CRC Report No. AVFL-16

FUELS TO ENABLE LIGHT-DUTY DIESEL ADVANCED COMBUSTION REGIMES

August 2012

COORDINATING RESEARCH COUNCIL, INC.
3650 MANSELL ROAD·SUITE 140·ALPHARETTA, GA 30022

The Coordinating Research Council, Inc. (CRC) is a non-profit corporation supported by the petroleum and automotive equipment industries. CRC operates through the committees made up of technical experts from industry and government who voluntarily participate. The four main areas of research within CRC are : air pollution (atmospheric and engineering studies); aviation fuels, lubricants, and equipment performance, heavy-duty vehicle fuels, lubricants, and equipment performance (e.g., diesel trucks); and light-duty vehicle fuels, lubricants, and equipment performance (e.g., passenger cars). CRC's function is to provide the mechanism for joint research conducted by the two industries that will help in determining the optimum combination of petroleum products and automotive equipment. CRC's work is limited to research that is mutually beneficial to the two industries involved, and all information is available to the public.

Center for Alternative Fuels, Engines & Emissions
West Virginia University

CRC AVFL-16

"Fuels to Enable Light-Duty Diesel Advanced Combustion Regimes"

Project Period: December 2008 – March 2012

Final Report – August 2012

Submitted to:

Dr. Chris J. Tennant
Coordinating Research Council, Inc.
3650 Mansell Rd, Suite 140
Alpharetta, GA 30022
ctennant@crcao.org

Dr. William J. Cannella
Senior Consultant – Fuels R&D
Chevron Energy Technology Co.
100 Chevron Way
Richmond, CA 94802
bijc@chevron.com

Submitted by:

Daniel Carder (Principal Investigator), Ross Ryskamp, John Nuszkowski*
Hailin Li, Nigel Clark, Gregory Thompson, Mridul Gautam, and Scott Wayne
Center for Alternative Fuels, Engines, and Emissions
West Virginia University
Department of Mechanical & Aerospace Engineering
Morgantown, WV 26506
daniel.carder@mail.wvu.edu

***University of North Florida**

August 23, 2012

WVU OSP Ref. No. - 08-258
***Project.Task.Award* –** 10012244.1.1004514R

Executive Summary

Advanced combustion strategies have gained significant attention within the last decade as a potential tool to comply with tightening emissions regulations. These strategies seek to minimize oxides of nitrogen (NO_X) and particulate matter (PM) emissions while increasing or retaining fuel efficiency typical of diesel combustion and are dependent on engine hardware, engine control strategy, and fuel properties. The goal of CRC AVFL-16, "Fuels to Enable Light-Duty Diesel Advanced Combustion Regimes," was to investigate the effects that diesel fuel properties might have on the combustion, emissions, and performance characteristics of light-duty production engines during advanced combustion operation.

To investigate the effect of fuel properties on advanced combustion, a comprehensive matrix of nine fuels (shown below) with varying cetane number (CN), aromatic content, and 90 percent distillation temperature (T90) was utilized with a split injection control strategy and a single injection control strategy on a GM Z19DTH light-duty compression-ignition engine. The matrix of Fuels for Advanced Combustion Engines (FACE) diesel fuels designed by CRC and commercialized by Chevron Phillips Chemical Co. was used. The FACE 2 fuel was replaced by an ultra low sulfur diesel (ULSD) certification fuel to facilitate a baseline comparison to previous studies at WVU.

Fuel Properties

Property	FACE 4	FACE 1	FACE 3	ULSD	FACE 7	FACE 9	FACE 8	FACE 6	FACE 5
Cetane Number	28.4	29.9	32.0	44.0	44.3	45.0	50.0	53.3	54.2
Aromatic Content (Mass %)	40.7	26.1	50.0	34.7	46.2	37.0	43.5	21.1	22.2
90% Distillation Temperature (°F)	639	517	518	582	513	610	648	646	528

A single engine operating condition consisting of a fixed engine speed of 2100 rpm and 3.5 bar brake mean effective pressure (BMEP) was utilized. The split injection control strategy involved varying the start of the pilot injection, start of the main injection, and fuel split ratio with a constant intake oxygen concentration of 16% and constant rail pressure of 1600 bar. In the single injection control strategy investigation, intake oxygen concentration was varied from 12 to 14% and injection pressures from 1200 to 1600 bar while controlling the injection timing to identify the operating conditions for 50% of the mass fraction burned (MFB) at 7° after top dead center (ATDC). The test matrix consisted of 60 individual test points per fuel. Each fuel was categorized as a low, medium, or high CN fuel (shown below) based on historical correlation of emissions and engine performance with CN.

Fuel Categories

Category	Criteria	Fuels
Low CN	CN< 40	FACE 1, 3, 4
Medium CN	40<CN<48	FACE 7, 9, ULSD
High CN	CN>48	FACE 5, 6, 8

A significant effort was required to establish the engine test platforms for this study. Initial experiments were performed using two different engines (a 16 valve GM Z19DTH engine and an 8 valve GM Z19DT engine) as well as three exhaust gas recirculation (EGR) coolers (sized for 1.9 L, 6.0 L, and 11.0L engine applications). The lower emissions, higher brake thermal efficiency (BTE), and more homogeneous combustion of the GM Z19DTH engine made it better suited for advanced combustion research than the GM Z19DT engine and so it was selected to complete the study. In initial tests on the FACE 4 (low CN) fuel, the 1.9 L EGR cooler achieved greater BTE and more stable combustion than the 6.0 L EGR cooler. However, with the FACE 5 (high CN) fuel, lower soot and NO_X emissions were produced with the 11.0 L EGR cooler compared to the 6.0 L EGR cooler. In an effort to reduce the influence of engine hardware when determining fuel property effects on emissions and performance, a decision was made to use the 6.0 L EGR cooler for all fuels.

A study of the repeatability in engine performance was conducted after the primary testing of the fuels to develop a standard by which differences in emissions and performance could be attributed to fuel property differences and not to the variability associated with the equipment, control strategy, or drift. Two different split injection control conditions using the ULSD fuel were chosen for this study. The first split injection control condition employed a main start of injection (SOI) timing of 6° before top dead center (BTDC), a pilot SOI timing of 40° BTDC, and a fuel split of 35% pilot. This split injection control condition was chosen based on low soot emissions observed during the primary testing of the ULSD fuel. The second split injection control condition employed a main SOI timing of -2° BTDC, a pilot SOI timing of 40° BTDC, and a fuel split of 30% pilot. This split injection control condition was chosen based on low NO_X emissions observed during the primary testing of the ULSD fuel. Tests using these control conditions were repeated 18 times each over the course of three days. Based on the outcome of this study, it was determined that any difference in emissions of greater than 4% for hydrocarbons (HC) and NO_X, 18% for carbon monoxide (CO), 27% for soot, and 2% for BTE, could be attributed to differences in the fuels rather than variability associated with the data.

The following conclusions can be drawn regarding both the split and single injection control strategies evaluated in this study:

1. A clear trend was observed between CN and HC emissions. Engine operation on the low CN fuels produced the highest levels of HC, while operation on the high CN fuels produced the lowest levels of HC. For example, FACE 4, the lowest CN fuel, produced the highest HC emissions.
2. FACE 8 and FACE 9, which both have high T90 and high aromatic content, exhibited the highest NO_X in their respective CN categories of medium CN and high CN.
3. The low CN fuels emitted significantly less (~4-84 times lower) soot than the high CN fuels.
4. Soot emissions were the highest for FACE 6 and 8 due to the high CN and high T90 of each fuel.
5. FACE 4 had the lowest BTE due to incomplete combustion caused by the fuel's low CN and low volatility.
6. The average BTE of all fuels decreased from approximately 32.6% using the single injection strategy to 30.1% using the split injection strategy, which represents an 8%

reduction at this operating condition (2100 RPM, 3.5 bar BMEP). In comparison, a stock GM Z19DTH engine operated with an original equipment manufacturer (OEM) engine control unit (ECU) at 2000 RPM produced 22.8% and 31.9% BTE at a BMEP of 2.1 bar and 5.4 bar, respectively. Note that the calibration for this OEM ECU may not have been the same as a production calibration. Additionally, these BTE values were not obtained with the same laboratory equipment as those used in the AVFL-16 study.

7. Accompanying the BTE reduction was an increase of HC, CO, and NO_X emissions by 50%, 18%, and 65%, respectively, for the split injection strategy compared to the single injection strategy. Soot emissions and in-cylinder pressure rise rate (PRR) decreased by 57% and 28%, respectively for the split injection strategy when compared to the single injection strategy.

Acknowledgement

West Virginia University acknowledges the support of the Coordinating Research Council for funding the project and the AVFL-16 technical leadership panel throughout the project. The technical leadership panel members were: Bill Cannella (Chevron), Scott Sluder (ORNL), Chris Tennant (CRC), and Robert Wagner (ORNL). Input was also provided by other AVFL-16 Panel members: Scott Jorgensen (GM), David Lax (API), Mani Natarajan (Marathon Petroleum), Stuart Neill (National Research Council Canada), Krystal Wrigley (ExxonMobil), and Ken Wright (ConocoPhillips).

Additionally, the authors acknowledge Dr. Benjamin Shade, Jason Ice, Ramamoorthy Balakrishnan, Peter Bonsack, Zac Luzader, Richard Atkinson, and Brad Ralston for their assistance and support throughout the project.

Table of Contents

List of Figures

List of Tables

List of Acronyms

ATDC – After Top Dead Center
AVFL – Advanced Vehicle, Fuel, and Lubricants Committee
BMEP – Brake Mean Effective Pressure
BPD – Bullet Proof Diesel
BSFC – Brake Specific Fuel Consumption
BTDC – Before Top Dead Center
BTE – Brake Thermal Efficiency
CA – Crank Angle
CAFEE – Center for Alternative Fuels, Engines, and Emissions
CA50 – Crank Angle of 50% MFB
CI – Compression Ignition
CLD – Chemiluminescence Detector
CN – Cetane Number
CO – Carbon Monoxide
CO_2 – Carbon Dioxide
COV – Coefficient of Variation
CR – Compression Ratio
CRC – Coordinating Research Council
CVS – Constant Volume Sampling
DAQ – Data Acquisition
ECU – Engine Control Unit
EERL - Engines and Emissions Research Laboratory
EGR – Exhaust Gas Recirculation
EOC – End of Combustion
EOI – End of Injection
FACE – Fuels for Advanced Combustion Engines
FID – Flame Ionization Detector
GM – General Motors
HC – Hydrocarbon
HCCI – Homogeneous Charge Compression Ignition
HDD – Heavy-Duty Diesel
HECC – High Efficiency Clean Combustion
HRR – Heat Release Rate
IMEP – Indicated Mean Effective Pressure
IO_2 – Intake Oxygen
ISFC – Indicated Specific Fuel Consumption
LTC – Low Temperature Combustion
MFB – Mass Fraction Burned
NDIR – Non-Dispersive Infrared
NO – Nitric Oxide
NO_X – Oxides of Nitrogen
O_2 – Oxygen
OEM – Original Equipment Manufacturer
PCCI – Premixed Charge Compression Ignition

PM – Particulate Matter
PRR – Pressure Rise Rate
RP – Rail Pressure
RPM – Revolutions per Minute
SOC – Start of Combustion
SOI – Start of Injection
SOP – Start of Injection Pulse
T90 – 90% Distillation Temperature
TDC – Top Dead Center
THC – Total Hydrocarbon
UHC – Unburned Hydrocarbon
ULSD – Ultra Low Sulfur Diesel
UNIBUS – Uniform Bulky Combustion System
VGT – Variable Geometry Turbocharger
VVA – Variable Valve Actuation
WVU – West Virginia University

1 Introduction

Advanced combustion strategies have gained significant attention within the last decade as a potential tool to comply with tightening emissions regulations for on and off-road applications. Emissions of oxides of nitrogen (NO_X) and particulate matter (PM) have, in particular, received increased scrutiny from federal and state regulators, resulting in near zero permissible levels of these pollutants. Furthermore, many strategies that decrease NO_X increase soot or decrease soot and increase NO_X. Advanced combustion strategies seek to simultaneously minimize the reactions that produce NO_X and PM emissions while retaining acceptable fuel efficiency. Achievement of such strategies depends on numerous variables, such as engine hardware, engine control strategy, and fuel properties.

Responding to the need for increased knowledge of fuel property effects on advanced combustion strategies, the Fuels for Advanced Combustion Engines (FACE) Working Group of the Advanced Vehicle, Fuel, and Lubricants Committee (AVFL) of the Coordinating Research Council (CRC) designed a comprehensive matrix of nine fuels for advanced combustion engine research [1, 2]. Development of the FACE diesel fuel matrix centered around three important fuel characteristics: auto-ignition quality, boiling range, and chemical composition. Respectively, these characteristics are represented by cetane number (CN), 90 percent distillation temperature (T90), and aromatic content. Project AVFL-16, "Fuels to Enable Light-Duty Diesel Advanced Combustion Regimes", was established to investigate the effects of these fuel properties on the combustion, emissions, and performance characteristics of a light-duty production engine during advanced combustion operation.

Much of the existing technical literature has focused on the interaction of fuel properties and conventional diesel combustion, whereas studies of fuel property effects on advanced combustion are less prevalent. Other organizations have researched and published FACE fuel effects on a variety of engines and operating conditions [3, 4, 5, 6], but West Virginia University (WVU), through the AVFL-16 project, seeks to augment this knowledge base with FACE fuel effects associated with a split injection control strategy. A single injection strategy was also investigated by WVU.

Both control strategies were implemented on a General Motors light-duty compression-ignition European production engine. No internal engine hardware modifications were made in an effort to retain the study's focus on fuel property effects. A single engine operating condition consisting of a fixed engine speed and load was selected to investigate each fuel during both fuel injection strategies. Research for the split injection control strategy involved varying the start of fuel injection timing and fuel injection quantity for two injection events, while keeping exhaust gas recirculation (EGR) rates and injection pressures constant. Investigation of the single injection control strategy entailed varying EGR rates and injection pressures while tailoring injection timing to obtain a constant combustion phasing among all fuels.

2 Literature Review

2.1 Advanced Combustion Strategies

Advances in engine technology have been driven by many factors since the inception of the internal combustion engine. In recent decades, several key laws have required engine manufacturers to decrease engine emissions in an effort to improve air quality. Concurrently, state and federal legislation as well as consumer demand for more fuel efficient vehicles have fueled research and development.

There is generally a tradeoff between compliance with emissions regulations and improving efficiencies in conventional engines. Exhaust aftertreatment systems and other methods of reducing regulated emissions generally affect engine performance and fuel economy negatively. Advanced combustion strategies seek to break this tradeoff by retaining acceptable thermal and combustion efficiency while simultaneously decreasing specific regulated emissions. In addition, advanced combustion strategies do not have the same added packaging volume, and mass associated with aftertreatment systems such as diesel particulate filters and selective catalytic reduction systems found on many conventional 2010 heavy-duty diesel engines.

Several methods of advanced combustion exist, but strategically they are all very similar. In essence, a homogeneous air and fuel mixture with combustion occurring at a low temperature can retain efficiencies while reducing NO_X and PM emissions. The strategies discussed in this document include low temperature combustion (LTC), premixed charge compression ignition (PCCI), and homogenous charge compression ignition (HCCI). Figure 1 displays the in-cylinder regions defined by local temperature and equivalence ratios (the actual ratio of fuel-to-air divided by the stoichiometric ratio of fuel-to-air) and conceptually where these advanced combustion strategies may be applied [7]. Conventional diesel combustion occupies the largest region in the figure with operating points located in heavy soot and nitric oxide (NO) formation regions, while LTC, PCCI and HCCI have a limited number of operating points in these regions.

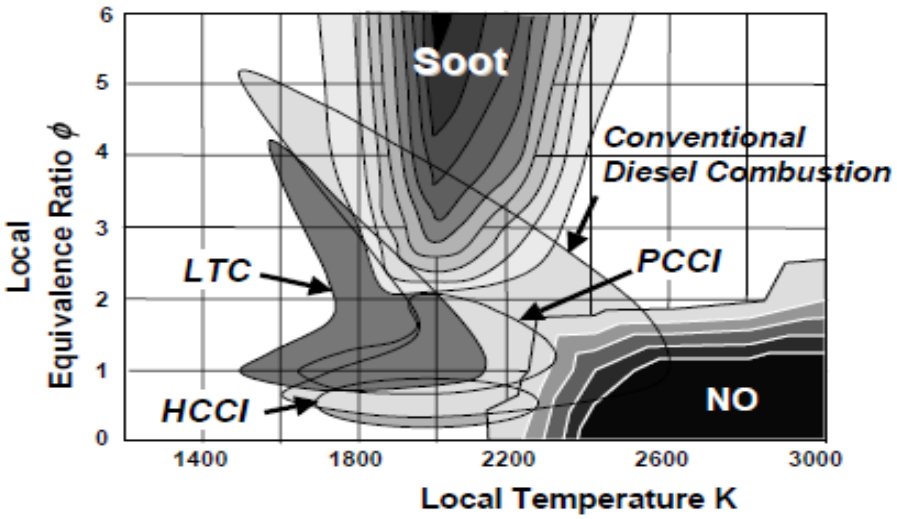

Figure 1: Temperature and Equivalence Ratio Regions for Advanced Combustion Strategies [7]

2.1.1 Low Temperature Combustion (LTC)

Formally introduced in the year 2000 under the name "low temperature oxidation" by Toyota Motor Corporation at the 9th Aachen Colloquium, LTC seeks a simultaneous reduction of NO_X and soot formation through decreased combustion temperatures at stoichiometric and locally rich air-to-fuel ratios [8]. The concept is shown visually in Figure 1 where the outlined LTC region exists at local combustion temperatures less than 2200°K and local equivalence ratios range from nearly stoichiometric to 4. LTC has a smaller operating area than conventional diesel combustion and lies outside of heavy soot and NO_X production zones. An apparent drawback of the decreased operating range is its general restriction of the attainment of LTC at higher loads due to high combustion temperatures, especially at the increased local equivalence ratios created by heavy fueling [7].

2.1.2 Premixed Charge Compression Ignition (PCCI)

Various organizations and manufacturers have demonstrated reductions in NO_X and PM emissions resulting from near homogeneous mixtures through the use of early injection timings and elevated EGR levels [6, 9, 10, 11]. By injecting fuel into the cylinder early and using EGR to control combustion phasing, more time for mixing is achieved, which avoids a stratified air and fuel charge typical of conventional diesel combustion. Figure 1 displays a narrower local equivalence operating range for PCCI when compared to LTC, but the presence of a larger combustion temperature range allows for more NO_X production. This limited area of operation presents issues when attempting to achieve PCCI at heavy and full load operating conditions, where heavy fueling is necessary and early injection timings may not be feasible due to the high pressure rise rates from combustion, leading to engine wear issues or engine failure.

2.1.3 Homogeneous Charge Compression Ignition (HCCI)

Examples of and research on HCCI combustion has existed for decades [12]. This research effort has grown considerably in recent years due to a desire for efficient, lower polluting internal combustion engines. The strategy of HCCI is similar to some elements of LTC and PCCI, in which a homogeneous, lean air and fuel mixture is combusted rapidly and uniformly without flame propagation at a low combustion temperature. Elimination of locally rich air and fuel mixtures decreases PM emissions, while low combustion temperatures reduce NO_X formation. Efficiencies comparable to modern compression ignition engines are retained through the use of increased compression ratios (compared to spark ignition engines), the absence of throttling losses, and rapid combustion of the homogeneous air and fuel mixture without flame propagation [13]. HCCI has been demonstrated for low to medium load operation, but, as with other advanced combustion strategies, heavy load operation is difficult to achieve. Thus, as demonstrated in Figure 1, the operating region for HCCI is the smallest for all of the combustion strategies presented. Additionally, HCCI combustion generally results in greater hydrocarbon (HC) and carbon monoxide (CO) emissions than typical diesel combustion.

2.2 Initiating and Controlling Advanced Combustion Strategies

In order to initiate and control any advanced combustion strategy, some modification to a conventional compression ignition engine must be performed. Hardware changes as well as modifications of engine control strategies can have a profound effect on engine operation. To adequately achieve some forms of advanced combustion, several modifications must be performed to work in conjunction with each other.

2.2.1 Fuel Injection and other Engine System Control Changes

2.2.1.1 Start of Injection Timing

One common method of promoting better mixing of the air and fuel charge is to advance the start of injection (SOI) timing. Injecting fuel into the cylinder earlier allows more time for the development of a well-mixed air and fuel mixture. In a conventional diesel combustion strategy, NO_X emissions increase as SOI timing is advanced, but researchers such as Kawano et al. have demonstrated on a single cylinder HCCI research engine that advanced SOI timing paired with increased injection pressure can reduce NO_X emissions for SOI timings greater than 30° before top dead center (BTDC) [14]. (See Figure 2.) This effect is likely a result of reduced diffusion flame zones, a major contributor of thermal NO formation, due to the absence of near stoichiometric air and fuel mixtures [15].

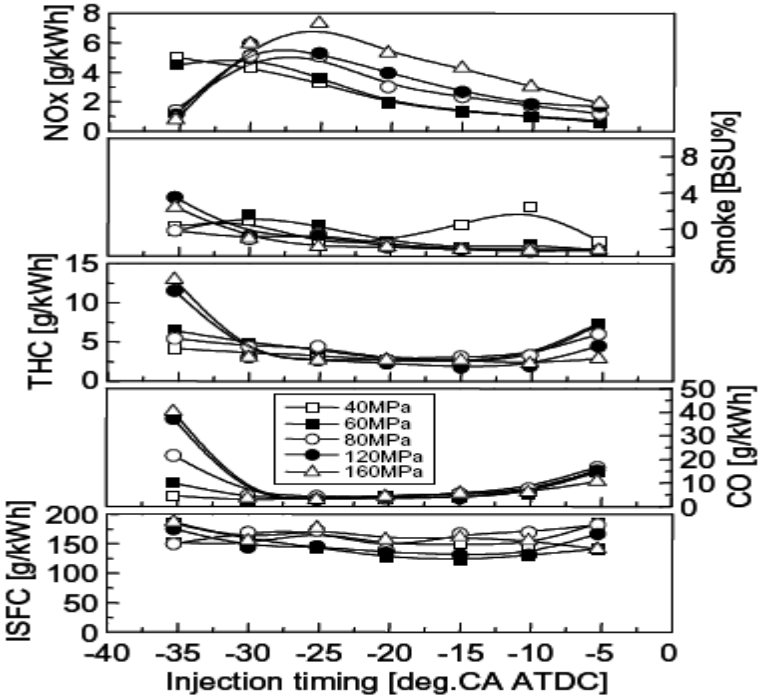

Figure 2: Brake Specific Emissions, Fuel Consumption & Smoke vs. Injection Timing [14]

Figure 2 shows a simultaneous decrease in NO_X, and an increase in CO and HC as HCCI combustion is targeted. The increases can be attributed to conditions such as wall wetting or raw fuel seeping into piston ring glands and other crevices where combustion will not occur. Additionally, increased pressure and pressure rise rates are common when advancing SOI timing. Engine durability becomes a concern under these conditions.

2.2.1.2 Fuel Split

Modern compression ignition (CI) engines equipped with electronically controlled direct fuel injection systems commonly use multiple injections (e.g., a pilot injection). Injection of a relatively small pilot quantity of fuel prior to the main injection event can reduce in-cylinder pressure rise rates (PRR) by reducing the amount of fuel burned during the premixed phase of combustion [16] and aid in optimizing combustion phasing for the main injection event. A decrease in audible noise emitted from the engine (a common characteristic of older CI engines) and lower in-cylinder temperatures accompany the reduction in PRR. The lower in-cylinder temperatures aid in reducing NO_X emissions.

Hasegawa et al. of Toyota Motor Corporation explored the effects of a multiple injection strategy on an HCCI concept termed Uniform Bulky Combustion System (UNIBUS) [12]. In this study, the test platform was a four cylinder, dual overhead camshaft engine with four valves per cylinder displacing three liters. The engine was also equipped with a common rail fuel injection system, variable nozzle turbocharger with intercooler, exhaust gas recirculation, and featured a compression ratio of 18.4: 1. Figure 3 compares the UNIBUS injection strategy (Double Injection) to a single injection strategy and the conventional diesel combustion strategy.

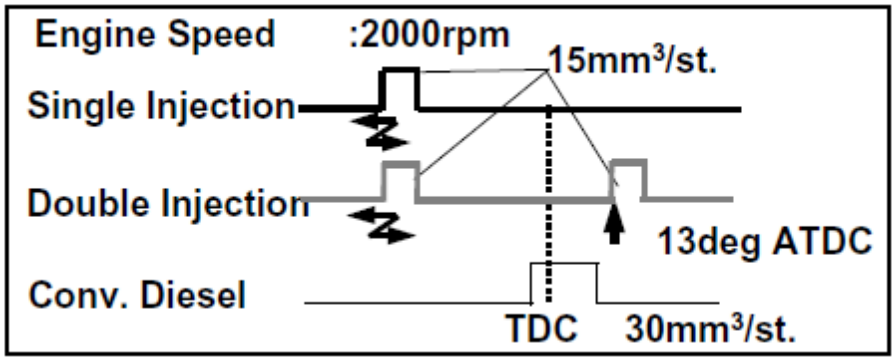

Figure 3: UNIBUS and Comparison Injection Strategies [12]

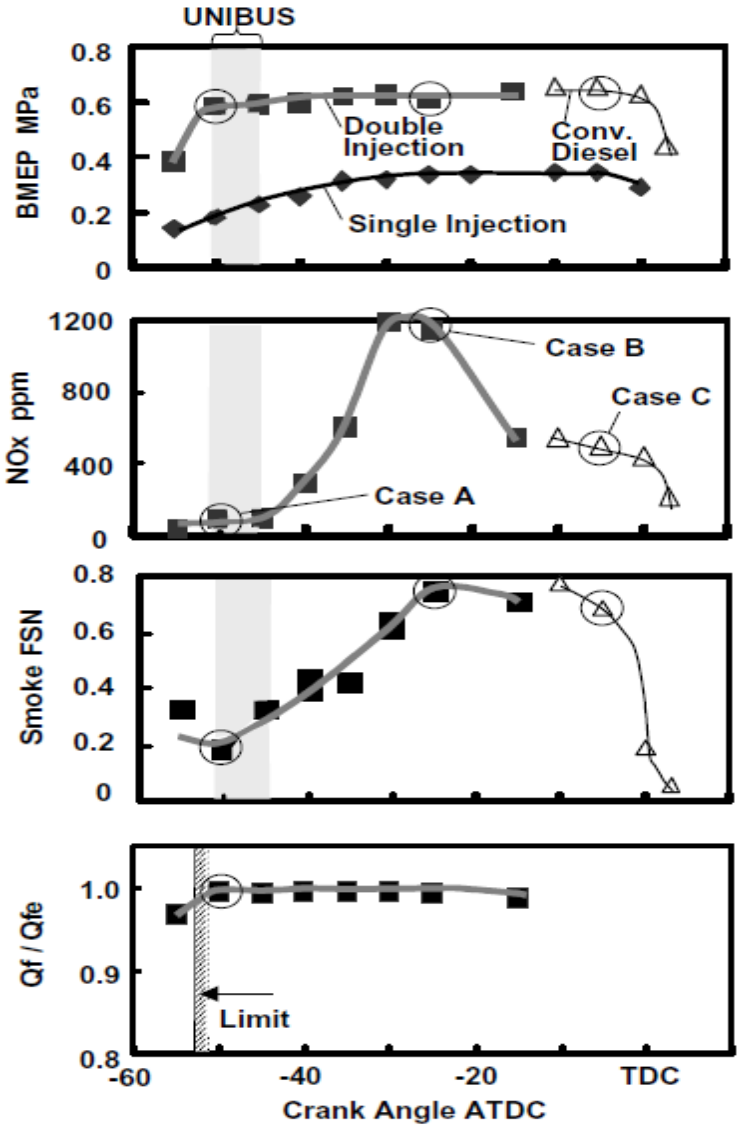

Figure 4: BMEP, NO_X and Smoke Emissions, and Rate of Effective Injection Quantity for UNIBUS and Comparison of Injection Strategies [12]

During the development of the UNIBUS concept, a number of tests were performed to compare and quantify the effects of a double injection strategy with varying SOI timing versus a conventional diesel combustion strategy. For the double injection tests, the main SOI was fixed at 13 ° after top dead center (ATDC) while the pilot SOI was varied. As displayed by Figure 3, the injection volume of fuel per stroke during the double injection strategy was held at 15 mm^3 for both injection events. The plot of brake mean effective pressure (BMEP) in Figure 4 shows that the UNIBUS strategy, as well as the majority of double injection strategy tests, are capable of achieving a BMEP close to that of conventional combustion with the same fuel quantity injected and while producing significantly lower NO_X and smoke emissions. Figure 4 also plots the rate of effective injection, which is the input injection quantity (Qf) divided by the injection quantity calculated by carbon number method (Qfe). This rate of effective injection shows that the UNIBUS strategy is very close to its performance limit. Unfortunately Hasegawa et al. did not report HC and CO emissions for the UNIBUS strategy; therefore, the overall effects of their

use of early pilot injection cannot be completely assessed. A study performed by Musculus et al. [17] provides some insight into the potential effects of using an injection event located near or after top dead center (TDC) in an LTC process such as the UNIBUS strategy. In this study, unburned hydrocarbon (UHC) emissions were attributed to over-mixing and the formation of locally lean mixtures (too lean for combustion) near the fuel injector shortly after the end of injection (EOI) in a single cylinder direct injection heavy-duty diesel engine operating at LTC conditions. Musculus et al. concluded that "immediately after EOI, mixtures near the injector rapidly mix with ambient gases so that the distribution [of equivalence ratios in the diesel jet] reverses, with equivalence ratios increasing with axial distance from the injector."

2.2.1.3 Rail Pressure

Modern compression ignition engines usually use a relatively new fuel injection technology labeled common rail injection. Common rail injection features a high pressure fuel rail which feeds electronically controlled injectors. Increasing the fuel rail pressure increases the fuel injection pressure. Increased fuel injection pressure can have varying effects on combustion phasing as well as emissions formation. Ideally, a greater fuel pressure will result in better fuel atomization, quicker delivery and ultimately a more globally homogeneous air and fuel mixture.

Figure 5 displays the effects of increased rail pressure on smoke and NO_X emissions for varying values of lambda (attributed to changes in EGR fraction). It shows that an increase in rail pressure at near stoichiometric conditions reduces smoke by over 50%. This phenomenon is most likely attributed to better fuel atomization and an overall more homogeneous air and fuel mixture. Increased rail pressure at a lean air-to-fuel ratio results in greater NO_X emissions, possibly linked to elevated cylinder temperatures from the lack of EGR.

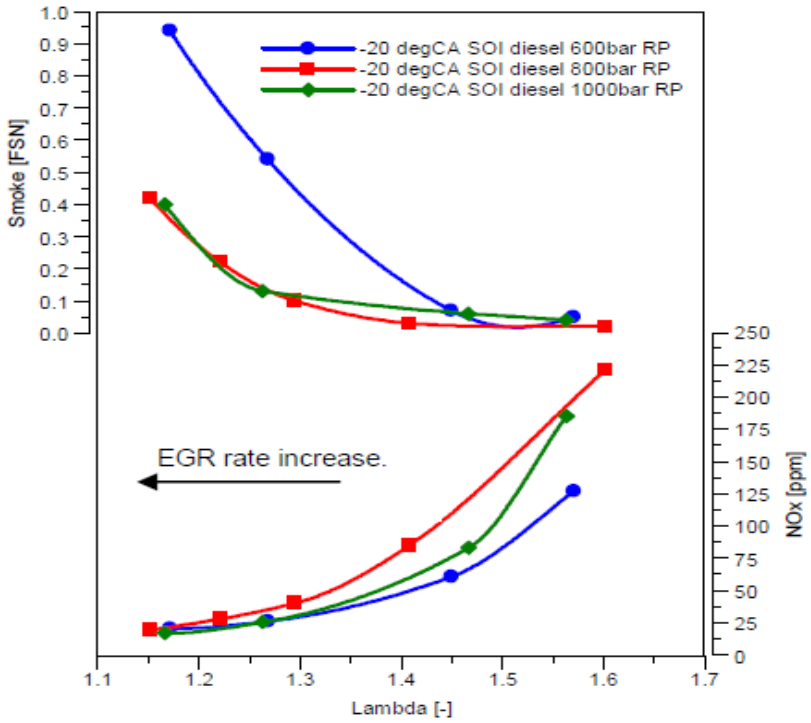

Figure 5: NO_X and PM Emissions a Function of Lambda for Varying Rail Pressure [18]

2.2.1.4 Exhaust Gas Recirculation (EGR)

Reintroduction of exhaust gas into the cylinder affects combustion phasing and emissions formation by acting as a diluent. The presence of this diluent (EGR) reduces in-cylinder temperature, pressure, and pressure rise rates. Through this reduction in temperature, decreased NO_X emissions are normally observed, while increased HC, CO and PM emissions are common as well as increased brake specific fuel consumption (BSFC). The NO_X and PM tradeoff created by EGR is exemplified in Figure 5. Development of cooled EGR has been shown to further reduce NO_X emissions while helping to improve BSFC. The tradeoff between NO_X emissions and BSFC for cooled and un-cooled EGR at varying injection timings is displayed in Figure 6.

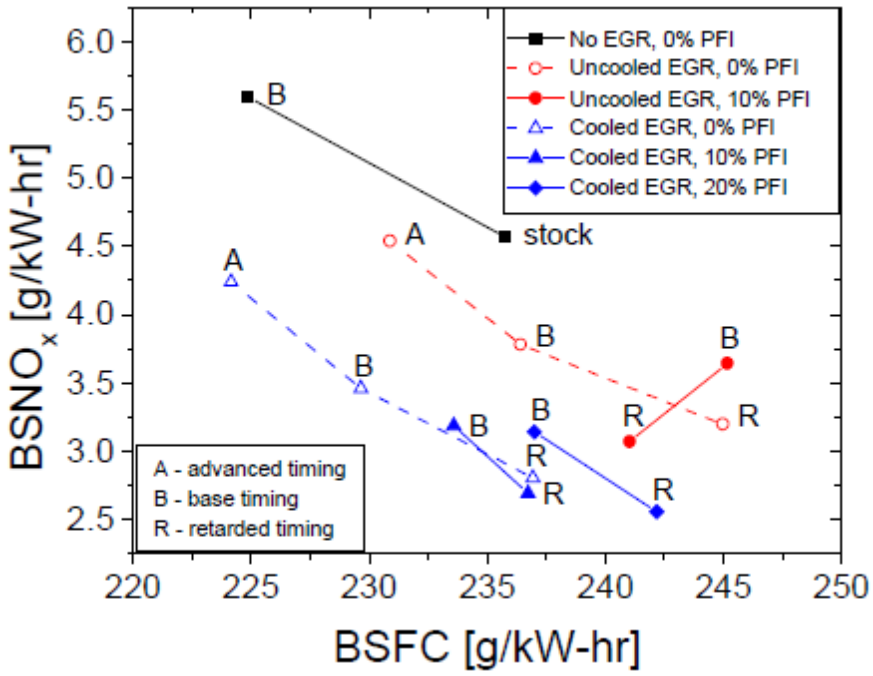

Figure 6: $BSNO_X$ Emissions vs. BSFC at Varying Injection Timing for Cooled and Un-Cooled EGR [9]

Besides lower combustion temperatures and NO_X emissions, the greatest benefit offered by incorporating EGR into an advanced combustion strategy is the ability to control combustion phasing and limit pressure rise rates that adversely affect engine durability. Figure 7 demonstrates longer ignition delay for greater EGR fractions. This is especially helpful when attempting to control combustion phasing or eliminate engine knock after an early injection event. The increase of EGR fraction from 0% to 60% as shown in Figure 8 results in approximately a 50% decrease in maximum cylinder pressure rise rate leading to greater engine durability under advanced combustion strategies.

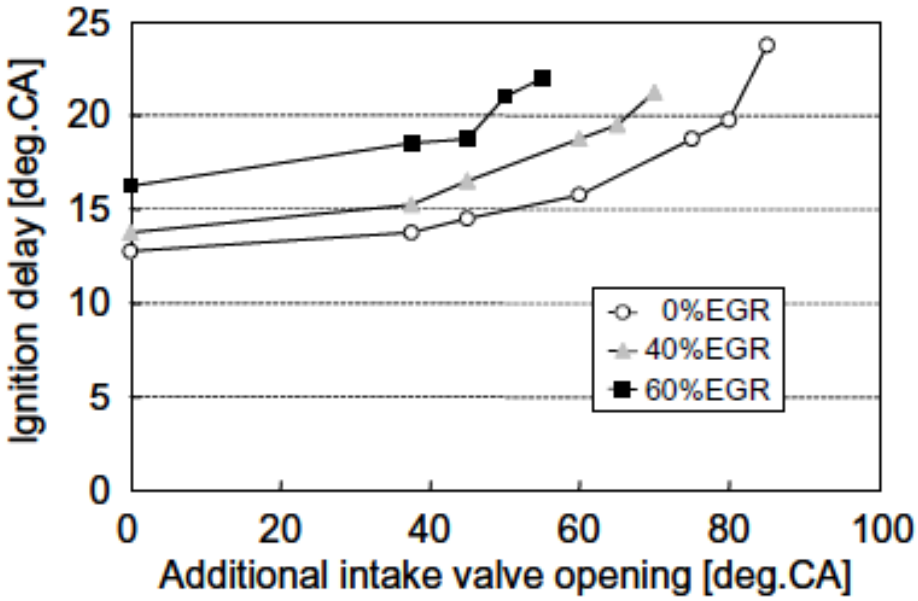

Figure 7: Ignition Delay for Additional Intake Valve Opening with Varying EGR Fraction [14]

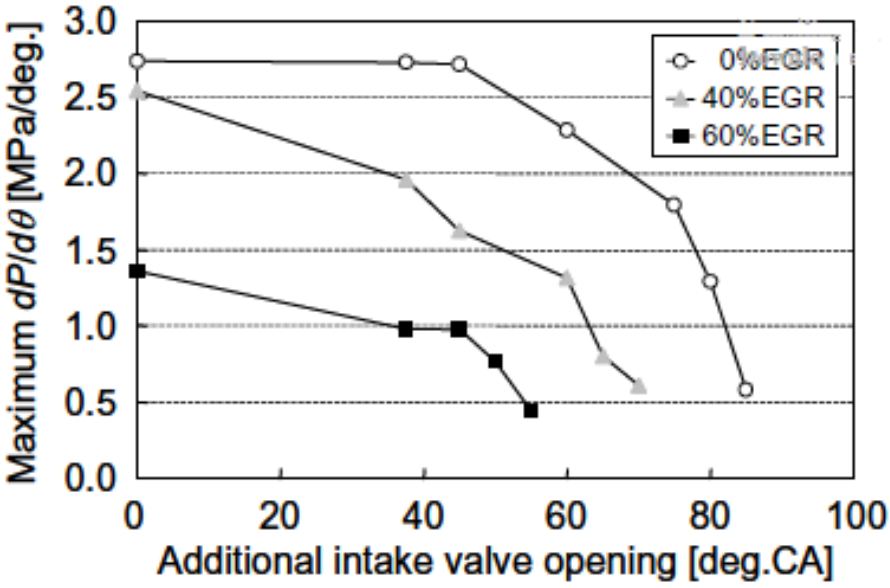

Figure 8: Maximum Pressure Rise Rate for Additional Intake Valve Opening with Varying EGR Fraction [14]

2.2.1.5 Intake Air Temperature

Changes in intake air temperature have a major effect on combustion and can be used to control combustion phasing. Elevating the intake air temperature will raise the bulk mixture of air and fuel closer to the ignition temperature, resulting in an earlier combustion event. In addition to combustion phasing, increased intake air temperatures generally promote better fuel atomization. Figure 9 shows cylinder pressure curves from an HCCI study on varying compression ratio, intake air temperature, and EGR [19]. The compression ratio was fixed at 14:1, and a relative high CN fuel was used (approximately 55) for the data presented. For the highest intake air temperature tested (60°C), combustion occurs earlier for similar EGR fractions. Figure 9 also shows the largest in-cylinder pressure and the steepest pressure rise for a 60°C intake air temperature test. This is beneficial during start up of a HCCI engine, as well as when using a lower CN fuel.

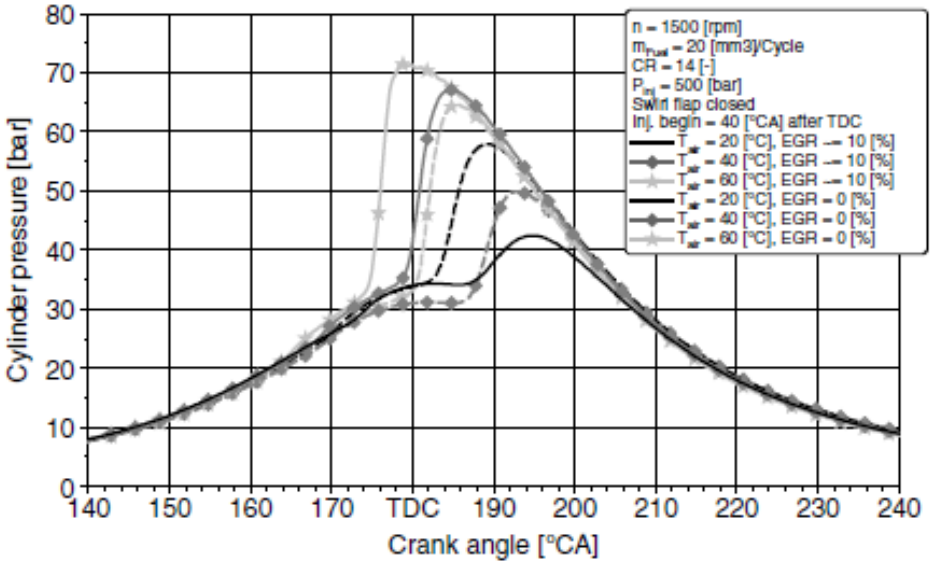

Figure 9: In-Cylinder Pressure Curves as a Function of Crank Angle for Varying Intake Air Temperatures [19]

2.2.1.6 Intake Manifold Pressure

Known also as boost pressure, intake manifold pressure is an essential feature of modern compression ignition engines. The forceful introduction of air into the intake manifold affects emissions, fuel consumption, and combustion-related characteristics. The value of boost on advanced combustion strategies is much more significant when paired with other technologies such as variable valve timing. Nevin et al. of the University of Wisconsin-Madison performed research on a single cylinder version of the Caterpillar 3406E equipped with artificial boost and variable valve timing [10]. Their experiments displayed reduced PM emissions for late valve closing conditions with elevated boost pressure. A nearly linear decrease in exhaust temperatures with the application of more boost pressure was also observed, but no real correlation to NO_X emissions reduction could be made. Negative effects of the increased boost pressure and decreased exhaust temperature were greater CO and HC emissions due to less oxidation, as well as increased BSFC.

2.2.2 Engine Hardware Modifications

2.2.2.1 Compression Ratio

An alteration of compression ratio (CR) may be necessary to transition a conventional compression ignition engine into an advanced combustion engine. This change may be performed statically or dynamically. A change in the dynamic compression ratio can be achieved through the application of variable valve actuation which is discussed in Section 2.2.2.3. A common method of changing the static compression ratio is the use of removable piston crowns. Depending on the strategy employed to achieve an advanced combustion method, the compression ratio may need to be decreased to ensure safe operation of the engine, or an increase may be necessary to ensure complete combustion without misfiring. Wagner et al. explored the effects of compression ratio on HCCI combustion [19]. The sweeps of compression ratio displayed in Figure 10 are for a fuel with a CN of approximately 55. Notice that as compression ratio increases, cylinder pressure increases, and the combustion phasing occurs earlier. This demonstrates that compression ratio is an important factor that affects combustion phasing. The pressure trace with a compression ratio of 14:1 and EGR fraction of 10% in Figure 10 shows weak and late combustion, flagging this as a non-optimal condition.

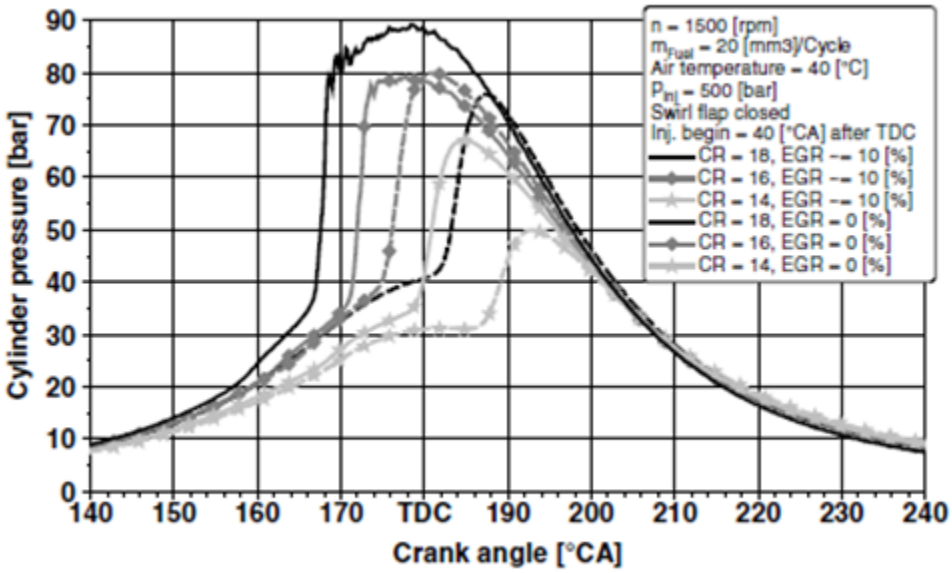

Figure 10: In-Cylinder Pressure as a Function of Crank Angle for Varying Compression Ratio [19]

2.2.2.2 Piston Design

Many different piston design concepts exist; the "Mexican hat" piston bowl design is common for compression ignition engines due to its swirl-invoking nature. Increased swirl in the combustion chamber leads to a more homogenous air and fuel mixture. Some advanced combustion studies rely on flat top pistons for simplicity's sake, but the complex geometric shapes of piston bowls can have varying effects on emissions and performance as demonstrated by Benajes et al. [11] and shown in Figure 11. These results reflect a medium load condition and display a tradeoff between NO_X emissions and reduced soot and fuel consumption for the differing piston bowl geometries.

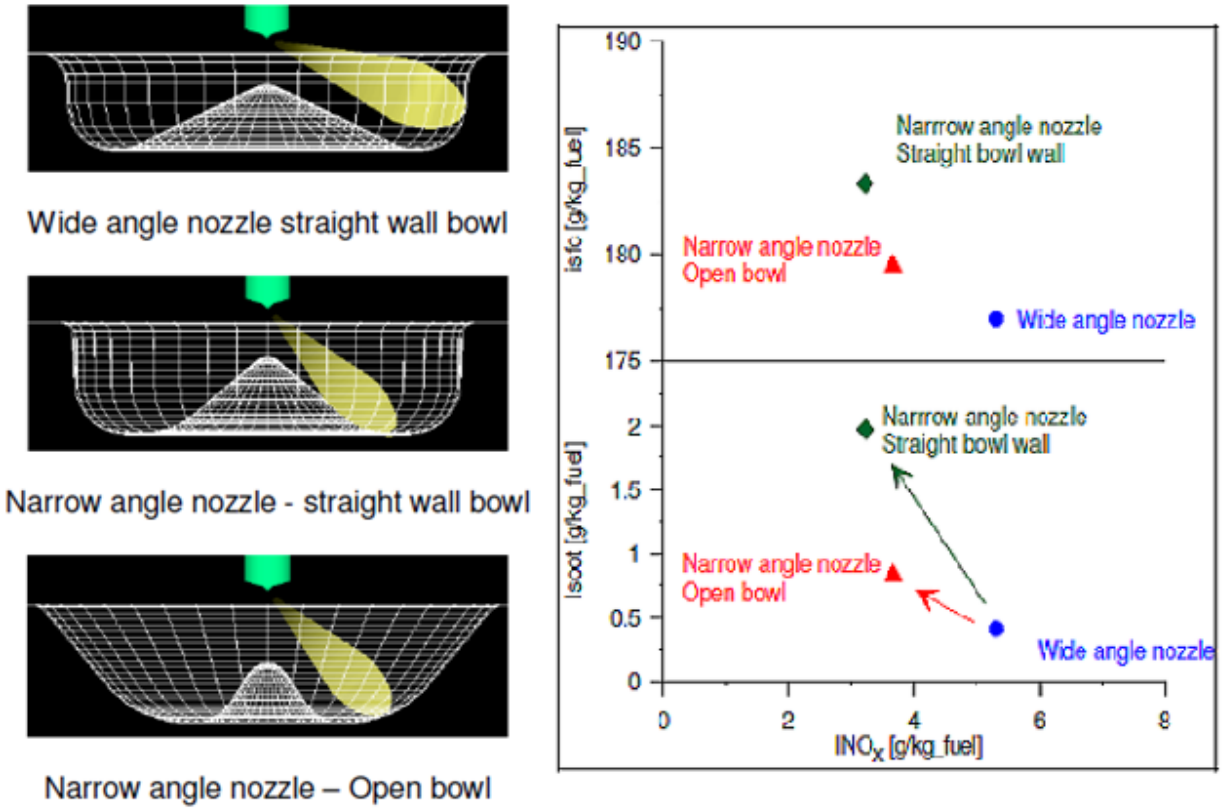

Figure 11: Various Piston Bowl Configurations and their Effects on Soot, Fuel Consumption, and NO_X [11]

2.2.2.3 Variable Valve Actuation

Modern variable valve actuation (VVA) systems are beginning to appear on compression ignition engines, but are generally found on research engines or retrofitted to a production engine for research purposes. The primary research focus of VVA for compression ignition engines is on the intake valve timing for the compression stroke. This variable plays a direct role in determining an engine's dynamic compression ratio. Besides mechanical operation, several methods of activating an engine's valves exist, including pneumatic, hydraulic, magnetic, electric, or a combination of these. Nevin et al. [10] and Kawano et al. [14] utilized an electrically operated high pressure hydraulic actuation method which holds the valve open longer after the mechanical lift has finished. Kawano et al. found additional intake valve opening resulted in decreased NO_X emissions and increased HC and CO emissions [14]. Fuel consumption remained fairly constant while smoke increased for the condition of no EGR and heavily extended valve opening. Other benefits include control of combustion phasing and cylinder pressure rise rate, as demonstrated in Figure 7 and Figure 8, respectively.

2.2.2.4 Injection Spray Angle

Employing an early injection event commonly results in fuel impinging on the cylinder walls, piston crown, and accompanying crevices. This phenomenon, known as wall wetting, can heavily increase HC and CO emissions and negatively affect engine performance due to copious amounts of unburned fuel. Implementing an injection angle that synchronizes with an early

injection strategy greatly reduces the effects of wall wetting. Trends can vary with widening or shortening the injection angle. Buchwald et al. found that a wide injection angle resulted in the best (lowest) overall NO_X, PM, and fuel consumption. This is heavily dependent on in-cylinder geometry and engine operating conditions [20]. Vanegas et al. produced similar results in research based around three different injection angles; concluding that the narrowest injection angle resulted in the greatest NO_X emissions and smoke [21]. The highest fuel consumption is found with the largest injection angle, while HC emissions are almost unanimously less with the narrow injection angle displayed in Figure 12. This signifies less wall wetting, especially at advanced start of injection pulse (SOP) timing (i.e., 50° BTDC).

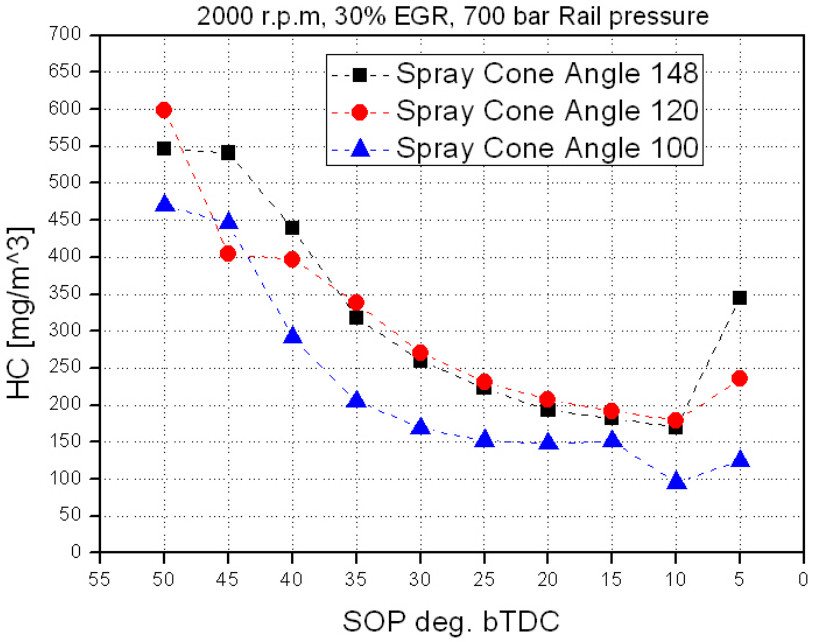

Figure 12: HC Emissions as a Function of Start of Injection Pulse for Varying Injection Angle [21]

2.3 Effect of Fuel Properties on Advanced Combustion Strategies

Fuel properties have a significant impact on the achievement of advanced combustion methods as well as the resulting emissions and engine performance. Methods of control and necessary modification of engine hardware can be solely dependent on the properties of a selected fuel. This has resulted in a considerable amount of research to determine which fuels are best suited for advanced combustion. CRC's FACE Working Group created a matrix of nine diesel fuels for use in advanced combustion research [1, 2]. The FACE group concluded that the three most important properties for advanced combustion research were CN, aromatic content, and T90 which they deem are "a measure of ignition quality," "a measure of chemistry," and a measure of "volatility," respectively [2]. The nine fuels comprising the FACE matrix were manufactured by Chevron Phillips Chemical Company; they include a mix of high and low CN, aromatic content, and 90% distillation temperature. Other researchers such as Kawano et al. have blended other fuels with conventional diesel fuel for use in advanced combustion research. Kawano et al. blended conventional diesel fuel with iso-octane, iso-paraffins, toluene, and MTBE to create a matrix of test fuels with varying properties [22].

2.3.1 Cetane Number (CN)

The ignition delay time of a particular fuel is quantified by its CN [23], where a high CN results in a shorter ignition delay and low CN results in a longer ignition delay. The effects of fuel CN on combustion phasing are important in advanced combustion. A study of the FACE matrix by Cho et al. explored the effects of CN on high efficiency clean combustion (HECC), an advanced combustion strategy related to LTC and PCCI [3]. Their research showed CN to be the main factor in determining acceptable injection timings for each fuel. Additionally, a study of the FACE matrix by Hosseini et al. determined that "cetane number clearly had the strongest effect" on combustion phasing [4]. Figure 13 demonstrates that in Cho et al.'s study, the shortest ignition delay was obtained for the high CN FACE diesel fuels (FACE 5 through 9). Therefore the allowable SOI timing range is more advanced for the low CN fuels. For both high and low CN fuels, Figure 13 shows combustion noise increases as SOI timing is advanced, with a slightly higher peak for the low CN fuels.

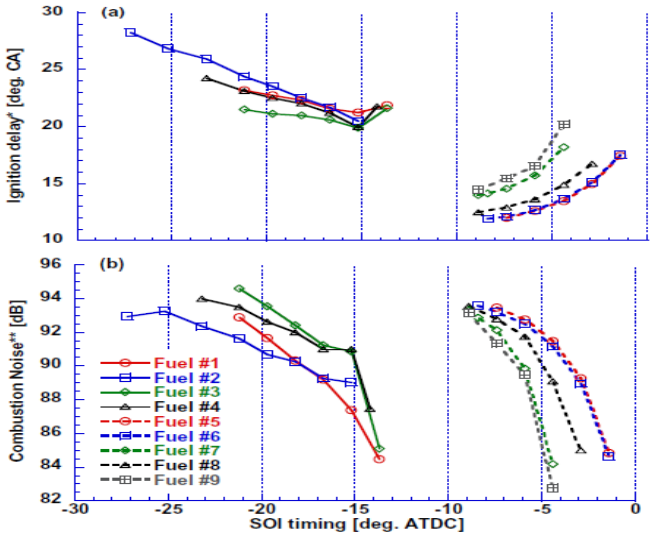

Figure 13: Ignition Delay and Combustion Noise as a Function of SOI Timing for the FACE Matrix [3]

Ignition quality and delay has a profound effect on in-cylinder temperatures, pressures, and bulk mixing, suggesting that CN has a direct influence on emissions formation. Results obtained by Bunting et al. from a single cylinder HCCI engine display a trend of decreasing NO_X emissions for fuels with higher CN [24]. This results from a lower combustion temperature due to a greater percent of low temperature heat release and a decreased intake air temperature (the minimum intake air temperature necessary to sustain combustion was used) [24]. They reported a slight decrease in HC emissions as CN increased while CO emissions tripled as CN rose from 30 to 55. Cho et al. [3] shows different trends in FACE fuel impacts on emissions due to differing engines and advanced combustion strategies. (See Figure 14.) An overall decrease in NO_X emissions for high CN fuels is present in the experiments by both Bunting et al. and Cho et al., but Cho et al. demonstrated lower CO emissions for high CN fuels while Bunting et al. observed higher CO emissions from high CN fuels (in comparison to the low CN fuels tested by both authors). PM emissions displayed in Figure 14 by Cho et al. are much greater for the high CN fuels while the BSFC for low CN fuels have a slightly lower maximum.

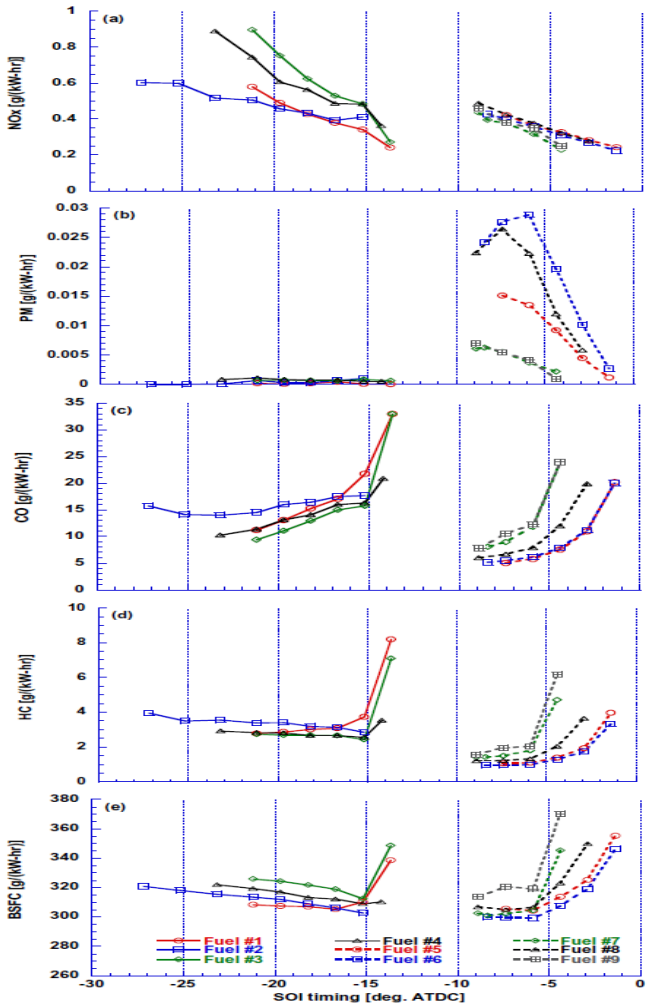

Figure 14: Emissions and Fuel Consumption at Varying SOI for the FACE Matrix [3]

Results of FACE matrix testing at low load conditions (5.5 bar indicated mean effective pressure (IMEP) in a 0.75 L single cylinder test engine) from De Ojeda et al. [5] agreed with those of Cho et al. De Ojeda et al. report that greater HC and CO emissions were observed during combustion

of the lower CN fuels when compared to the higher CN fuels. Additionally, it was noted that the lower CN fuels offered a better NO_X vs. soot tradeoff but lower fuel conversion efficiency due to the "considerable amount of fuel energy" contained in the elevated HC and CO emissions.

2.3.2 Aromatic Content

Described previously as "a measure of chemistry" [2] aromatics "have high densities in the liquid state and thus have high energy content per unit volume" [23]. Results from Cho et al., when operating the test engine in HECC mode (Figure 14), show lower NO_X emissions for fuels 1 and 2 which have a lower aromatic content than fuels 3 and 4. De Ojeda et al. also made comparisons between FACE fuels 1 and 2 versus FACE fuels 3 and 4, reporting that a higher aromatic content resulted in a longer ignition delay [5]. De Ojeda et al. noted that at low load conditions the highest HC and CO emissions were observed during combustion of FACE 3 and FACE 4 (low CN with high aromatic content).

2.3.3 90 Percent Distillation Temperature (T90)

The temperature at which 90 percent of the distillation process has occurred for a given fuel is often used to draw conclusions about the back-end volatility of that fuel. Fuels having a lower back-end volatility (i.e. higher T90's and end boiling points) are expected to be more difficult/take longer to completely volatilize and thus may lead to more PM/soot emissions. Figure 15 demonstrates the ASTM D86 measured T90 values for the FACE matrix. An interesting comparison is the volatility of fuels 1 and 2. The temperature curves up to approximately 80 percent distillation (T80) for both fuels are nearly identical. However at that point the curves diverge with fuel 2 having a T90 value of 346°C while the T90 value for fuel 1 (284°C) is considerably lower. So the front-end volatilities of these two fuels are very similar, but the back-end volatilities are very different.

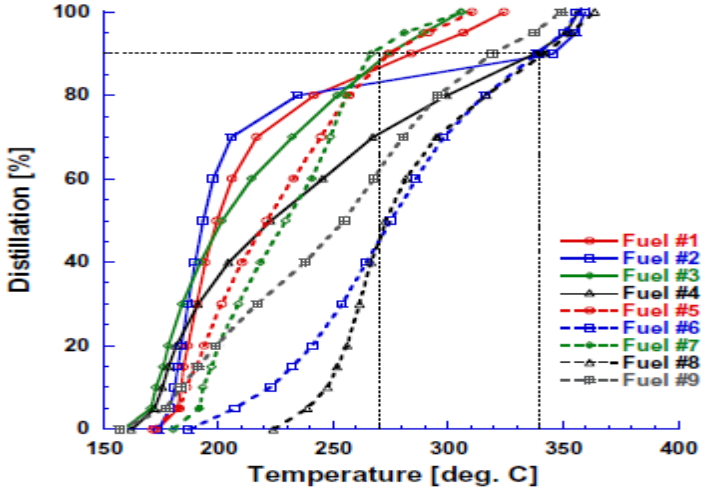

Figure 15: Distillation Percentage as a Function of Temperature for the FACE Matrix [3].

Although Hosseini et al. determined CN to have the most profound impact on combustion phasing, it was also reported that a lower T90 could be linked to advanced combustion phasing [4]. T90 has also been linked to PM formation; this is exemplified by Cho et al. in Figure 14 for the high CN fuels [3]. Fuels 5 and 7 exhibit a T90 of less than 275°C, while fuels 6 and 8 have a T90 of approximately 340°C and produced nearly double the PM emissions at their peaks.

3 Experimental Setup

3.1 Introduction

All testing discussed in this section of the document was conducted at West Virginia University's Center for Alternative Fuels, Engines and Emissions (CAFEE) and performed in the Engines and Emissions Research Laboratory (EERL). A full-scale constant volume sampling (CVS) dilution tunnel (Figure 16) was used in conjunction with a Horiba MEXA-7200 Gaseous Emissions analyzer to characterize gaseous emissions. Soot emissions were measured from the raw exhaust stream with the use of an AVL MS 483 micro-soot sensor. Test engines used during the project included a GM Z19DT (8 valve) model and a GM Z19DTH (16 valve) model; studies have been conducted at national laboratories, universities and research centers using the Z19DTH model.

Figure 16: CAFEE CVS Tunnel

3.2 Fuel Properties

Eight out of nine fuels of the FACE diesel matrix were utilized. Instead of testing FACE 2, the CRC AVFL-16 Project Panel decided to test a common reference fuel, which has also been tested in other studies at WVU: Chevron Phillips Chemical Company ultra low sulfur diesel (ULSD) 2007 certification fuel. Table 1 displays the nine fuels classified by CN category (high, medium, and low). Additional fuel properties (e.g., aromatic content, T90, etc.) within each of the CN categories are shown in Table 2 [1, 2]. Figure 17 illustrates the targeted values of each of the three primary fuel properties for each of the FACE diesel fuels used during this study.

Table 1: Description of Fuel Categories

Category	Criteria	Fuels
Low CN	CN < 40	FACE 1, 3, 4
Medium CN	40 < CN < 48	FACE 7, 9, ULSD
High CN	CN > 48	FACE 5, 6, 8

Table 2: Fuel Properties [1, 2]

Property	FACE 4	FACE 1	FACE 3	ULSD	FACE 7	FACE 9	FACE 8	FACE 6	FACE 5
Cetane Number	28.4	29.9	32.0	44.0	44.3	45.0	50.0	53.3	54.2
Aromatic Content (Mass %)	40.7	26.1	50.0	34.7	46.2	37.0	43.5	21.1	22.2
90% Distillation Temperature (°F)	639	517	518	582	513	610	648	646	528
Specific Gravity	0.8355	0.8084	0.8401	0.8496	0.8375	0.8465	0.8682	0.8411	0.8086
HC Ratio	1.819	1.956	1.749	1.796	1.773	1.788	1.704	1.871	1.967
Net Heat of Combustion (BTU/LB)	18269	18402	18120	18425	18211	18257	18141	18399	18443

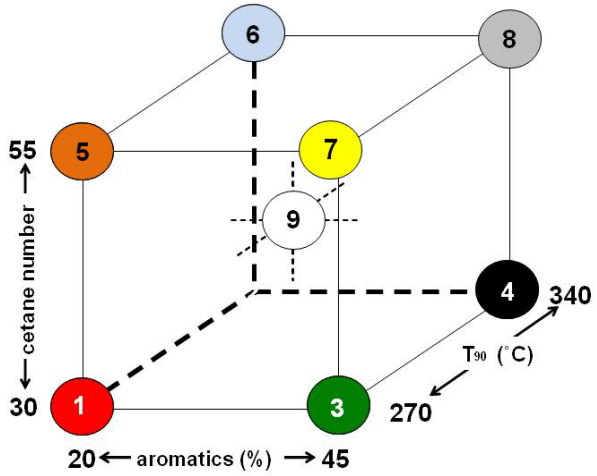

Figure 17: FACE Diesel Fuels Design Matrix

3.3 Test Engine

The AVFL-16 study initially used a General Motors (GM) Z19DT (eight valve cylinder head) engine. This engine was purchased by WVU and featured two valves per cylinder, cooled EGR and a variable geometry turbocharger (VGT). After some initial testing, it was replaced with a GM Z19DTH engine (obtained from WVU's Department of Energy sponsored Challenge X program), which employs essentially the same architecture, except the Z19DTH has four valves per cylinder and swirl control valves. These valves control air flow in the second intake runner for each cylinder. The inherently better mixing and flow characteristics of the Z19DTH engine 16 valve cylinder head made it a more suitable platform for advanced combustion research.

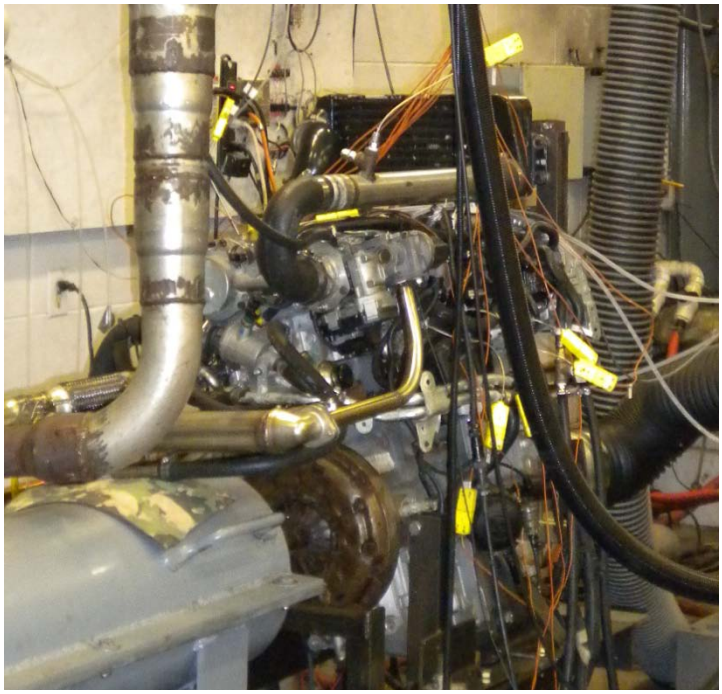

Figure 18: GM Z19DTH Test Engine

During the research, both engines were instrumented with thermocouples measuring engine lubricant, coolant, intake manifold, and exhaust manifold temperatures. Pressure transducers measured inlet depression, exhaust backpressure and intake manifold pressure. The advanced combustion research performed on both engines utilized EGR rates that were higher than those of the original equipment manufacturer (OEM). As a result, larger EGR coolers were fitted to both engines to reduce elevated intake manifold temperatures. For the final testing of the FACE diesel fuels, the Z19DTH engine utilized an EGR cooler from a 2003 Ford 6.0 L Powerstroke engine which was rebuilt by Bullet Proof Diesel (BPD). Table 3 shows specifications of this test engine used by WVU. No internal engine modifications were implemented during the study.

Table 3: Test Engine Specifications

Type	CDTi Diesel Engine
Manufacturer	General Motors
Model	Z19DTH
Valve Configuration	4 Valves per Cylinder
Year	2005
Configuration	In-line 4 Cylinder
Displacement	1.9 L
Bore	82 mm
Stroke	90.4 mm
Compression Ratio	17.5:1
Injection System	Common Rail
EGR	Cooled, External
Rated Power	110 kW

3.4 In-Cylinder Pressure Measurement

To determine the in-cylinder pressure during engine operation, a single Kistler 6058A1 piezoelectric crystal pressure sensor (Figure 19) was installed into cylinder number three (oriented from the front of the engine). The sensor was adapted into the engine cylinder head via a custom glow plug adapter that replaced the stock glow plug, as seen in Figure 20. Due to the accumulation of carbon on the pressure sensor, cleaning was crucial in obtaining accurate combustion data. Cleaning was periodically performed on the sensor with a special solvent, while the adapter was cleaned with traditional oven cleaner. Each end of the sensor wire, which connects to the charge amplifier, was also cleaned with special solvent to remove any accumulation of oil and surface debris.

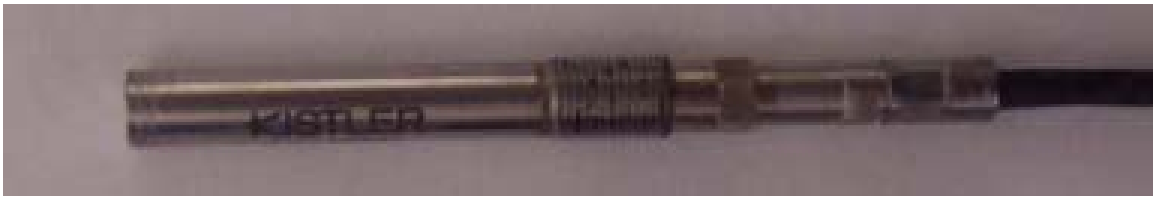

Figure 19: Kistler Pressure Sensor

Figure 20: Pressure Sensor Glow Plug Adapter

A custom analysis software and data acquisition system, developed by Dr. John Nuszkowski of West Virginia University, was used for the combustion analysis. The custom software allowed plots of pressure, temperature, heat release rates (HRR) and, mass fraction burned (MFB) to be generated and accessed on-line in real-time during testing to verify engine operation and/or misfiring events. Numerous derived and calculated combustion characteristics such as the

maximum pressure, pressure rise rates, start of combustion, end of combustion, maximum temperature, etc. were also available in real-time during testing. Figure 21 depicts a real-time screenshot captured during a testing event.

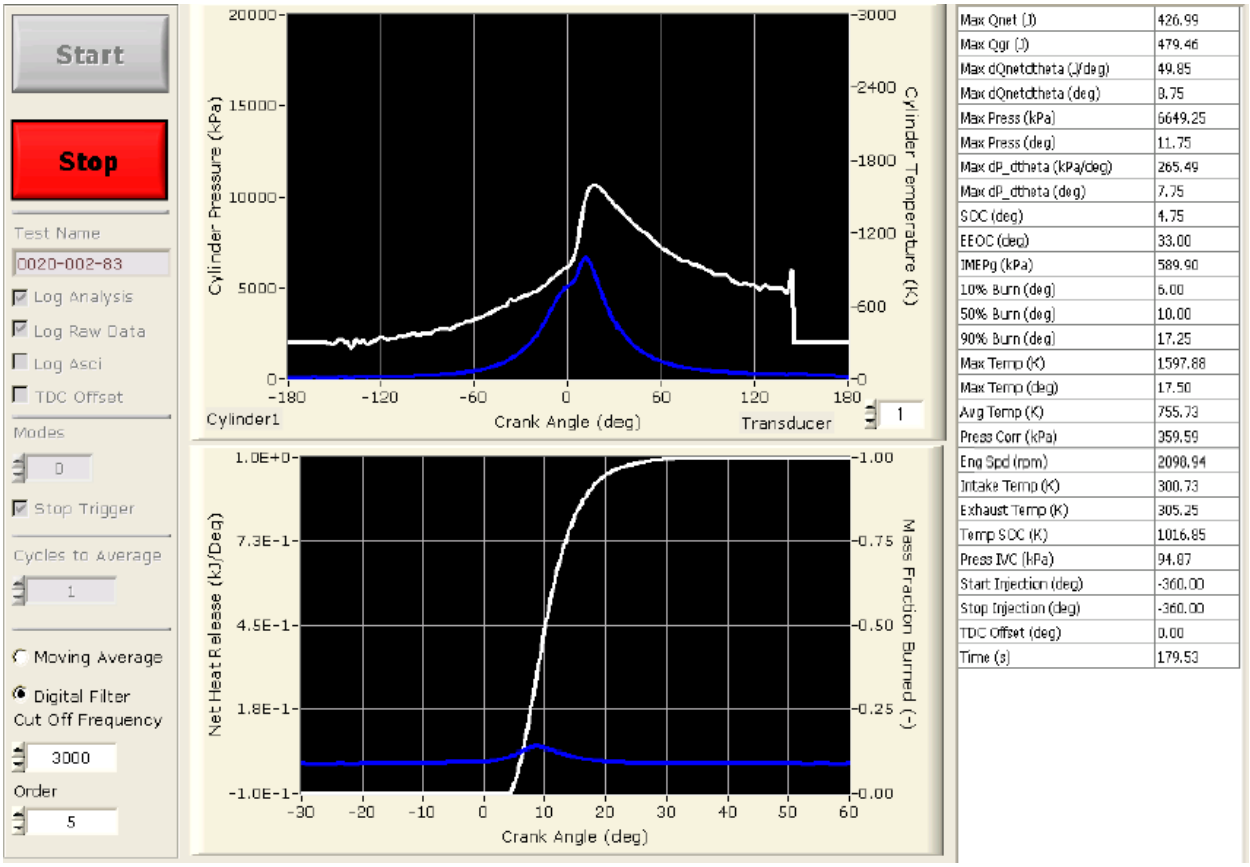

Figure 21: In-Cylinder Combustion Software

3.5 Measured and Calculated Combustion Parameters

Most of the combustion parameters were calculated using in-cylinder pressure measurements via pressure sensors. However, intake temperature, exhaust temperature and engine speed were recorded as separate parameters. Intake and exhaust temperature were recorded from K-type thermocouples, installed in the intake and exhaust manifold, respectively, of the engine, while engine speed was measured via a BEI shaft encoder connected to the engine crank via a helical coupling.

3.5.1 In-Cylinder Pressure

As mentioned in Section 3.4, the in-cylinder pressure was obtained from a piezoelectric crystal pressure sensor signal which was then converted to a voltage by a charge amplifier. Through this direct measurement, both the magnitude and the location of the maximum in-cylinder pressure were calculated. These parameters were useful for identifying potential engine integrity issues associated with high pressures. The dynamic pressure signal from each sensor was referenced by assuming a constant polytropic coefficient to give an absolute pressure measurement [25]. A low-pass filter with a cut-off frequency of 3000Hz was applied to the in-cylinder pressure signal to reduce the high frequency combustion noise. The low-pass filter

employed an averaging algorithm to reduce noise; this unfortunately caused a reduction in combustion spikes. It was assumed that since this averaging was applied to all data equally, the relative differences between fuels should not be impacted significantly.

3.5.2 Heat Release Rate (HRR)

HRR is an important tool for interpreting engine performance and emissions data. For example, higher HRR is generally associated with higher NO_X emissions [26]. The heat release rate in the combustion chamber is a well-known and highly utilized method for analyzing combustion characteristics. Utilizing the first law of thermodynamics and assuming a uniform pressure, uniform temperature, and ideal gas with the substitution of the specific heat ratio (γ) and the substitution of crank angle for time reduces to an expression for the gross heat release rate (Equation 1). A relationship for the heat transfer to the walls is required when using the gross heat release rate. The Woschni equation was used for this study [27].

$$\left[\frac{dQ}{d\theta}\right]_{gross} = \left(\frac{\gamma}{\gamma-1}\right) * P * \frac{dV}{d\theta} + \left(\frac{1}{\gamma-1}\right) * V * \frac{dP}{d\theta} + \left[\frac{dQ}{d\theta}\right]_{ht} \quad \textbf{(1)}$$

Where Q is the heat transfer, θ is the crank angle, "gross" indicates the overall heat transfer in the cylinder, γ is the ratio of specific heats, P is the pressure, V is the volume, and "ht" indicates the heat loss to the cylinder walls. From the heat release data, parameters such as maximum HRR, location of maximum HRR, net heat released during combustion, gross heat released during combustion and fuel flow can be determined. Equations 2 and 3 show the calculation for determining net and gross heat released during combustion from the start of combustion (SOC) to the estimated end of combustion (EOC).

$$Q_{net} = \sum_{SOC}^{EOC} dQ_{net} \quad \textbf{(2)}$$

$$Q_{gross} = \sum_{SOC}^{EOC} dQ_{gross} \quad \textbf{(3)}$$

Because of cycle-to-cycle combustion variation, multiple steady state cycles are normally collected after the engine has reached thermal equilibrium to provide for an average cylinder pressure trace before the heat release analysis is performed. For this study, 2000 in-cylinder pressure cycles were averaged. The calculated heat release rate showed a small heat release peak after the main combustion event due to the high frequency combustion noise caused during rapid combustion for the Z19DTH engine. This event is apparent, in Figure 26, at 15° ATDC and 20° ATDC for the 6.0 L EGR cooler and at 10° and 15° ATDC for the 11.0 L EGR cooler. Reduction of the cut-off frequency for the low pass filter would reduce this combustion noise, but at the expense of reducing combustion spikes.

3.6 Control of Engine Operating Parameters

The ability to control engine operating parameters is crucial for obtaining advanced combustion. Accessing the engine's engine control unit (ECU) allows for full control of operating parameters such as SOI timing, number of fuel injection events, fuel injection duration, rail pressure, EGR rate, VGT rack position, etc. To access such operating parameters, WVU purchased an open engine controller based on National Instrument hardware developed by Drivven, Inc. (Figure 22).

Figure 22: Open Engine Controller Purchased from Drivven, Inc

The Drivven engine controller was pre-programmed with baseline operating parameters relative to the test engine as purchased by WVU. A portion of these baseline operating parameters relative to fuel injection is shown in the lookup table (torque map is displayed) in the center of Figure 23. This particular tab of the Drivven engine controller interface allows the user to modify SOI timing, fuel split, injection duration, and many other fuel injection parameters. Other interfaces listed at the top of Figure 23 allow the modification of EGR rate, VGT rack position, fuel rail pressure, and offer full control of other engine systems and sensors.

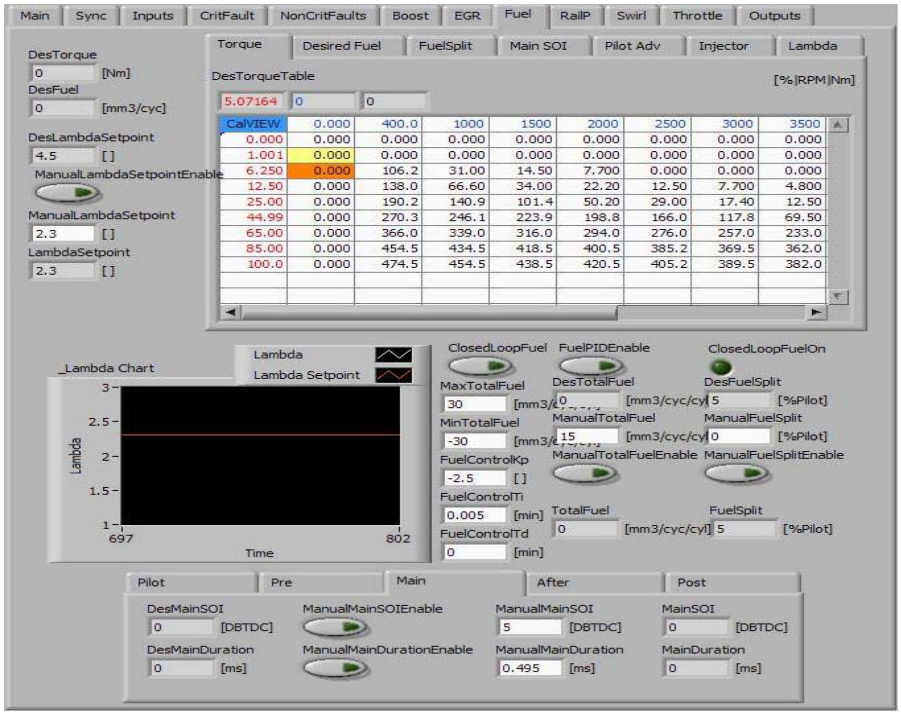

Figure 23: Drivven Engine Controller Fuel Injection Interface

3.7 Emissions Measurement

3.7.1 Gaseous Emissions Measurement

Gaseous emissions measured and recorded during the AVFL-16 study included total HC, NO_X, oxygen (O_2), CO and carbon dioxide (CO_2). Gaseous emissions measurements were performed on the diluted exhaust gases in the CVS system, raw exhaust gases, and gases in the intake manifold by several separate analyzers.

3.7.1.1 Horiba MEXA-7200D

Dilute exhaust emissions sampled from WVU's CVS system were analyzed by a Horiba MEXA-7200D. The MEXA-7200D contains several gaseous analyzers and accompanying equipment necessary to perform gaseous emissions measurements, analyzer calibrations and verifications. Gaseous analyzers contained in the MEXA-7200D used for this study include a flame ionization detector (FID) used to measure HC emissions, a chemiluminescence detector (CLD) used to measure NO_X emissions, and two non-dispersive infrared (NDIR) analyzers used to measure CO and CO_2 emissions.

3.7.1.2 Horiba MEXA 720 ZrO2

Intake manifold and raw exhaust gas oxygen concentrations were measured by Horiba MEXA-720 analyzers. The MEXA-720 employs a heated zirconium oxide sensor to provide O_2 concentrations. This study relied heavily on the intake oxygen concentration measurement as one of the primary controlled operating variables. Additionally, raw exhaust oxygen concentration was used in conjunction with intake oxygen concentration to calculate EGR fraction.

3.7.2 AVL MS 483 Soot Measurement

Soot concentrations of raw exhaust gases were measured with the use of an AVL 483 Micro Soot Sensor. The AVL 483 employs a photo-acoustic method to measure and quantify soot concentration. To ensure that the measurement chamber did not become contaminated, the micro soot sensor was zeroed with dilution air between measurements, and the measurement chamber was periodically cleaned.

3.8 Laboratory and Dynamometer Control

For the AVFL-16 study, the GM Z19DTH engine was coupled to an AC dynamometer operated in speed mode. Torque was controlled autonomously by a proportional–integral–derivative throttle controller integrated into WVU's data acquisition (DAQ) system. WVU's DAQ system is based around National Instruments hardware using software written by WVU CAFEE employees. The DAQ system operates based on Title 40 CFR Part 1065.

4 Results

The results are presented in four sections. The first section, 4.1, details the selection of the engine and the EGR cooler. Section 4.2 presents results from a repeatability study that offer a standard by which emissions and performance changes among the fuels could be attributed to fuel property differences and not to the variability associated with the equipment or control strategy. Sections 4.3 and 4.4 present results from the split injection control strategy and single injection control strategy, respectively. Within these sections, subsections detailing "optimal tests," "comparable tests," and "emissions and fuel property trends" exist. The "optimal tests" enable comparisons between fuels without the restriction of using the same fuel injection settings since each fuel may have higher brake thermal efficiency (BTE), lower NO_X and/or lower PM at different injection settings. Alternative optimal tests whose selection criteria are within +/- 0.5% of the optimal value have also been identified. These alternative tests are provided to demonstrate to the reader that the method of optimal tests selection can alter the differences observed when comparing the fuels. The "comparable tests" allows comparisons between fuels at identical fuel injection settings. The "emissions and fuel property trends" subsection provides scatter plots containing data from the "optimal tests" and "comparable tests." These plots allow for a more global overview of the emissions and performance characteristics exhibited by each fuel. By considering the results of all three methods of comparison, conclusions based upon fuel properties can be obtained with confidence.

4.1 Engine Test Platform Selection

During the AVFL-16 study, initial experiments were performed using two different engines, as well as three differently sized EGR coolers. The following sections compare and contrast the hardware and provide reasoning for the final engine and EGR cooler selection.

4.1.1 Z19DT (8 Valve) vs. Z19DTH (16 Valve) Comparison

In an effort to determine whether the Z19DT or Z19DTH engine produced the lowest emissions and highest BTE operating in advanced combustion regimes, the following tests were performed at 2100 RPM, targeting 3.5 bar BMEP with ULSD (CPChem 2007 Cert ULSD). Both engines were operated with the Drivven engine controller. A split injection strategy was implemented for all tests. The in-cylinder pressure and accompanying calculations were obtained from cylinder 3 (oriented from the front of the engine).

The fuel injection settings and engine operating conditions presented in Table 4 reveal that the tests selected for comparison were not identical, but they were sufficiently similar to establish a relative comparison. It should be noted that the higher rail pressure used during the 16-valve engine tests could lead to lower soot emissions. Additionally, the lower intake oxygen concentration used for the 16-valve engine tests leads to lower NO_X emissions at the expense of HC, CO, and soot emissions. Regardless of these differences in operating conditions, it is evident from results provided in Table 5 that the Z19DTH engine is capable of producing similar, if not lower emissions (with the exception of CO for this comparison) while operating at a significantly higher BTE than the Z19DT engine. It was inferred from Figure 24 and the lower emissions results that the Z19DTH engine had better mixing characteristics than the Z19DT engine. The lower heat release in the first peak (before TDC) exhibited by the Z19DTH engine displayed in Figure 24 suggests that a more homogenous air and fuel mixture is present

after the pilot injection and thus resists combustion at lower in-cylinder temperatures. The more pronounced heat release rate peak after TDC (i.e., main combustion event) exhibited by the Z19DTH engine also suggests the presence of a more homogenous air and fuel mixture and thus faster flame propagation, leading to a sharper and more pronounced heat release rate curve once a significant ignition temperature is reached.

Table 4: Operating Conditions and Injection Parameters for Engine Comparison

Test ID	Engine	BMEP (bar)	Main SOI (° BTDC)	Pilot SOI (° BTDC)	Fuel Split (% Pilot)	Rail Pressure (bar)
8V-1	Z19DT (8 Valve)	3.49	0	40	40	1200
8V-2		3.26	0	40	50	1200
8V-3		3.32	0	50	40	1200
8V-4		3.70	0	50	50	1200
16V-1	Z19DTH (16 Valve)	3.46	0	40	35	1600
16V-2		3.46	0	40	40	1599
16V-3		3.53	0	45	35	1600
16V-4		3.45	0	45	40	1600

Table 5: Intake Oxygen Concentration, Brake Specific Emissions and Thermal Efficiency for Engine Comparison

Test ID	Intake O_2 (%)	HC (g/kW-hr)	NO_x (g/kW-hr)	CO (g/kW-hr)	Soot (mg/kW-hr)	BTE (%)
8V-1	16.7	5.17	0.837	20.3	59.5	27.1
8V-2	17.0	4.66	1.737	13.3	69.7	25.0
8V-3	17.0	6.08	0.995	21.2	51.9	24.6
8V-4	15.7	6.14	0.490	12.5	99.6	26.4
16V-1	16.0	4.50	0.332	22.0	62.1	29.7
16V-2	16.0	4.73	0.362	19.5	98.7	29.4
16V-3	16.0	5.41	0.315	25.2	30.4	29.8
16V-4	16.1	5.49	0.330	23.9	47.1	29.7

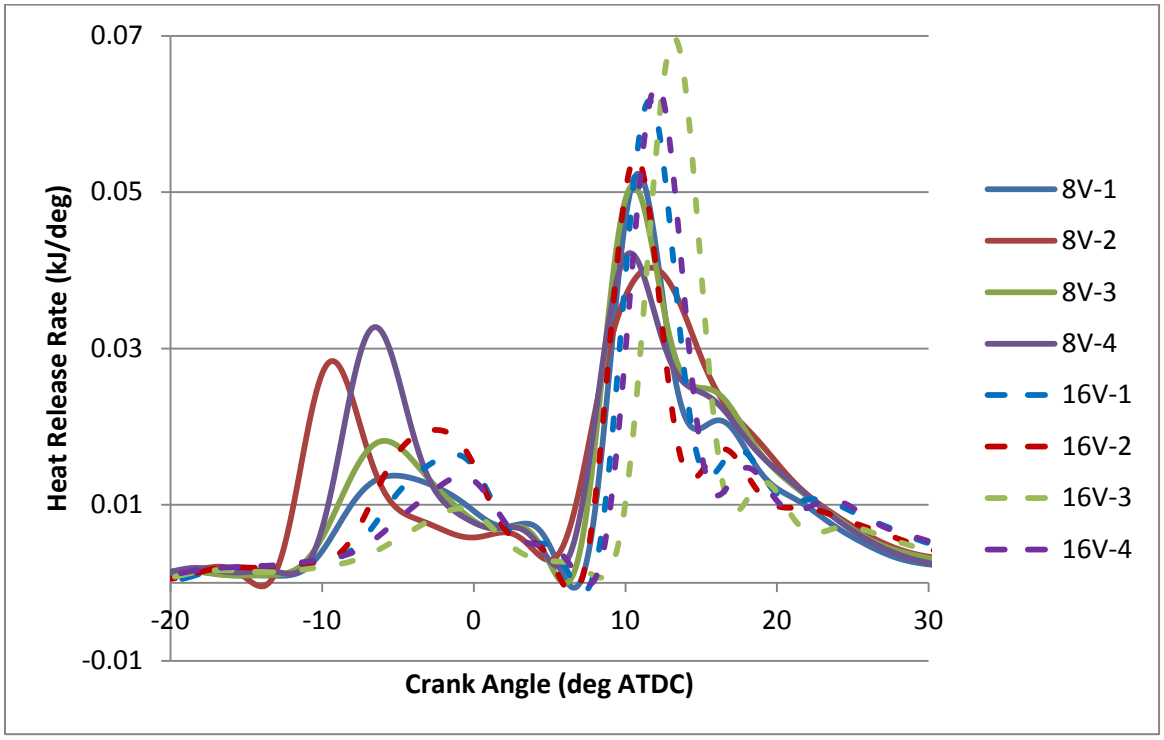

Figure 24: Calculated Heat Release Rate for Engine Comparison

4.1.2 EGR Cooler

Due to concerns regarding intake manifold temperatures associated with the use of an oversized EGR cooler (sourced from a Mack 11.0 L MP7 heavy-duty diesel (HDD) engine), WVU purchased and installed an EGR cooler sourced from a Ford 6.0 L Powerstroke engine. This specific cooler was rebuilt by Bullet Proof Diesel to minimize wear during testing that could cause leaking of engine coolant into the exhaust system. Data presented below were obtained during tests performed at 2100 RPM, targeting 3.5 bar BMEP with the FACE 4 and FACE 5 fuels. FACE 4 was chosen based on its low CN, high aromatic content and high T90, while FACE 5 was chosen base on its high CN, low aromatic content and low T90 in an effort to obtain results from both ends of the fuel properties spectrum.

4.1.2.1 FACE 4

Results presented within this section were performed with the FACE 4 (low CN) fuel using the OEM 1.9 L EGR cooler as well as the Bullet Proof Diesel Ford 6.0 L Powerstroke EGR cooler. The in-cylinder pressure and accompanying calculations were obtained from cylinder 3(oriented from the front of the engine). Split and single injection strategies were tested. Operating conditions and injection parameters for each of these strategies are provided in Table 6.

Intake manifold temperatures with the use of FACE 4 and the 6.0 L EGR cooler were over 10°C cooler when compared to the original OEM 1.9 L EGR cooler as displayed by Table 7. This resulted in lower NO_X and soot emissions at the expense of increased HC and CO emissions as well as lower BTE as demonstrated in Table 8. Higher intake manifold temperatures created by the use of the 1.9 L EGR cooler provided more stable combustion and allowed for a larger operating range (without misfire) in terms of fuel injection settings.

Focusing on the heat release data presented in Figure 25, the 6.0 L EGR cooler resulted in retarded combustion phasing, while the 1.9 L EGR cooler exhibited sharper heat release rate peaks and slightly shorter combustion duration with the use of a low CN fuel (FACE 4).

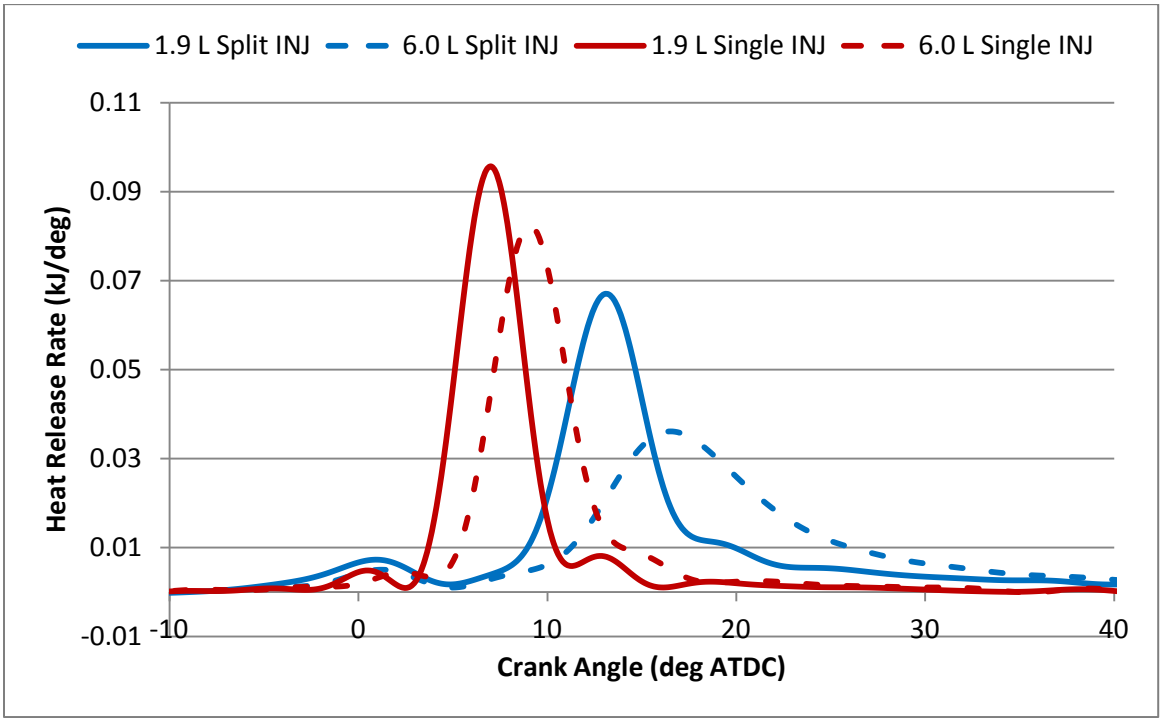

Figure 25: Calculated Heat Release Rate for EGR Cooler Comparison with FACE 4

Table 6: Operating Conditions & Injection Parameters for EGR Cooler Comparison with FACE 4

Description	BMEP (bar)	Main SOI (° BTDC)	Pilot SOI (° BTDC)	Fuel Split (% Pilot)	Rail Pressure (bar)
1.9 L Split INJ	3.61	2	40.0	30	1399
6.0 L Split INJ	3.48	2	40.0	30	1400
1.9 L Single INJ	3.49	26	N/A	N/A	1400
6.0 L Single INJ	3.50	26	N/A	N/A	1400

Table 7: Engine Operating Conditions for EGR Cooler Comparison with FACE 4

Description	Intake Manifold Temperature (°C)	Exhaust Manifold Temperature (°C)	Maximum Pressure Rise Rate (bar/deg)	CA50 (deg)
1.9 L Split INJ	100.1	364	3.07	13.75
6.0 L Split INJ	89.4	368	1.66	18.75
1.9 L Single INJ	109.9	334	7.34	7.25
6.0 L Single INJ	96.9	334	5.56	9.50

Table 8: Intake Oxygen Concentration, Brake Specific Emissions and Thermal Efficiency for EGR Cooler Comparison with FACE 4

Description	Intake O_2 (%)	HC (g/kW-hr)	NO_X (g/kW-hr)	CO (g/kW-hr)	Soot (mg/kW-hr)	BTE (%)
1.9 L Split INJ	16.1	7.17	0.403	19.6	22.10	30.4
6.0 L Split INJ	16.1	12.35	0.293	27.1	8.19	27.5
1.9 L Single INJ	13.2	3.37	0.241	8.5	1.66	32.5
6.0 L Single INJ	13.2	4.63	0.188	11.1	1.40	32.1

4.1.2.2 FACE 5

Results presented within this section were performed with the FACE 5 (high CN) fuel using the Mack 11.0 L EGR cooler**,** as well as the 6.0 L EGR cooler. The in-cylinder pressure and accompanying calculations were obtained from cylinder 3 (oriented from the front of the engine). A split and single injection strategy were each tested. Operating conditions and injection parameters for each of these strategies are provided in Table 9.

Table 10 demonstrates intake manifold temperatures significantly greater (approximately 30° C for the split injection strategy and 40° C for the single injection strategy) with the use of the 6.0 L EGR cooler and FACE 5 when compared to those of the 11.0 L EGR cooler. Use of the 11.0 L EGR cooler resulted in lower NO_X (10-26% decrease) and soot emissions with elevated but still reasonable HC emissions (25-46% increase) and CO emissions (46% increase) and comparable BTE (1.3% decrease to 2.7% increase) displayed by Table 11. A heavy penalty in terms of soot emissions (~3 times higher) is incurred with the use of the 6.0 L EGR cooler, although for the split injection strategy tests this may be in part due to lower rail pressures used for this configuration.

Figure 26 demonstrates more pronounced heat release rate peaks with less heat released during the first heat release rate peak for the split injection tests with the use of the 11.0 L EGR cooler.

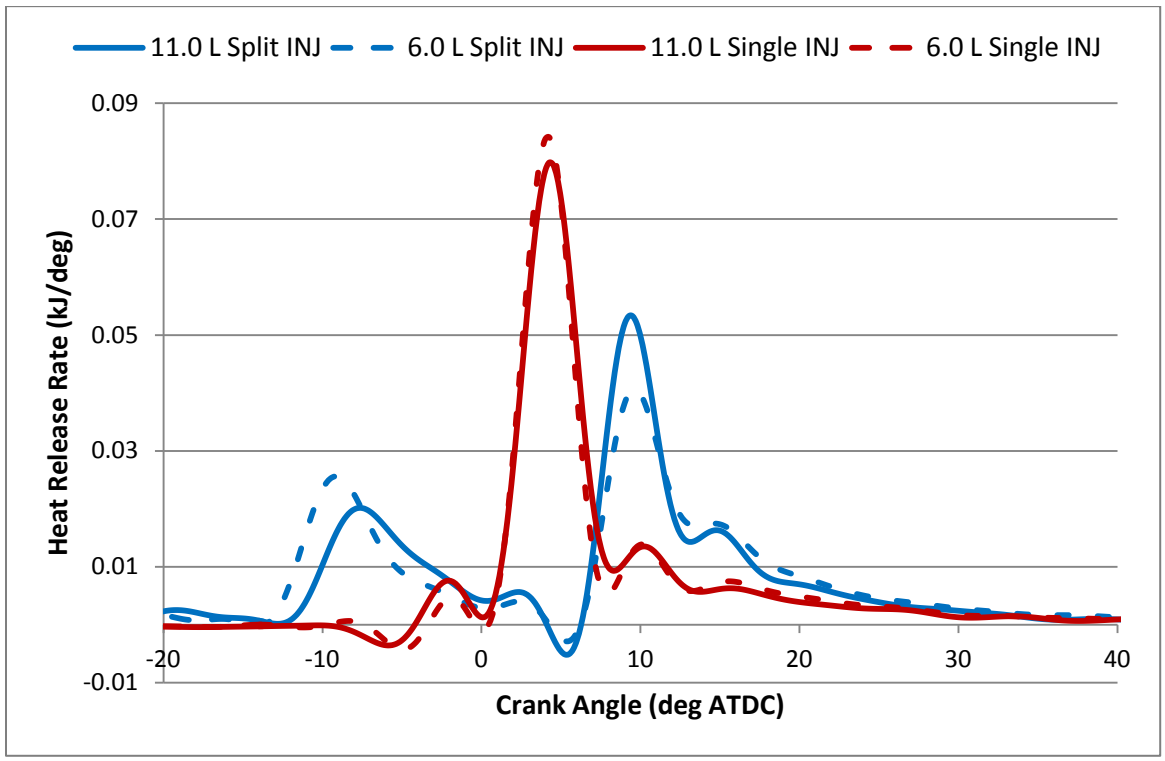

Figure 26: Calculated Heat Release Rate for EGR Cooler Comparison with FACE 5

Table 9: Operating Conditions and Injection Parameters for EGR Cooler Comparison with FACE 5

Description	BMEP (bar)	Main SOI (° BTDC)	Pilot SOI (° BTDC)	Fuel Split (% Pilot)	Rail Pressure (bar)
11.0 L Split INJ	3.36	0	40	40	1800
6.0 L Split INJ	3.48	0	40	40	1399
11.0 L Single INJ	3.59	13.2	N/A	N/A	1399
6.0 L Single INJ	3.56	11.5	N/A	N/A	1400

Table 10: Engine Operating Conditions for EGR Cooler Comparison with FACE 5

Description	Intake Manifold Temperature (°C)	Exhaust Manifold Temperature (°C)	Maximum Pressure Rise Rate (bar/deg)	CA50 (deg)
11.0 L Split INJ	60.3	317	3.70	9.50
6.0 L Split INJ	89.7	336	4.23	10.00
11.0 L Single INJ	63.7	321	7.11	5.25
6.0 L Single INJ	104.8	345	7.41	5.25

Table 11: Intake Oxygen Concentration, Brake Specific Emissions and Thermal Efficiency for EGR Cooler Comparison with FACE 5

Description	Intake O_2 (%)	HC (g/kW-hr)	NO_X (g/kW-hr)	CO (g/kW-hr)	Soot (mg/kW-hr)	BTE (%)
11.0 L Split INJ	16.0	4.05	0.430	16.82	61.5	30.0
6.0 L Split INJ	16.0	2.83	0.478	11.50	181.2	30.4
11.0 L Single INJ	13.0	1.35	0.123	10.57	37.1	34.3
6.0 L Single INJ	13.0	1.08	0.166	7.20	110.4	33.4

4.1.3 Final Engine Test Platform Selection

The GM Z19DTH engine (16-valve) was chosen for the remainder of the advanced combustion tests due to the lower emissions, higher BTE, and reduced HRR during the first heat release section compared to the GM Z19DT engine (8-valve). The EGR cooler comparisons made in section 4.1.2 presented the benefits and shortcomings of using the 6.0 L EGR cooler versus the 1.9 L or 11.0 L EGR coolers. Greater BTE and more stable combustion was achieved by the use of the 1.9 L EGR cooler for FACE 4 (low CN), while less soot and NO_X emissions were produced when the 11.0 L EGR cooler was used with FACE 5 (high CN). From initial testing (data not shown), use of the 1.9 L EGR cooler for medium and high CN fuels produced intake temperatures that were too high to provide sufficient ignition delay for the split and single fuel injection strategies. Additionally from initial testing (data not shown), employing the 11.0 L EGR cooler during combustion of low CN fuels resulted in low intake manifold temperatures that led to erratic combustion and misfire at many of the proposed split and single fuel injection settings. In an effort to reduce the influence of engine hardware when attempting to determine and compare fuel property effects, a compromise was made to use the 6.0 L EGR cooler for all fuels, noting that more desirable results could be achieved with the use of EGR coolers specifically matched to a specific fuel's properties.

4.2 Repeatability Study

4.2.1 Introduction

A study of the repeatability of test data generated from two split injection control strategies was performed with the ULSD fuel. The purpose of this effort was to develop a standard by which emissions and performance changes among the fuels could be attributed to fuel property differences and not to the variability associated with the equipment or control strategy.

The details of these tests, such as injection control parameters and engine conditions, can be found in Section 4.3 Split Injection Control Strategy. Test 5, which is described in Table 16, was selected because of the low soot production that was observed during the initial testing (see 7.3 Appendix C). Test 40, described in Table 16, was selected based on the low NO_X emissions observed during the original testing.

Each selected test was repeated three times in the morning and evening. This daily routine was repeated for three days providing data for 18 repeats of each test. From this data, the percent difference of the original test and average of the repeated tests was quantified. The standard deviation and coefficient of variation (COV) was also calculated for the repeat tests and is presented in the subsequent section. It should be noted that the original test was conducted four months prior to the 18 repeat tests and consisted of one test.

4.2.2 Discussion

Table 12 and Table 13 present the results of the repeatability study for test 5 and test 40, respectively. For both test 5 and test 40, the COV for the HC emissions, NO_X emissions, and BTE were less than 3%. The COV for the CO emissions and soot emissions were elevated from the other constituents as traditionally observed, and test 40 exhibited a higher COV for these emissions species than those of test 5. The percent difference between the original and repeated tests for both test 5 and test 40 offered a similar trend. HC emissions, NO_X emissions, and BTE all retained a percent difference of less than 1%. The percent difference for the CO emissions and soot emissions were considerably higher for both test 5 and test 40. Test 5 exhibited the worst percent difference for CO emissions at nearly 14.5%, while test 40 exhibited the worst percent difference for soot emissions at approximately 18%.

Table 12: Test 5 Repeatability

Description		HC (g/kW-hr)	NO_x (g/kW-hr)	CO (g/kW-hr)	Soot (mg/kW-hr)	BTE (%)
Original Test		2.08	0.660	10.54	55.4	31.4
Repeated Tests	Average	2.07	0.655	9.21	51.1	31.2
	Standard Deviation	0.05	0.018	0.30	2.92	0.2
	COV	2.22%	2.67%	3.28%	5.72%	0.75%
Difference – Original vs. Repeat		0.8%	0.8%	14.5%	8.5%	0.6%

Table 13: Test 40 Repeatability

Description		HC (g/kW-hr)	NO_X (g/kW-hr)	CO (g/kW-hr)	Soot (mg/kW-hr)	BTE (%)
Original Test		2.74	0.352	14.5	104.5	29.7
Repeated Tests	**Average**	2.72	0.350	13.47	88.4	29.7
	Standard Deviation	0.06	0.010	0.48	7.73	0.3
	COV	2.35%	2.81%	3.58%	8.75%	0.99%
Difference – Original vs. Repeat		0.7%	0.7%	7.4%	18.2%	0.04%

Consideration of the COV and percent differences for HC emissions, NO_X emissions, and BTE displayed in and Table 12 and Table 13 allowed for comparisons and conclusions to be made for these constituents in the subsequent sections with a relatively high level of confidence. In many instances, especially for soot emissions the measured difference between fuels is an order of magnitude. In those cases, sound conclusions can still be made despite the variability presented in this section. Based on the outcome of this repeatability study, it was determined that any difference in HC emissions or NO_X emissions greater than 4% and any difference in BTE greater than 2% could be deemed significant and thus attributed to differences in the fuels rather than variability associated with the data. Similarly for CO emissions and soot emissions, a difference greater than 18% and 27% respectively, could also be deemed significant. These criteria were developed by summing the observed COV and percent difference for each constituent. Although the repeatability criteria for CO emissions and soot emissions were significantly higher than the other constituents presented, the values were not unexpected for a modern compression ignition engine equipped with EGR and VGT and controlled with a non-OEM open engine controller while operating in an advanced combustion regime.

4.3 Split Injection Control Strategy

4.3.1 Introduction

A significant portion of the research performed during the AVFL-16 study involved the use of a split injection strategy. This strategy was selected for its characteristic ability to reduce PRR (compared to a single injection strategy) and limit soot production, especially for the higher CN fuels. The general concept, termed UNIBUS, was developed by Hasegawa et al. [12]. The UNIBUS strategy was then further refined by WVU for use with the GM Z19DTH engine platform and the fuels to be used during the AVFL-16 study. Due to the significantly different properties of fuels tested during the AVFL-16 study, fuels were divided into three CN groups for the split injection strategy as displayed in Table 1. The fuel injection parameters (namely main SOI timing and pilot SOI timing) comprising the split injection test matrices were then applied according to CN category. In subsequent tests, 50 percent mass fraction burned (CA50) was not held constant and varied among all fuels tested. A more advanced range of main SOI timing for the low CN fuels (when compared to medium and high CN fuels) was established to limit misfire at retarded main SOI timing resulting from the longer ignition delay provided by these fuels. The shorter ignition delay exhibited by the medium and higher CN fuels required that the range of main SOI timing be retarded (from that of low CN fuels) in order to achieve safe pressure rise rates and reasonable NO_X emissions (less than 1 g/kW-hr). Pilot SOI timings were also adjusted for each CN category to limit heat release before the main injection event; low CN fuels tolerated a more advanced range of pilot SOI timing, while the range of pilot SOI timing for medium and high CN fuels had to be retarded. The tests matrices for low, medium and high CN fuels can be found in Table 15, Table 16, and Table 17, respectively. Note that the SOI timing values found in these tables refer to control signal SOI timing; actual SOI timing may differ. Regardless of CN category, all tests were performed at an engine speed of 2100 RPM, targeting 3.5 bar BMEP with an intake oxygen concentration of 16% and a rail pressure of 1600 bar. These operating conditions can also be found in Table 14. The swirl control valves were fixed at the “fully open” position for all tests.

Table 14: Split Injection Control Strategy Operating Conditions

Engine Speed	2100 RPM
BMEP	3.5 bar
Intake Oxygen Concentration	16%
Rail Pressure	1600 bar
Fuel Temperature	31° C
Coolant Temperature	86° C

Table 15: Low Cetane (FACE 4, FACE 1, FACE 3) Split Injection Test Matrix

Test #	Main SOI (°BTDC)	Pilot SOI (°BTDC)	Fuel Split (%)	Test #	Main SOI (°BTDC)	Pilot SOI (°BTDC)	Fuel Split (%)
1	10	40	30	28	4	40	30
2	10	40	35	29	4	40	35
3	10	40	40	30	4	40	40
4	10	45	30	31	4	45	30
5	10	45	35	32	4	45	35
6	10	45	40	33	4	45	40
7	10	50	30	34	4	50	30
8	10	50	35	35	4	50	35
9	10	50	40	36	4	50	40
10	8	40	30	37	2	40	30
11	8	40	35	38	2	40	35
12	8	40	40	39	2	40	40
13	8	45	30	40	2	45	30
14	8	45	35	41	2	45	35
15	8	45	40	42	2	45	40
16	8	50	30	43	2	50	30
17	8	50	35	44	2	50	35
18	8	50	40	45	2	50	40
19	6	40	30				
20	6	40	35				
21	6	40	40				
22	6	45	30				
23	6	45	35				
24	6	45	40				
25	6	50	30				
26	6	50	35				
27	6	50	40				

Table 16: Medium Cetane (ULSD, FACE 7, FACE 9) Split Injection Test Matrix

Test #	Main SOI (°BTDC)	Pilot SOI (°BTDC)	Fuel Split (%)	Test #	Main SOI (°BTDC)	Pilot SOI (°BTDC)	Fuel Split (%)
1	6	35	30	28	0	35	30
2	6	35	35	29	0	35	35
3	6	35	40	30	0	35	40
4	6	40	30	31	0	40	30
5	6	40	35	32	0	40	35
6	6	40	40	33	0	40	40
7	6	45	30	34	0	45	30
8	6	45	35	35	0	45	35
9	6	45	40	36	0	45	40
10	4	35	30	37	-2	35	30
11	4	35	35	38	-2	35	35
12	4	35	40	39	-2	35	40
13	4	40	30	40	-2	40	30
14	4	40	35	41	-2	40	35
15	4	40	40	42	-2	40	40
16	4	45	30	43	-2	45	30
17	4	45	35	44	-2	45	35
18	4	45	40	45	-2	45	40
19	2	35	30				
20	2	35	35				
21	2	35	40				
22	2	40	30				
23	2	40	35				
24	2	40	40				
25	2	45	30				
26	2	45	35				
27	2	45	40				

Table 17: High Cetane (FACE 8, FACE 6, FACE 5) Split Injection Test Matrix

Test #	Main SOI (°BTDC)	Pilot SOI (°BTDC)	Fuel Split (%)	Test #	Main SOI (°BTDC)	Pilot SOI (°BTDC)	Fuel Split (%)
1	4	30	30	28	-2	30	30
2	4	30	35	29	-2	30	35
3	4	30	40	30	-2	30	40
4	4	35	30	31	-2	35	30
5	4	35	35	32	-2	35	35
6	4	35	40	33	-2	35	40
7	4	40	30	34	-2	40	30
8	4	40	35	35	-2	40	35
9	4	40	40	36	-2	40	40
10	2	30	30	37	-4	30	30
11	2	30	35	38	-4	30	35
12	2	30	40	39	-4	30	40
13	2	35	30	40	-4	35	30
14	2	35	35	41	-4	35	35
15	2	35	40	42	-4	35	40
16	2	40	30	43	-4	40	30
17	2	40	35	44	-4	40	35
18	2	40	40	45	-4	40	40
19	0	30	30				
20	0	30	35				
21	0	30	40				
22	0	35	30				
23	0	35	35				
24	0	35	40				
25	0	40	30				
26	0	40	35				
27	0	40	40				

4.3.2 Optimal Split Injection Tests

There are a number of different methods to compare the performances of the fuels. Recognizing the large number of tests performed for each fuel and accompanying data, the method used here was to select three optimal split injection tests for each fuel as one basis of comparison (note that these tests do not represent "optimized" settings or conditions based on a particular fuel but rather represent the best settings for a specific attribute [BTE, soot, NO_X] among the 45 tests conducted for each fuel). These optimum tests were determined by first identifying the ten tests with the highest BTE. From these ten tests were selected the test with the highest BTE, the test with the lowest soot emissions, and the test with the lowest NO_X emissions. Isolating and selecting from the ten tests with the highest BTE ensured that tests meeting the other optimal criteria (low soot and low NO_X emissions) were not selected without regard to BTE and ultimately combustion stability. The test numbers, main SOI timing ("Main" degrees BTDC), pilot SOI timing ("Pilot" degrees BTDC), and fuel split ("FS" percent pilot) for the selected optimal tests are displayed in Table 18. The test numbers correspond to those found in Table 15**,** Table 16, and Table 17 with regards to the CN category of each fuel.

Table 18: Optimal Split Injection Tests

Fuel	FACE4	FACE1	FACE3	ULSD	FACE7	FACE9	FACE8	FACE6	FACE5
High BTE Test	Test 10 Main 8° Pilot 40° FS 30%	Test 10 Main 8° Pilot 40° FS 30%	Test 1 Main 10° Pilot 40° FS 30%	Test 21 Main 2° Pilot 35° FS 40%	Test 1 Main 6° Pilot 35° FS 30%	Test 4 Main 6° Pilot 40° FS 30%	Test 1 Main 4° Pilot 30° FS 30%	Test 14 Main 2° Pilot 35° FS 35%	Test 11 Main 2° Pilot 30° FS 35%
Low Soot Test	Test 5 Main 10° Pilot 45° FS 35%	Test 5 Main 10° Pilot 45° FS 35%	Test 4 Main 10° Pilot 45° FS 30%	Test 14 Main 4° Pilot 40° FS 35%	Test 5 Main 6° Pilot 40° FS 35%	Test 1 Main 6° Pilot 35° FS 30%	Test 5 Main 4° Pilot 35° FS 35%	Test 8 Main 4° Pilot 40° FS 35%	Test 4 Main 4° Pilot 35° FS 30%
Low NO_X Test	Test 20 Main 6° Pilot 40° FS 35%	Test 19 Main 6° Pilot 40° FS 30%	Test 28 Main 4° Pilot 40° FS 30%	Test 29 Main 0° Pilot 35° FS 35%	Test 20 Main 2° Pilot 35° FS 35%	Test 21 Main 2° Pilot 35° FS 40%	Test 13 Main 2° Pilot 35° FS 30%	Test 16 Main 2° Pilot 40° FS 30%	Test 29 Main -2° Pilot 30° FS 35%

Although the optimal tests presented in Table 18 represent those with the maximum BTE, minimum soot emissions or minimum NO_X emissions for the given selection criteria, there were alternative tests with similar values for the given constituent that also exhibited more optimal values of the other parameters. Conditions have been identified that provide values within +/- 0.5% of the optimal value. For instance, test 14 on the FACE 6 fuel (a "High BTE Test" shown in Table 18) had a BTE within 0.5% of test 6, but test 6 produced 0.46 times the soot emissions and 1.26 times the NO_X emissions of test 14. Additionally, test 11 (the high BTE test for the FACE 5 fuel) had a BTE within 0.5% of test 15, but test 15 produced 0.91 times the NO_X emissions and 0.52 times the soot emissions of test 11. Results from these tests can be found in Appendix C. Other alternative tests could also be identified using the results of the repeatability study found in Section 4.2 (rather than values within +/- 0.5% of the optimal value). Ultimately, the identification of alternative tests serves the purpose of informing the reader that other methods of selection exist which could provide different results when comparing fuels. To simplify the comparative analyses, only the tests identified in Table 18 are discussed further.

Trends in SOI timing and fuel split were observed as a function of CN category for the three optimal conditions presented in Table 18. For all fuels, the highest BTE was achieved at either the first or second most advanced main SOI timing set point, with the exception of the ULSD. All of the low CN fuels achieved the highest BTE at the most retarded pilot SOI timing (40° BTDC) and lowest fuel split tested (30% pilot) for this CN category. Main SOI timing for the low soot test was the most advanced set point for all fuels, with the exception of the ULSD. Additionally, for the low CN fuels, all the low soot tests occurred with a pilot SOI timing of 45° BTDC, but it should be noted that soot production was minimal for all the tests with the low CN fuels. With regards to the low NO_X test, the low CN fuels and medium CN fuels all utilized the most retarded pilot SOI timing setting, 40° BTDC and 35° BTDC respectively. Trends among the high CN fuels based on the low NO_X test were not discernible. These observations indicate that further adjustment of a particular parameter could improve BTE, soot emissions, or NO_X emissions, but it is important to point out that improvement of one of these constituents would likely have a negative impact on other emissions or performance constituents. In certain situations, achievement of a more ideal measurement was constrained by other parameters. For example, advancing the main SOI timing further for certain fuels to achieve a greater BTE could increase PRR to potentially unsafe levels and produce greater NO_X emissions.

Hydrocarbon emissions produced during the optimal tests, selected for each fuel, trended primarily with CN. Figure 27 demonstrates that HC emissions are greatest for the low CN fuels (FACE 4, 1, and 3). The medium and high CN fuels both produced much lower HC emissions, with FACE 5 demonstrating the lowest overall HC emissions. Among the low CN fuels, HC production was less for fuels with lower T90 (FACE 1 and FACE 3), with no apparent aromatic content influence. This T90 and HC emissions correlation was upheld with the high CN fuels as well, where FACE 5 (lowest T90) exhibited the lowest HC emissions. Among the medium CN fuels, FACE 7 (lowest T90) produced the lowest HC measurements with the exception of the low soot test. Hosseini et al. [4] observed a similar result in which FACE 5 and 7 produced the lowest indicated specific HC emissions. Contrary to these results, other FACE studies [3, 5] have concluded that low CN fuels with higher aromatics generated greater HC and CO emissions.

CO emissions for the optimal tests also were highest for the low CN fuels (Figure 28). Measurements of CO for the low CN fuels were relatively similar, with that for FACE 4 being the highest. CO emissions for the medium CN fuels also were very similar with the exception of the low soot tests. For those fuels, the low soot tests show the greatest CO emissions for FACE 7 and the ULSD and the lowest for FACE 9. Correlations based on the three primary fuel properties (CN, aromatics and T90) are not apparent. The likely cause may be both the high variability in the CO emissions measurement (noted previously in Section 4.2) as well as differences related to the pilot SOI timing. The low soot test FACE 9 employed a pilot SOI timing of 30° BTDC, while FACE 7 and the ULSD were fixed at 35° BTDC.

Among the high CN fuels, CO emissions were greatest for FACE 6. Again correlations based on the three primary fuel properties were not apparent, but FACE 6 did use a more advanced pilot SOI timing than the other high CN fuels for each optimal test.

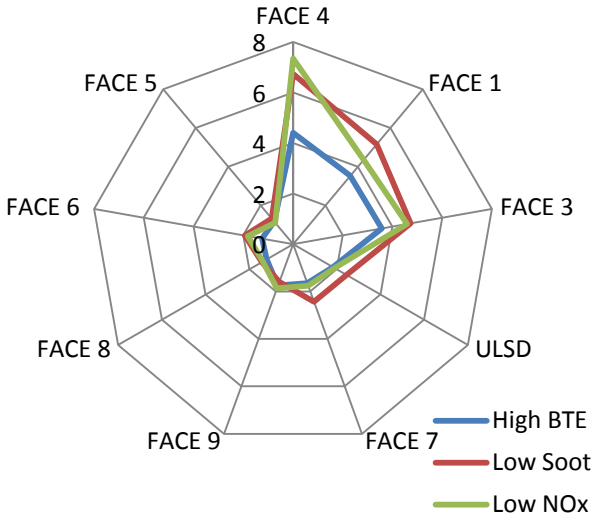

Figure 27: HC Emissions (g/kW-hr) for Optimal Split Injection Tests

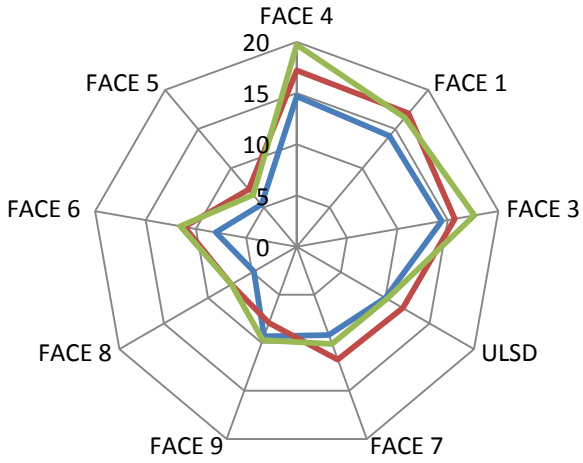

Figure 28: CO Emissions (g/kW-hr) for Optimal Split Injection Tests

For all fuels, the highest NO_X emissions were observed during the low soot tests (Figure 29), although for some fuels the same NO_X emissions values were obtained in the high BTE tests. The low CN fuels produced the highest NO_X emissions of all fuels during the low soot tests. Consideration of only the low NO_X tests demonstrates that most fuels produce very similar levels around approximately 0.5 g/kW-hr. It was observed by Cho et al. [3] and Dumitrescu et al. [6] that, among low CN fuels, fuels with lower aromatic content produced less NO_X. For the high BTE and low soot tests of the low CN fuels, NO_X emissions from FACE 1 (low aromatic content) were similar (2% greater) or up to 23% less than that of FACE 4 and FACE 3 (both high aromatic content) partially agreeing with previous findings [3, 6]. A higher NO_X measurement (13-15% increase) was observed for FACE 1 (low aromatic content) versus FACE 3 and FACE 4 (high aromatic content) for the low NO_X tests, which made this NO_X emissions-aromatic content observation not valid universally. The NO_X emissions generated using medium and high CN fuels also did not unanimously support this observation. However, FACE 9 and 8 produced the greatest NO_X emissions for their respective CN categories, and they are the only medium and high CN fuels to have simultaneously high aromatic content and T90.

Soot emissions varied widely among the fuels tested (Figure 30). FACE 8 and FACE 6 produced, by far, the most soot (1.6 to 82 times greater than the other fuels, which are much higher than the variation presented in Section 4.2); levels for the low CN fuels (especially FACE 4 and FACE 1) were below 5 mg/m^3 engine out soot concentration. Several other FACE studies [3, 5, 6] have observed similar results with FACE 8 and 6, providing a solid basis for the high CN fuels observation that T90 plays a significant role (lower T90, less soot) in soot formation. A similar soot emissions observation based on aromatic content and T90 could not be reached for the low and medium CN fuels, since even the fuel with the third highest T90 (FACE 4) produced very little soot.

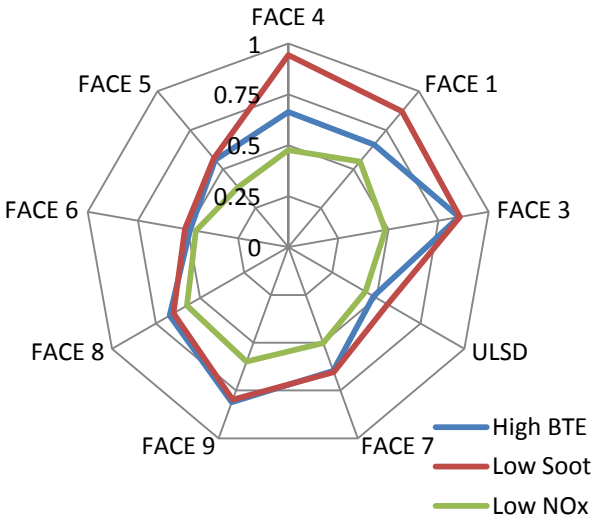

Figure 29: NO_X Emissions (g/kW-hr) for Optimal Split Injection Tests

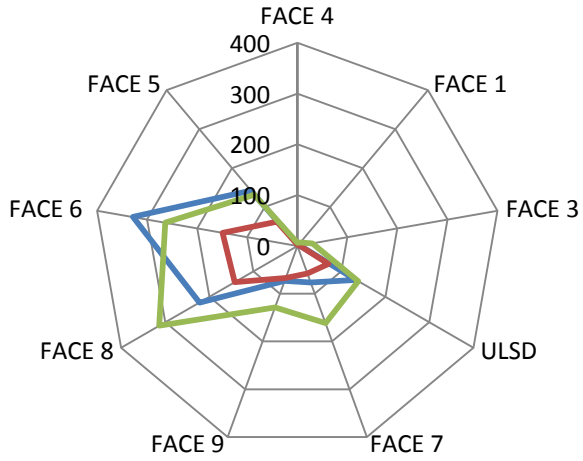

Figure 30: Soot Emissions (mg/kW-hr) for Optimal Split Injection Tests

Brake thermal efficiency was lowest for the low CN category (Figure 31). FACE 4 exhibited an especially low BTE (3-10% decrease) in comparison to all other fuels. This low BTE was a direct result of elevated HC and CO emissions, which contained a significant portion of unburned fuel energy as well as retarded combustion phasing. BTE did not prove to be dependent on CN with regards to the medium and high CN fuels; the highest BTE was observed during the combustion of FACE 9, a medium CN fuel, but not for the other two optimal cases. Furthermore, considering only the medium and high CN fuels, fuels with a higher T90 resulted in greater BTE than their lower T90 counterparts. We know of no explanation for this phenomenon based on combustion phasing.

PRR and heat release rate curve characteristics depended heavily on CN. The highest PRR were observed for the low CN fuels as a result of their increased ignition delay (Figure 32), and the lowest PRR were observed for the high CN fuels. Heat release rate curves (Figure 34, Figure 35, and Figure 36) for the low CN fuels demonstrated main heat release rate peaks with the greatest magnitudes and minimal amount of heat released prior to TDC. Higher CN fuels demonstrated more heat release prior to the main heat release event as a result of limited ignition delay. Although it is difficult to discern whether the first HRR event was more of a fuel reformation event or a combustion event, it was suspected that smaller, less rapid first HRR events were more indicative of advanced combustion (limited burning of the pilot injection) while the sharper more pronounced first HRR peaks (observed especially for high CN fuels) were indicative of combustion of the pilot injection. Among the medium and high CN fuels, a low T90 provided the highest peak PRR (during the low soot test); this is likely related to the higher volatility of these fuels and subsequent quicker vaporization causing the fuel to be more susceptible to combustion. When considering all fuels, a higher PRR did not correlate with a higher BTE (Figure 31 and Figure 32), and in many instances an inverse correlation was observed; lower PRR accompanied greater BTE.

The CA50 is presented in Figure 33. Due to the fact that main and pilot SOI timing and fuel split were not held constant for these tests, CA50 varied inconsistently among the different fuels. As expected, CA50 for the low NO_X tests was more retarded than the CA50 observed for the high BTE and low soot tests.

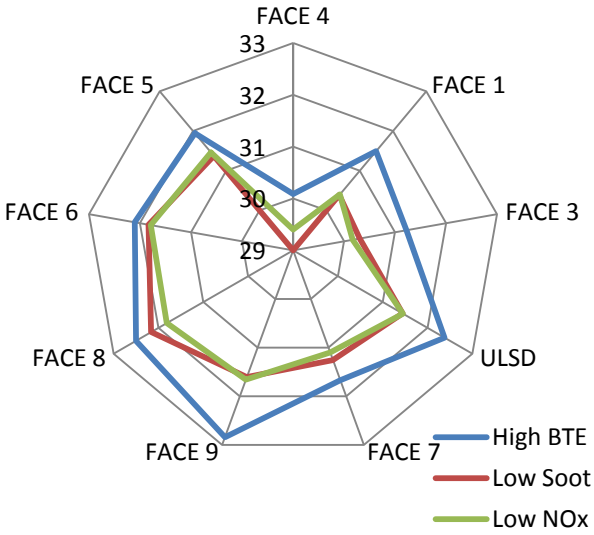

Figure 31: BTE (%) for Optimal Split Injection Tests

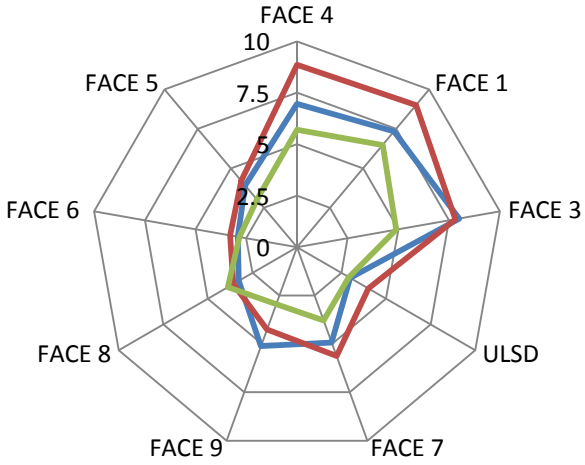

Figure 32: PRR (bar/deg) for Optimal Split Injection Tests

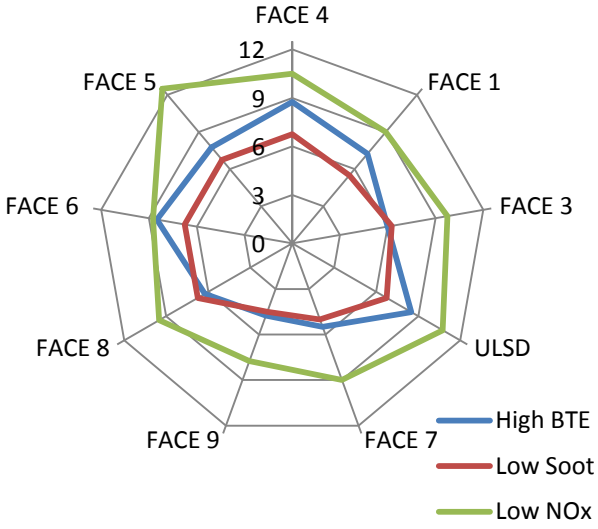

Figure 33: CA50 (deg ATDC) for Optimal Split Injection Tests

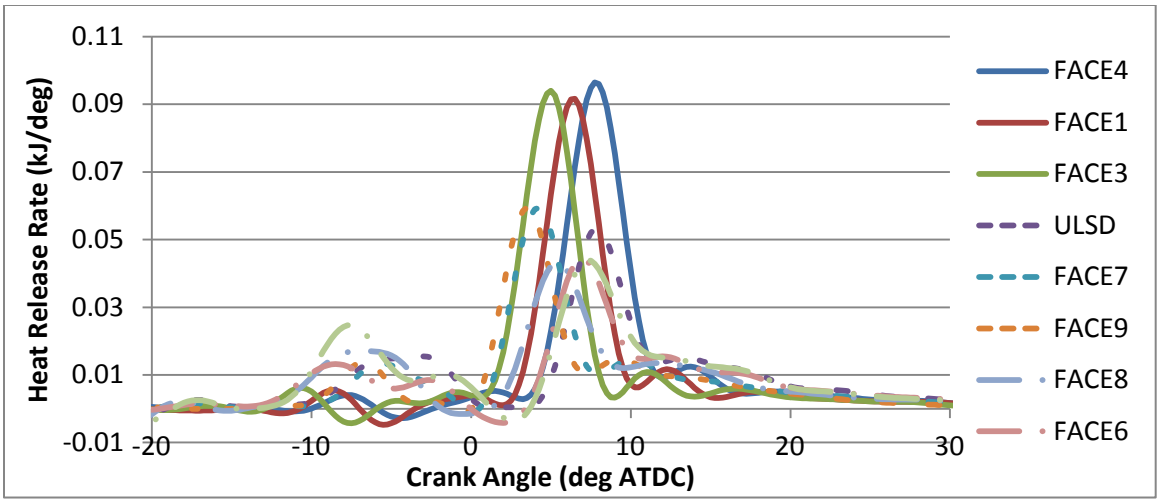

Figure 34: Calculated Heat Release Rate for Split Injection High BTE Tests

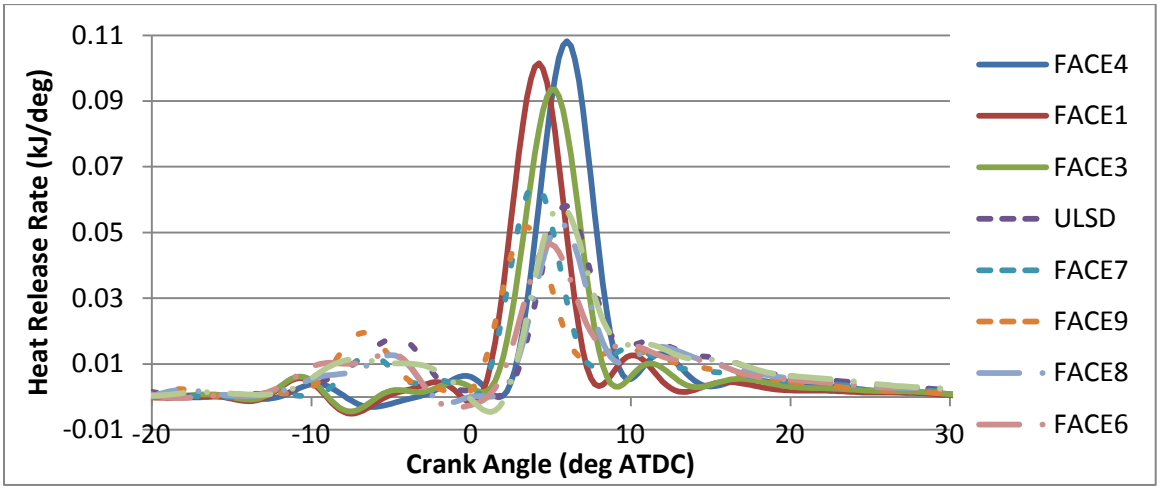

Figure 35: Calculated Heat Release Rate for Split Injection Low Soot Tests

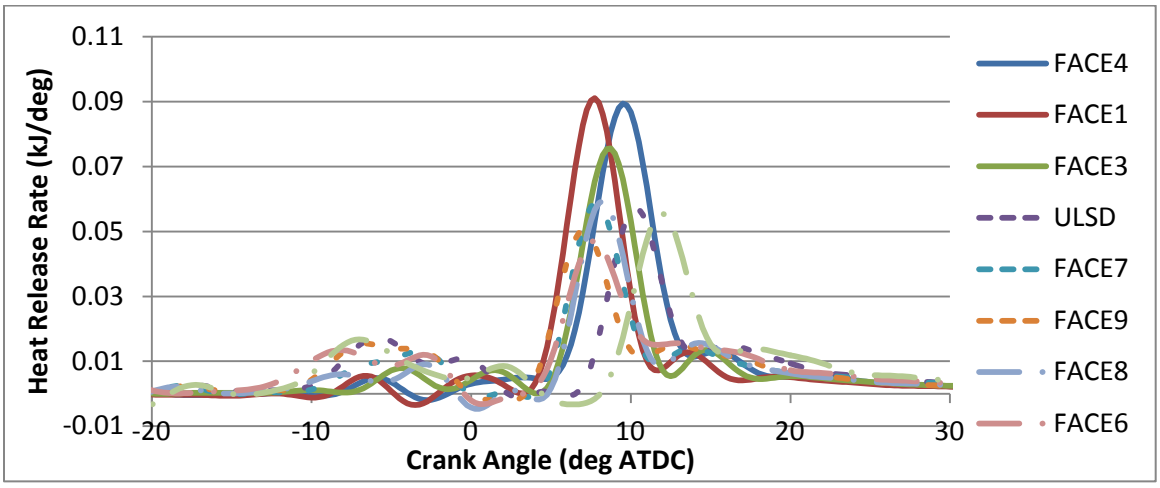

Figure 36: Calculated Heat Release Rate for Split Injection Low NO_X Tests

4.3.3 Comparable Split Injection Tests

In addition to the optimal tests selected for the split injection strategy, each fuel tested shared six tests with identical injection parameters regardless of CN category. The injection parameters for these tests include a main SOI timing of 4° BTDC, pilot SOI timing of 40° BTDC, with a fuel split of 30%, 35%, and 40%, as well as a main SOI timing of 2° BTDC, pilot SOI timing of 40° BTDC, with a fuel split of 30%, 35%, and 40%.

Similar to the optimal tests presented in the prior section, HC and CO emissions trended with CN (Figure 37, Figure 38, Figure 39, and Figure 40). Again, the low CN fuels produced the highest HC and CO emissions, especially FACE 4's HC emissions. HC and CO emission measurements for the medium and high CN fuels were generally higher in magnitude for these direct comparison tests versus the optimal tests presented in the prior section. Additionally, the effect of lower HC emissions with lower T90 for the high and medium CN fuels did not hold true for these tests, which indicates that this effect may have been due to changes in injection timing. HC emissions for FACE 7 and FACE 5 (low T90 fuels) were either on par or in many instances greater than those of other fuels within their respective CN categories. Increasing the fuel split (injecting more fuel during the pilot injection) resulted in greater HC production for all fuels (except FACE 4) and may be attributed to wall wetting or an over-mixing condition mentioned in Sections 2.2.1.1 and 2.2.1.2 respectively. Explanations of why this phenomenon was not observed for FACE 4 may be linked to the combined effect of low CN, low volatility (high T90) and subsequent ignition delay. Additionally, the heat release rate curves plotted in Figure 51 through Figure 56 reveal that injecting more fuel during the pilot injection (higher fuel split) shortened the ignition delay of the main combustion event for the low CN fuels. Increasing the fuel split for all fuels, with the exception of FACE 4, reduced the peak of the main heat release rate curve.

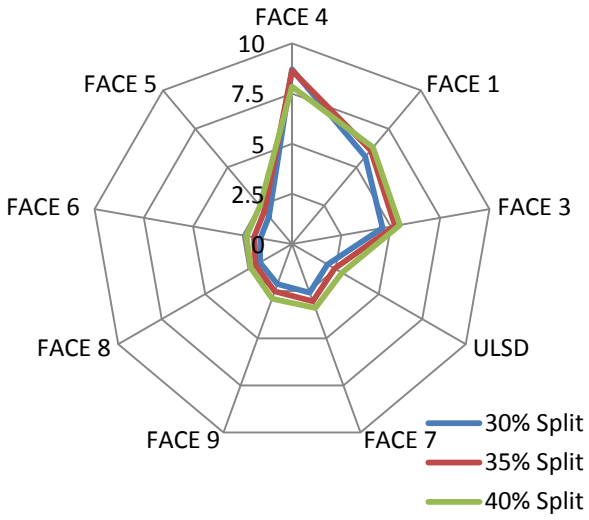

Figure 37: HC Emissions (g/kW-hr) with 4° BTDC Main SOI

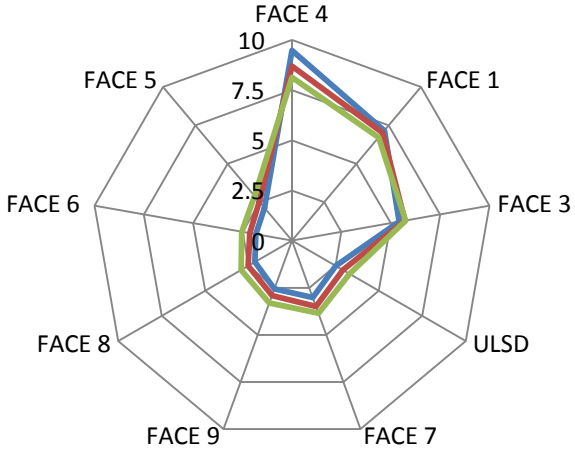

Figure 38: HC Emissions (g/kW-hr) with 2° BTDC Main SOI

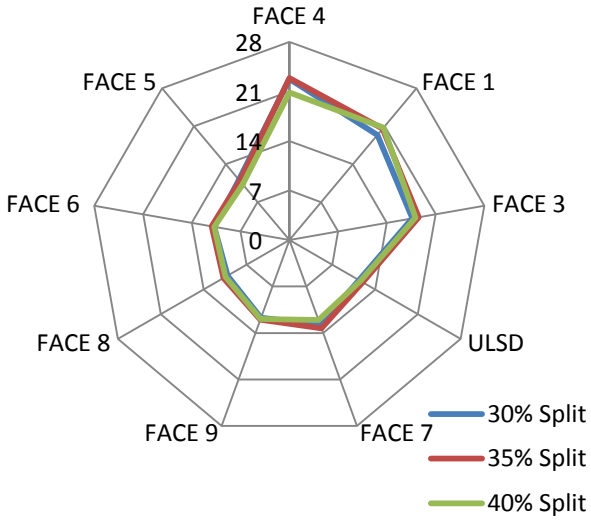

Figure 39: CO Emissions (g/kW-hr) with 4° BTDC Main SOI

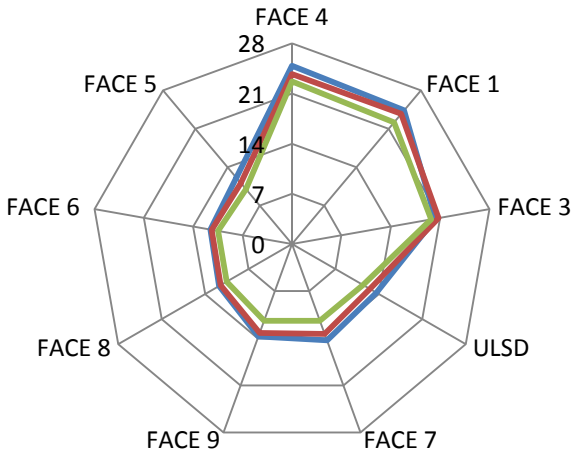

Figure 40: CO Emissions (g/kW-hr) with 2° BTDC Main SOI

NO_X emissions behaved as expected from the literature, noting a decrease in overall NO_X emissions as main SOI timing was retarded for all fuels (Figure 41 and Figure 42). Additionally, the low CN fuels emitted lower levels of NO_X than those of higher CN fuels, due primarily to retarded combustion phasing associated with the lower CN. Within their respective CN categories, FACE 9 and FACE 8 retained the highest NO_X emissions. FACE 8 had a higher aromatic content than either FACE 5 or FACE 6, and FACE 9 had a higher T90 than either FACE 7 or the ULSD. Observations regarding the individual effects of either T90 or aromatics on NO_X emissions could not be formed based on these test results. FACE 8 and FACE 9 were the only two medium and high CN fuels in the test matrix that had simultaneously high T90 and aromatic contents.

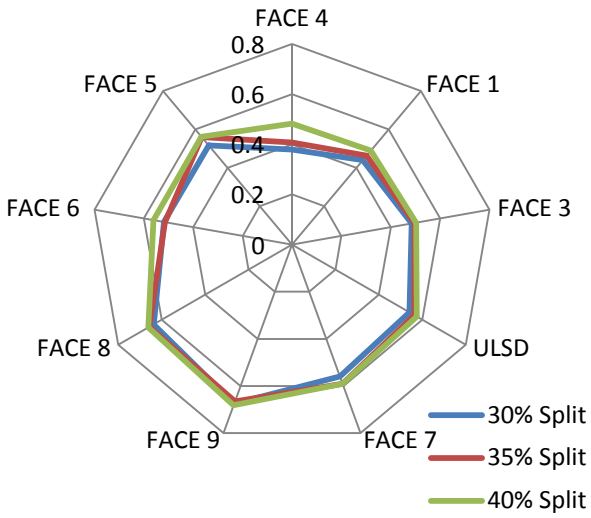

Figure 41: NO_X Emissions (g/kW-hr) with 4° BTDC Main SOI

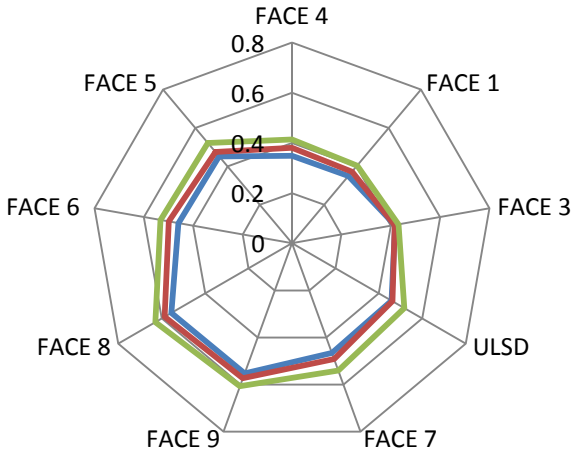

Figure 42: NO_X Emissions (g/kW-hr) with 2° BTDC Main SOI

Retarding the main SOI timing by only 2° for the medium and high CN fuels significantly increased soot emissions (Figure 43 and Figure 44). Low CN fuels produced very little soot, but soot from FACE 3 was 2-4 times greater than that of FACE 4 and FACE 1. The increase in observed soot for FACE 3 when going from a main SOI timing of 4° BTDC to 2° BTDC was likely a result of the higher CN for this fuel in comparison to that of the other low CN fuels. Among the high CN fuels, FACE 6 and FACE 8 (high T90) again produced more soot (2-3 times more) than FACE 5 (low T90). This has been observed in other FACE studies [3, 5, 6]. A similar T90 trend was not observed for the medium CN fuels. At a main SOI timing of 4° BTDC, soot emissions from FACE 7 (low T90) were comparable (±15%) to those of the ULSD and FACE 9 (higher T90), while at a main SOI timing of 2° BTDC, soot emissions from FACE 7 were 5-24% greater than the other medium CN fuels, especially for the 40% fuel split condition (although this could be partly attributed to the variance in soot emissions presented in Section 4.2 Repeatability Study). FACE 7 had the highest aromatic content of all medium CN fuels. Additionally, at the 4° BTDC main SOI and 40% split condition; FACE 8 demonstrated the highest soot emissions (1.2-2.6 times greater than the other fuels) and had the highest aromatic content among the high CN fuels.

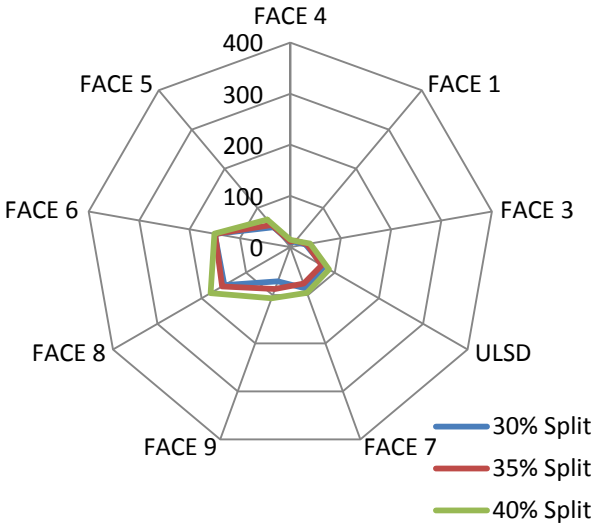

Figure 43: Soot Emissions (mg/kW-hr) with 4° BTDC Main SOI

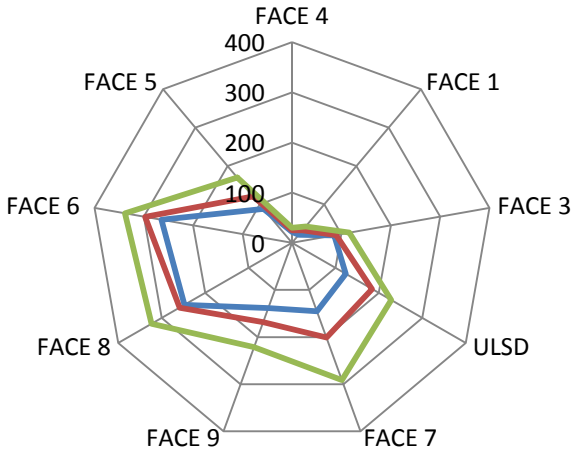

Figure 44: Soot Emissions (mg/kW-hr) with 2° BTDC Main SOI

Advancing the main SOI timing slightly improved the peak BTE for each fuel tested (Figure 45 and Figure 46). Low CN fuels demonstrated the lowest BTE, particularly FACE 4. This is explained by both lower combustion efficiency (Figure 62) and retarded combustion phasing (Figure 49 and Figure 50) that directly resulted from a main SOI timing that was too retarded for the CN of these fuels. Among the medium and high CN fuels, FACE 9 and FACE 6, respectively, retained the highest BTE at the 30% fuel split condition. This result may be attributed to a main SOI timing that was more ideal for these particular fuels compared to others in the same CN category. Longer ignition delays led to higher PRRs for the low CN fuels compared to the medium and high CN fuels for the 4° BTDC main SOI timing condition (Figure 47).

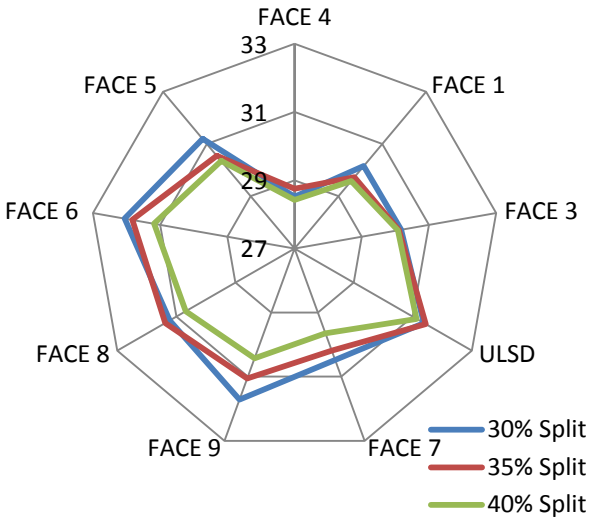

Figure 45: BTE (%) with 4° BTDC Main SOI

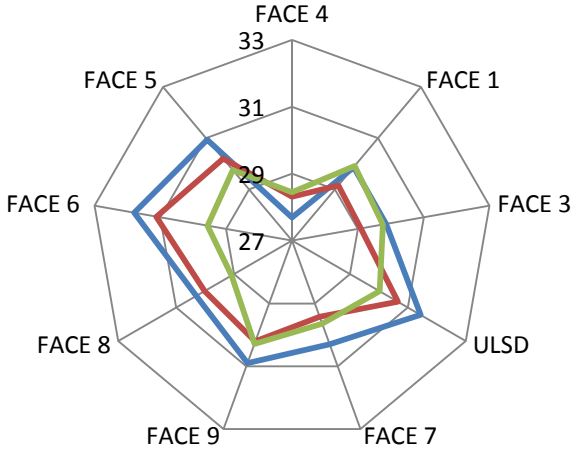

Figure 46: BTE (%) with 2° BTDC Main SOI

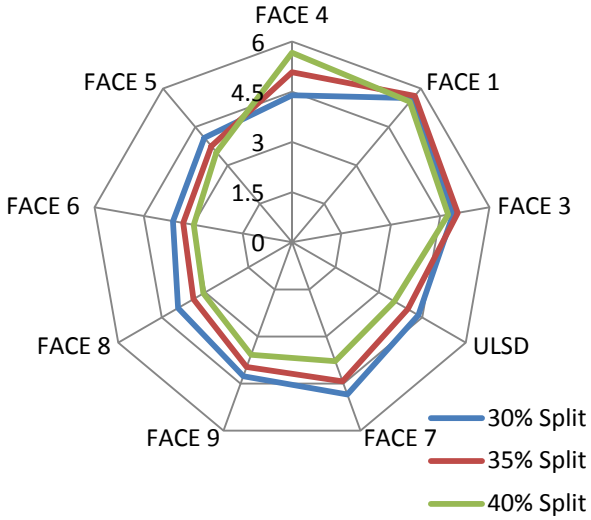

Figure 47: PRR (bar/deg) with 4° BTDC Main SOI

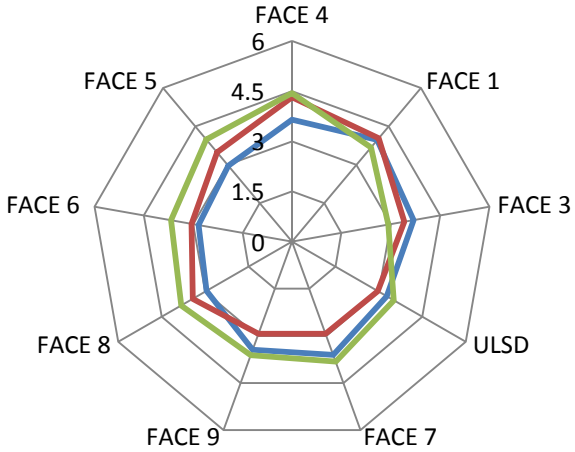

Figure 48: PRR (bar/deg) with 2° BTDC Main SOI

Combustion phasing as represented by CA50 is presented in Figure 49 and Figure 50 for the comparable split injection tests. For both Main SOI timing conditions presented, a higher fuel split resulted in more advanced combustion phasing. This was a direct result of greater HRR before the main HRR event evidenced by Figure 51 through Figure 56.

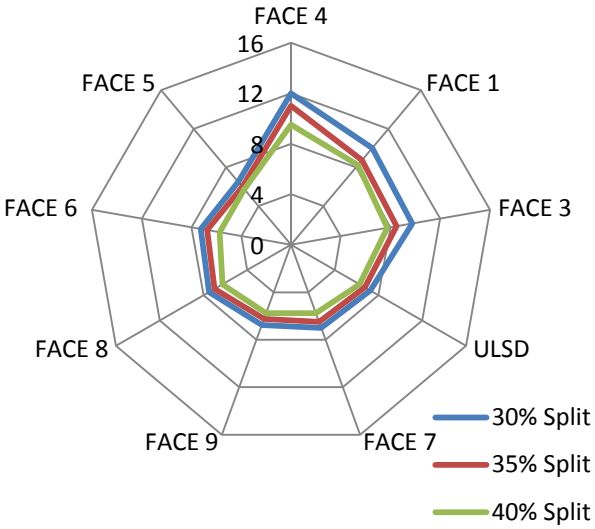

Figure 49: CA50 (deg ATDC) with 4° BTDC Main SOI

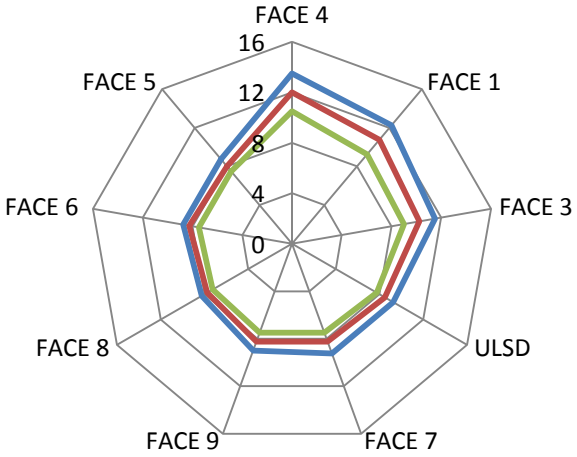

Figure 50: CA50 (deg ATDC) with 2° BTDC Main SOI

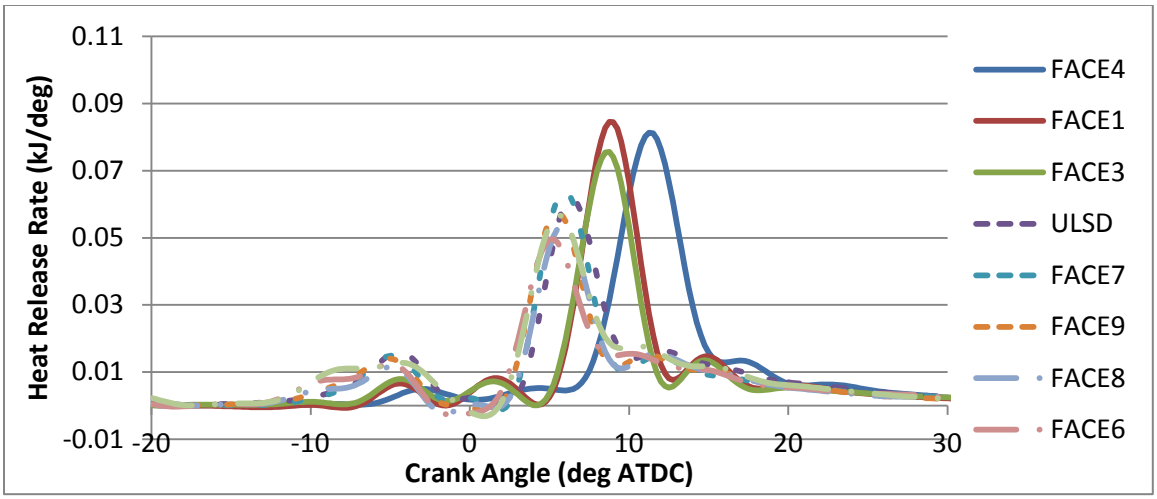

Figure 51: Calculated Heat Release Rate for 4° BTDC Main 40° BTDC Pilot 30% Split

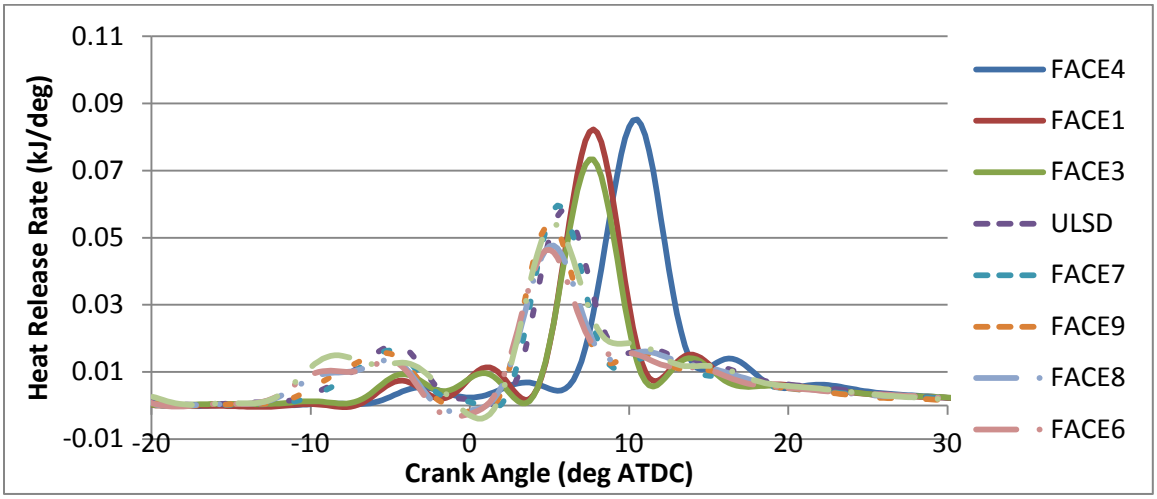

Figure 52: Calculated Heat Release Rate for 4° BTDC Main 40° BTDC Pilot 35% Split

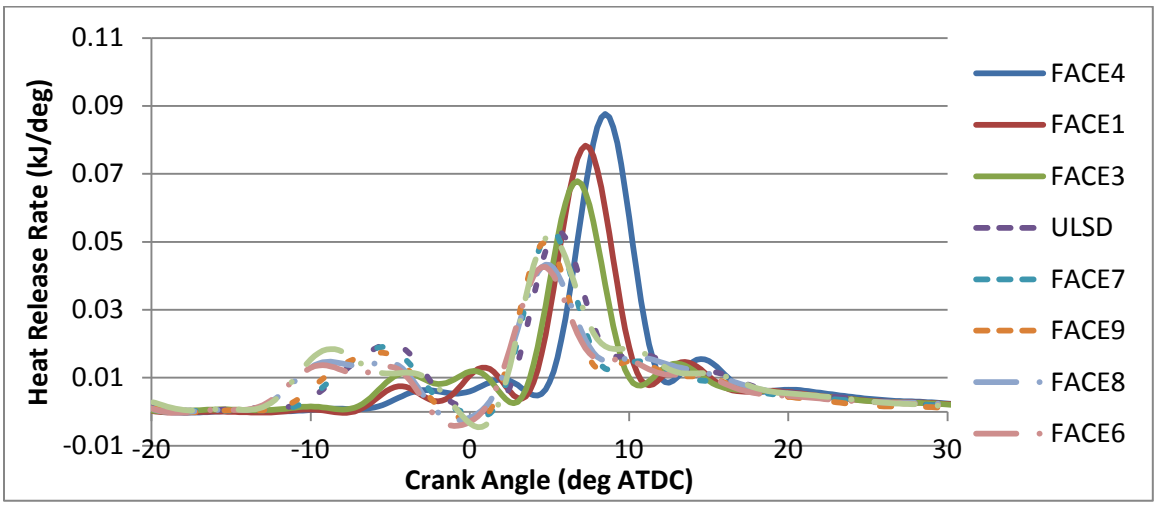

Figure 53: Calculated Heat Release Rate for 4° BTDC Main 40° BTDC Pilot 40% Split

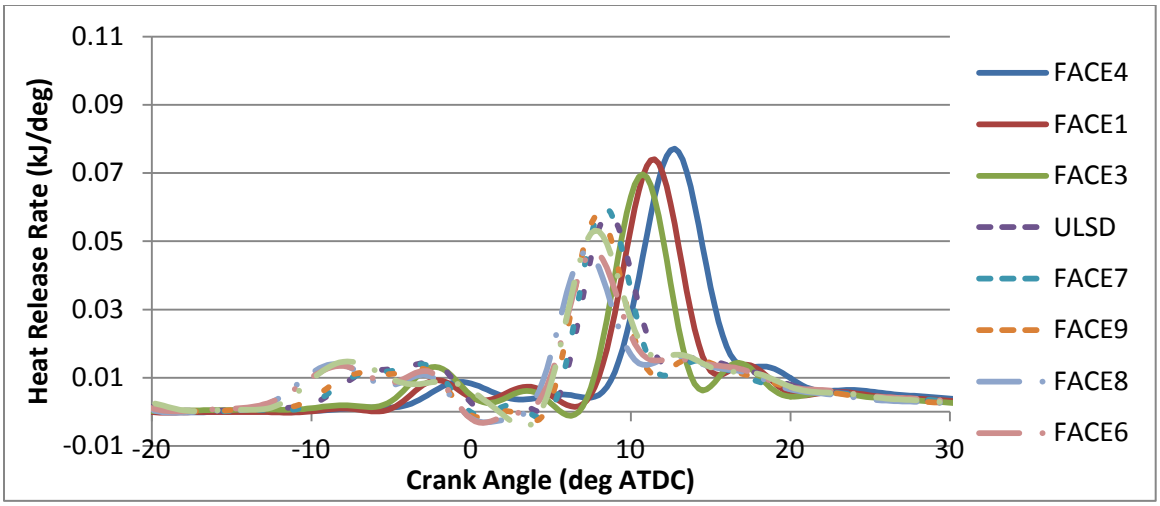

Figure 54: Calculated Heat Release Rate for 2° BTDC Main 40° BTDC Pilot 30% Split

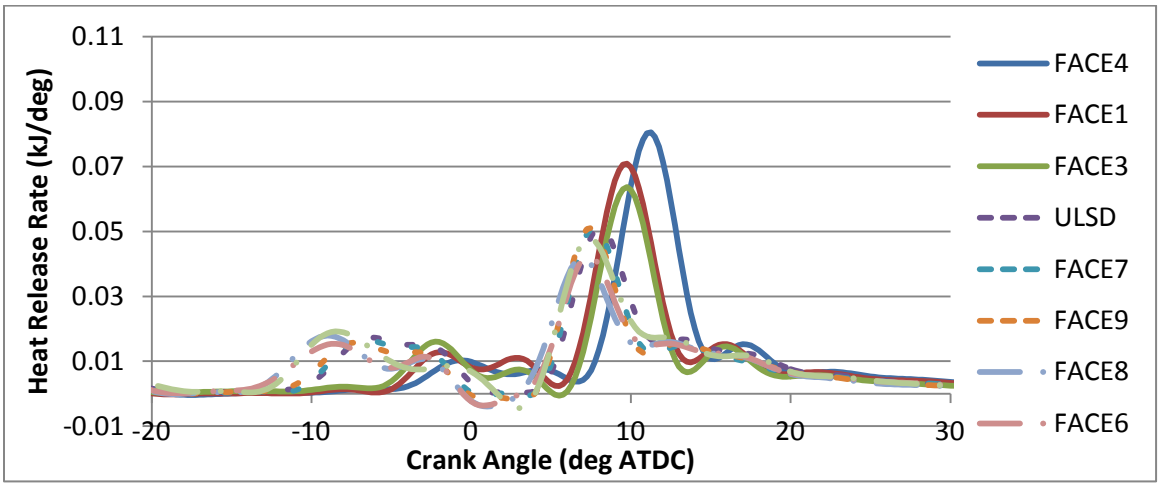

Figure 55: Calculated Heat Release Rate for 2° BTDC Main 40° BTDC Pilot 35% Split

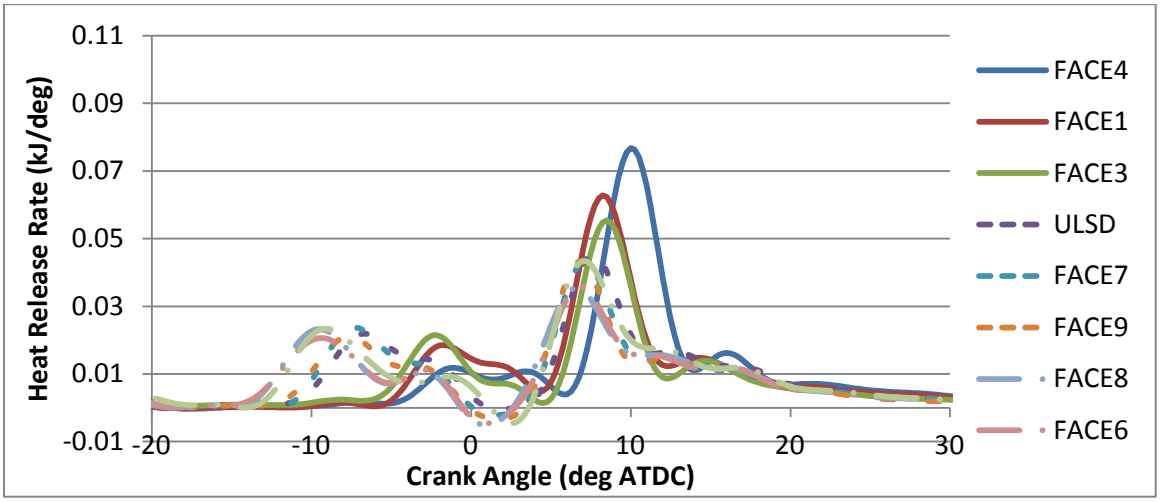

Figure 56: Calculated Heat Release Rate for 2° BTDC Main 40° BTDC Pilot 40% Split

4.3.4 Split Injection Emissions and Fuel Property Trends

Two dimensional scatter plots were made to better identify correlations of emissions, engine performance, and fuel properties. These plots contain data from the three optimal and six comparable split injection tests for each fuel. Note that for some fuels nine data points do not appear. This is due to some optimal and comparable tests occurring at the same test conditions for a given fuel and/or some tests having similar, overlapping values for particular parameters. Select plots are discussed in this Section. A complete set of plots of emissions and engine performance versus fuel properties is included in Section 7.2 Appendix B.

Operating the GM Z19DTH engine on the FACE diesel fuel matrix with a split injection strategy produced a trend in HC emissions as a function of CN. That trend is demonstrated in Figure 57. Elevated HC emissions for the low CN fuels may be attributed to an over-mixing condition related to their increased ignition delay. Adjusting the swirl valves to limit mixing may have reduced HC emissions for these fuels, but it negatively affected emissions and performance characteristics of the higher CN fuels. The correlation of CO emissions to CN was similar to that of HC emissions (see in Figure 124 Appendix B). Figure 58 demonstrated a correlation between HC and CO emissions for most of the fuels tested. This relationship was nearly linear for the low CN fuels. An offset was present for the FACE 4 CO emissions versus HC emissions data when compared to the other low CN fuels. Although a definitive conclusion on this phenomenon cannot be formed, it may be related to even greater unburned HC emissions (compared to other low CN fuels) due to over-mixing as a result of the increased ignition delay of FACE 4 observed in Figure 51 through Figure 56. The poor repeatability of CO emissions discussed earlier in Section 4.2 could also have an impact on the observed offset.

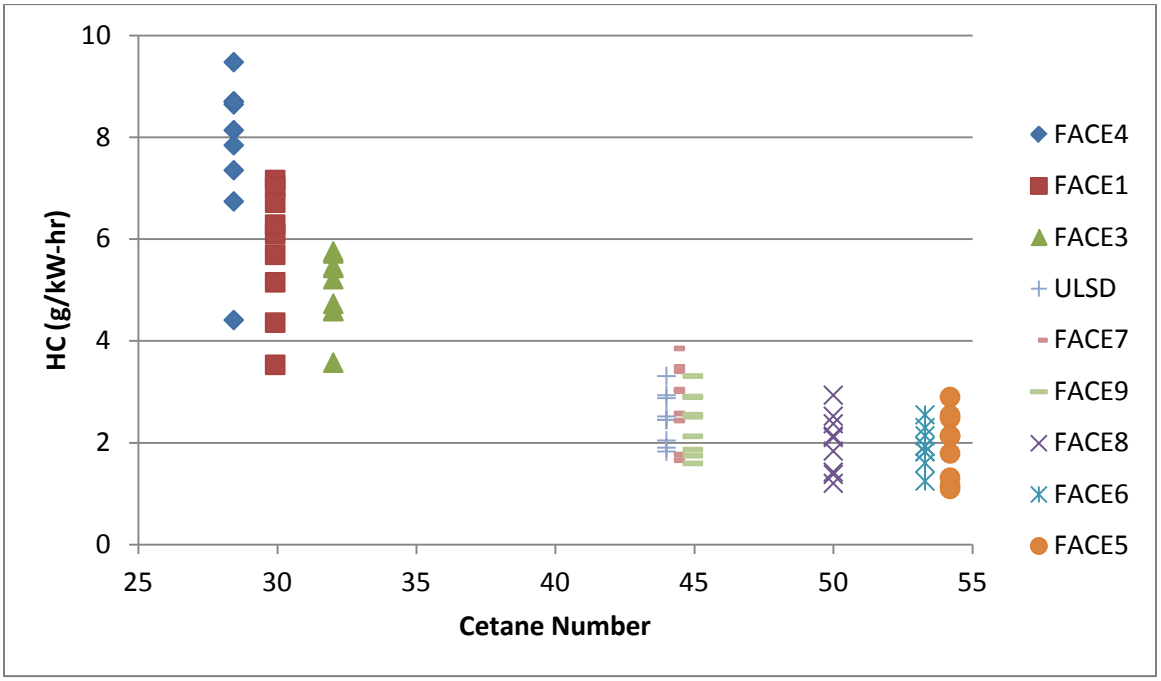

Figure 57: HC Emissions vs. CN for Split Injection Control Strategy

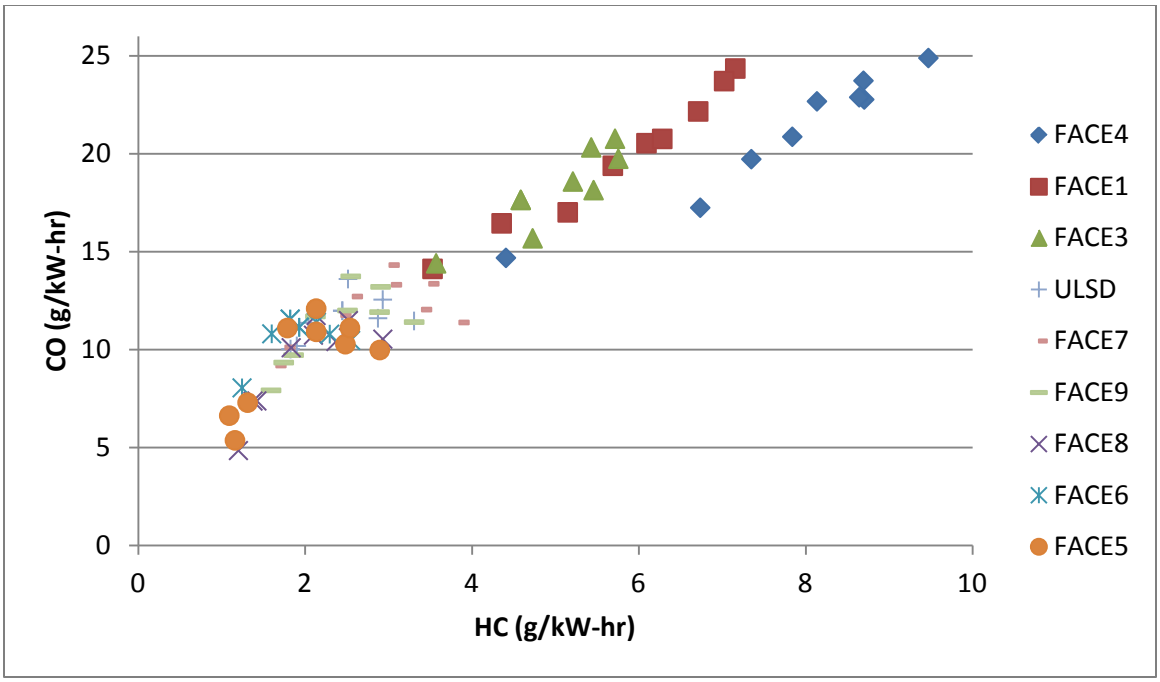

Figure 58: CO Emissions vs. HC Emissions for Split Injection Control Strategy

Figure 59 shows that low CN fuels offered the best tradeoff between soot and NO_X emissions. Figure 60 and Figure 61 reveal that, while using low CN fuels in conjunction with the split injection strategy could provide simultaneously low NO_X and soot, this occurred at the expense of elevated HC (and CO) emissions and reduced BTE. The medium CN fuels and FACE 5 offered a reasonable compromise in the tradeoff of soot emissions versus NO_X emissions while retaining reasonable HC emissions and BTE. The high CN, high T90 fuels, FACE 6 and 8, offered the worst tradeoff of soot emissions versus NO_X emissions due to their significant soot production.

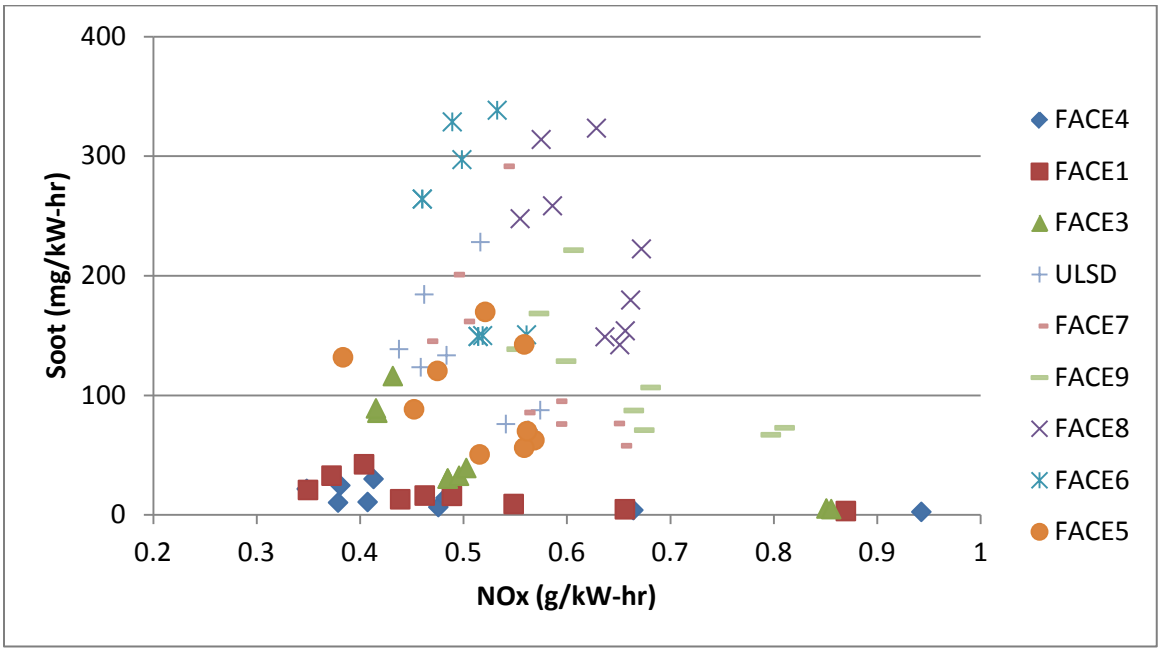

Figure 59: Soot Emissions vs. NO_X Emissions for Split Injection Control Strategy

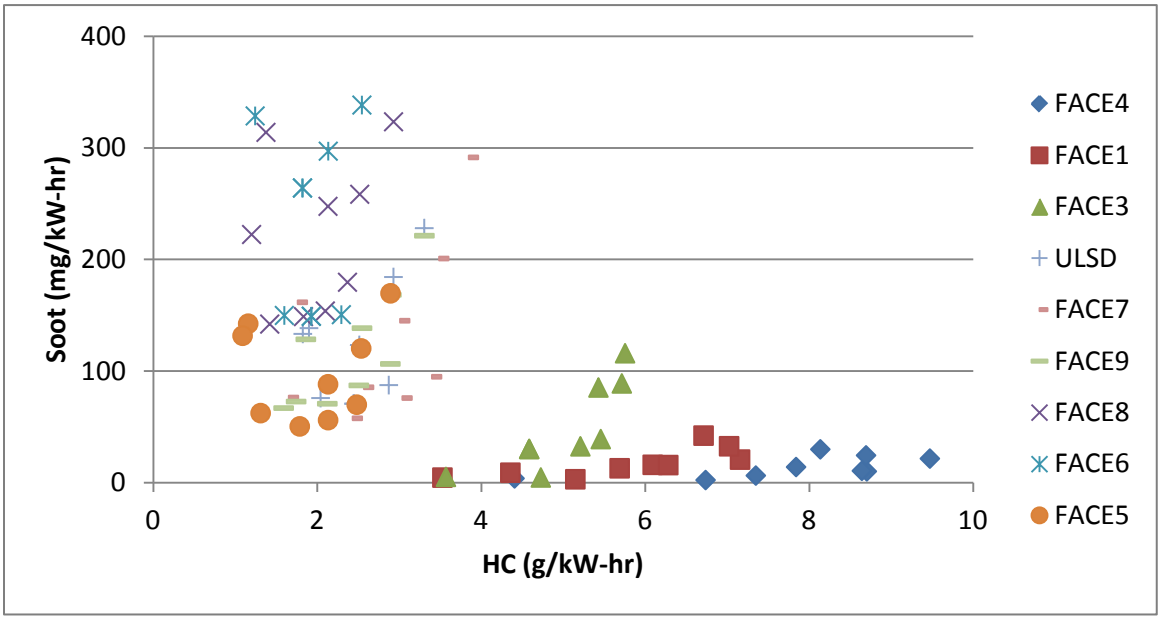

Figure 60: Soot Emissions vs. HC Emissions for Split Injection Control Strategy

The notion that the chemical energy contained in the CO and HC emissions directly affected BTE is reinforced in Figure 61 and Figure 58, which demonstrate that the highest BTE efficiency for each fuel was observed when HC and CO emissions were at a minimum. Additionally, Figure 62 shows that combustion efficiency had a leading role in the resulting BTE of all fuels. It is important to note that for the low CN fuels, combustion phasing (CA50) also affected BTE, while for medium and high CN fuels this effect was less pronounced.

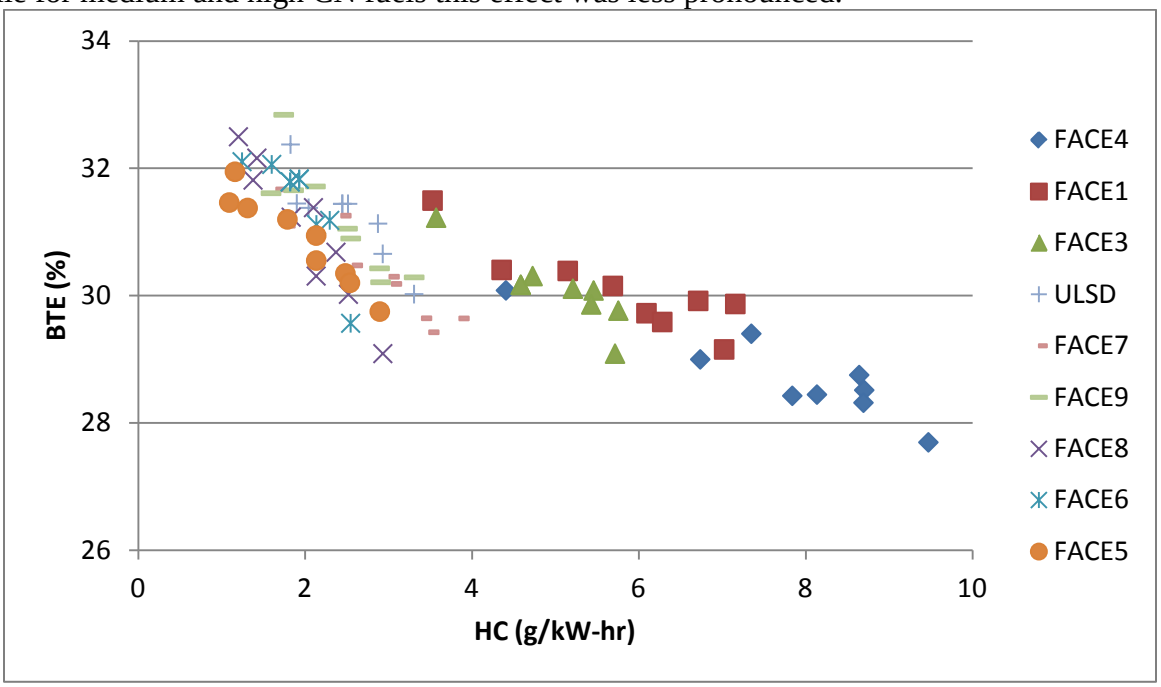

Figure 61: BTE vs. HC Emissions for Split Injection Control Strategy

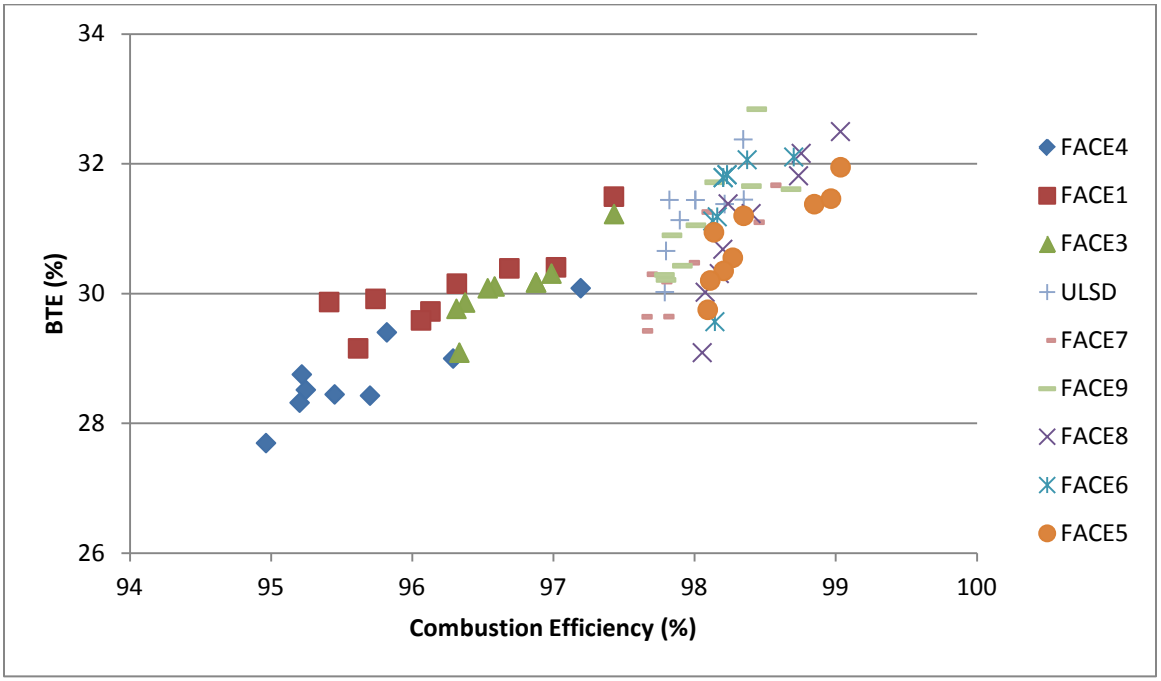

Figure 62: BTE vs. Combustion Efficiency for Split Injection Control Strategy

Figure 63 demonstrates that at soot levels below 100 mg/kW-hr, lower soot production was achieved at greater PRR, which is characteristic of advanced combustion. This also indicates that the soot reduction shown by the use of higher CN fuels was not necessarily related solely to fuel properties. Achievement of a higher PRR to reduce soot formation by these fuels was limited by the interaction of an array of variables including engine hardware, operating conditions (e.g., fuel injection settings, EGR, load, bulk mixture temperature, etc.) and fuel properties. For example, modifying engine hardware and adjusting the fuel injection settings for FACE 5 to safely achieve a higher PRR may result in reduced soot production.

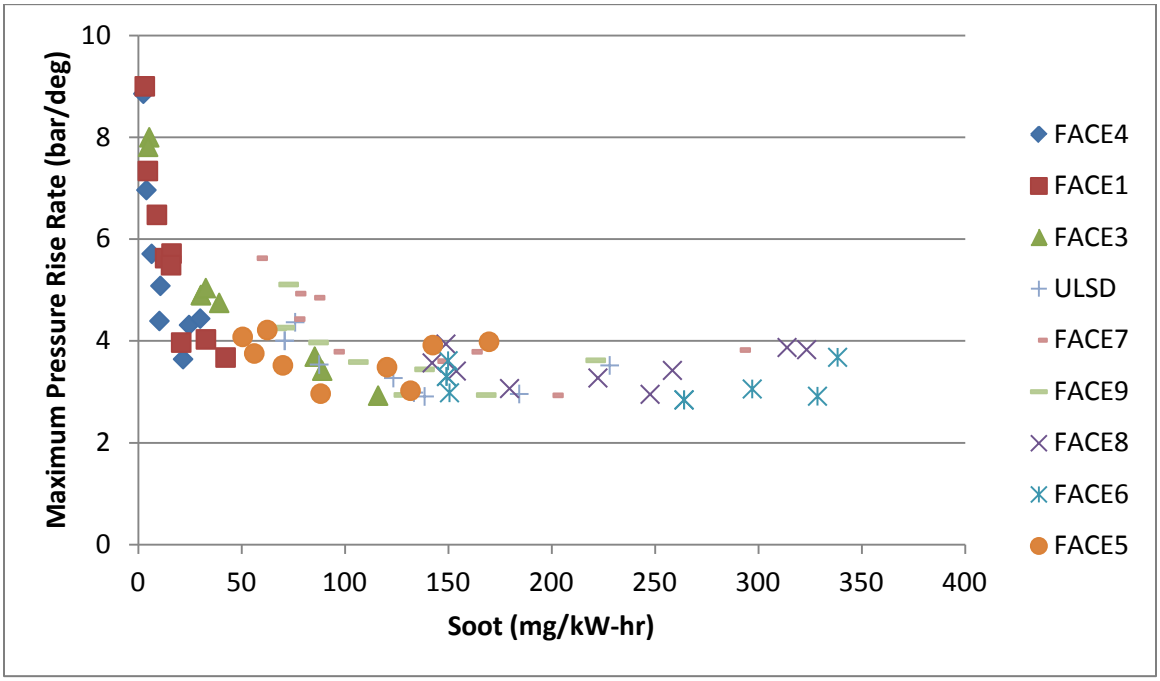

Figure 63: Max PRR vs. Soot Emissions for Split Injection Control Strategy

Figure 64 and Figure 65 offer insight into the implications of CN on NO_X and soot emissions. The highest NO_X emissions measurements were observed for the low CN fuels, while the highest soot emissions measurements were observed for the high CN fuels (except for FACE 5). For low CN fuels, a wide range of NO_X emissions (80-120% variation) were observed based on fuel injection settings with less variation, 35-52% on soot. In contrast, a wider range of soot measurements (33-73% variation) is displayed by higher CN based on fuel injection settings with less of an impact on NO_X emissions (19-36% variation).

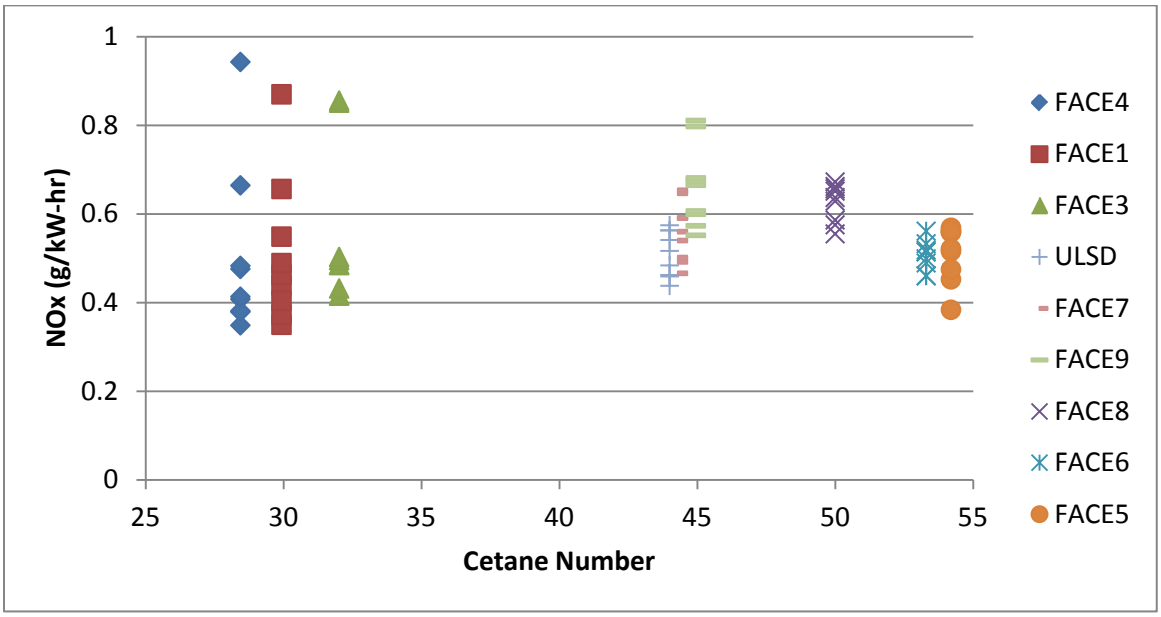

Figure 64: NO_X Emissions vs. CN for Split Injection Control Strategy

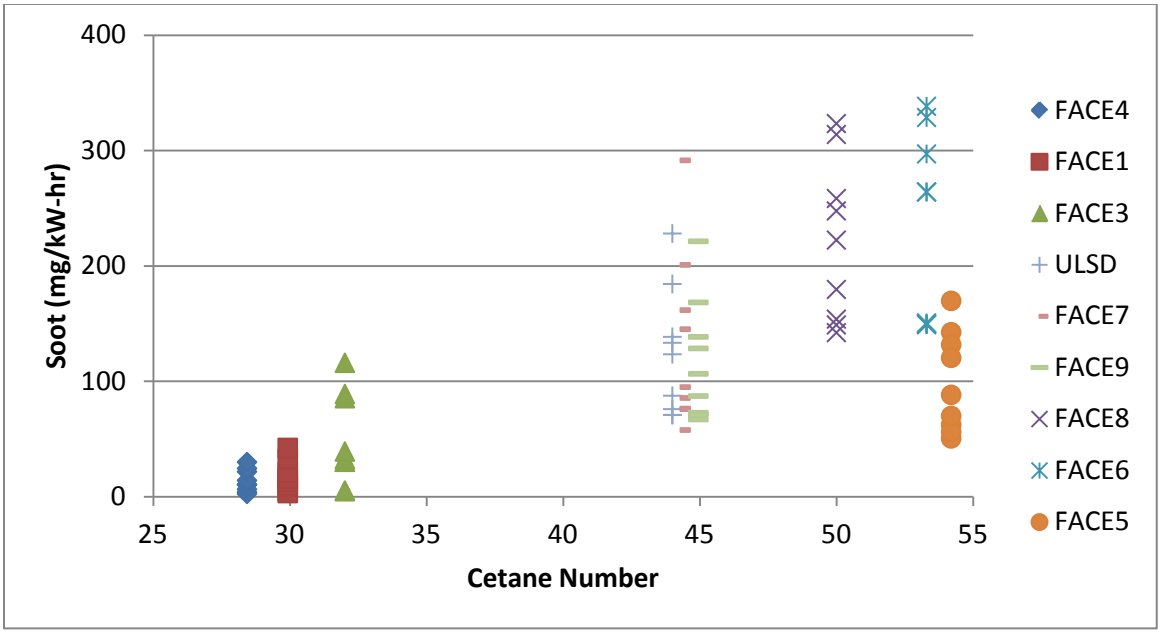

Figure 65: Soot Emissions vs. CN for Split Injection Control Strategy

4.4 Single Injection Control Strategy

4.4.1 Introduction

In addition to the split injection strategy, WVU also explored a single injection strategy for each of the fuels comprising the AVFL-16 study. The single injection test matrix (Table 20) used for all fuel categories was based on varying intake oxygen concentration and rail pressure while holding the CA50 at 7° ATDC by adjusting the SOI timing for each test and fuel. This CA50 of 7° ATDC was chosen in an effort to achieve the most advanced combustion phasing while retaining safe pressure rise rates. In several instances (particularly low CN fuels), a CA50 of 7° ATDC was not achievable regardless of further advancing the SOI timing; therefore, the most advanced CA50 was sought. Additionally, the low CN fuels experienced misfire at intake oxygen concentrations less than 12.5%; thus, they were not tested at those conditions. Similar to the split injection strategy, the engine was operated at an engine speed of 2100 RPM while targeting a BMEP of 3.5 bar. These operating conditions can also be found in Table 19. The swirl control valves were fixed at the "fully open" position for all tests.

Table 19: Single Injection Control Strategy Operating Conditions

Engine Speed	2100 RPM
BMEP	3.5 bar
CA50	7° ATDC
Fuel Temperature	32° C
Coolant Temperature	84° C

Table 20: Single Injection Test Matrix

Test #	Intake O_2 (%)	Rail Pressure (bar)
46	12	1200
47	12	1400
48	12	1600
49	12.5	1200
50	12.5	1400
51	12.5	1600
52	13	1200
53	13	1400
54	13	1600
55	13.5	1200
56	13.5	1400
57	13.5	1600
58	14	1200
59	14	1400
60	14	1600

4.4.2 Optimal Single Injection Tests

Three optimal single injection tests for each fuel were chosen using a procedure similar to the split injection strategy, except that all tests were considered (not only the top ten with the highest BTE as was done for the optimal split injection tests) due to the smaller test matrix for the single injection strategy. Tests 46 through 48 (for the low CN fuels) were not completed, as mentioned above. Ranking all single injection tests for each test fuel, the three tests with the highest BTE, lowest soot emissions, and, and the lowest NO_X emissions, respectively, were selected. The test number and subsequent intake oxygen (IO_2 %) and rail pressure (RP bar) chosen for each of these conditions for a particular fuel is presented in Table 21. Figure 66 displays the SOI timing for each of the optimal single injection tests.

Table 21: Optimal Single Injection Tests

Fuel	FACE4	FACE1	FACE3	ULSD	FACE7	FACE9	FACE8	FACE6	FACE5
High BTE Test	Test 58 IO_2 14% RP 1200	Test 59 IO_2 14% RP 1400	Test 49 IO_2 12.5% RP 1200	Test 49 IO_2 12.5% RP 1200	Test 47 IO_2 12% RP 1400	Test 47 IO_2 12% RP 1400	Test 58 IO_2 14% RP 1200	Test 46 IO_2 12% RP 1200	Test 53 IO_2 13% RP 1400
Low Soot Test	Test 59 IO_2 14% RP 1400	Test 56 IO_2 13.5% RP 1400	Test 53 IO_2 13% RP 1400	Test 60 IO_2 14% RP 1600	Test 60 IO_2 14% RP 1600	Test 60 IO_2 14% RP 1600	Test 60 IO_2 14% RP 1600	Test 60 IO_2 14% RP 1600	Test 60 IO_2 14% RP 1600
Low NO_X Test	Test 50 IO_2 12.5% RP 1400	Test 51 IO_2 12.5% RP 1600	Test 49 IO_2 12.5% RP 1200	Test 47 IO_2 12% RP 1400	Test 47 IO_2 12% RP 1400	Test 47 IO_2 12% RP 1400	Test 46 IO_2 12% RP 1200	Test 48 IO_2 12% RP 1600	Test 46 IO_2 12% RP 1200

The tests presented in Table 21 represent the absolute maximum value of BTE and/or minimum values of soot emissions or NO_X emissions for a given fuel. However, as previously noted there are other tests with very similar values, yet more optimal values for other parameters. Conditions have been identified that provide values within +/- 0.5% of the optimal value. For example, for the high BTE test for FACE 1, test 56 (32.95% BTE) and test 53 (32.89% BTE) produced BTE values within 0.5% of test 59 (33.04% BTE). However test 56 and test 53 produced only 71% and 53%, respectively, of the NO_X emissions and 77% and 87%, respectively, of the soot emissions of test 59. For the ULSD, test 46 provided a NO_X value within 0.5% of test 47 (0.1191 vs. 0.1185 g/kW-hr, respectively), a slightly higher BTE (33.58% vs. 33.21%), but also a significantly higher soot value (462 vs. 211 mg/kW-hr, respectively). With regard to the highest BTE condition for FACE 9, test 46 (33.78% BTE) and test 49 (33.74% BTE) produced BTE within 0.5% of test 47 (33.81% BTE). However, test 47 produced lower soot and lower NO_X emissions than both of the mentioned tests. For FACE 8, test 49 had a BTE value within 0.5% of test 58 (33.79% vs. 33.87%, respectively), 53% lower NO_X emissions (0.191 vs. 0.357 g/kW-hr, respectively), but more than twice as much soot (1073 vs. 473 mg/kW-hr, respectively). For the highest BTE condition for FACE 6, test 52 (33.72% BTE) and test 60 (33.66% BTE) produced BTE values within 0.5% of test 46 (33.79% BTE). Both have significantly higher NO_X than test 46, but both produced lower soot emissions; test 60 produced 78% less soot than test 46. For FACE 5, the high BTE test (test 53) had a BTE within 0.5% of test 47, but test 47 produced 30% lower NO_X emissions and 7% higher soot emissions than test 53. Also with regard to the lowest soot condition for FACE 5, test 54 had a nearly

identical soot value and BTE as test 60, however test 54 produced 32% lower NO_X. These results demonstrate that by adjusting operating conditions, performance and emissions trade-offs can be obtained. As previously noted in Section 4.3.2, other alternative tests could also be identified using the results of the repeatability study found in Section 4.2 (rather than values within +/- 0.5% of the optimal value). Ultimately, the identification of alternative tests serves the purpose of informing the reader that other methods of selection exist which could provide different results when comparing fuels.

Certain trends existed for each of the optimal conditions displayed in Table 21. All fuels performed best at the lower rail pressures (1200 or 1400 bar) for the high BTE test. The highest intake oxygen concentration (14%) and rail pressure setting (1600 bar) were best for the low soot test for all of the medium and high CN fuels. Regarding the low NO_X test, the lower oxygen concentrations were best for all fuels, with 12.5% oxygen for the low CN fuels and 12.0% oxygen for the medium and high CN fuels. Although some of the optimal parameters were at the lowest or highest end of the ranges tested, expansion of the range of these operating parameters to achieve more ideal BTE, soot emissions, or NO_X emissions would likely have a detrimental impact on other emissions and performance constituents. For example, decreasing the intake oxygen concentration to achieve lower NO_X emissions would likely result in misfire, particularly for the low CN fuels.

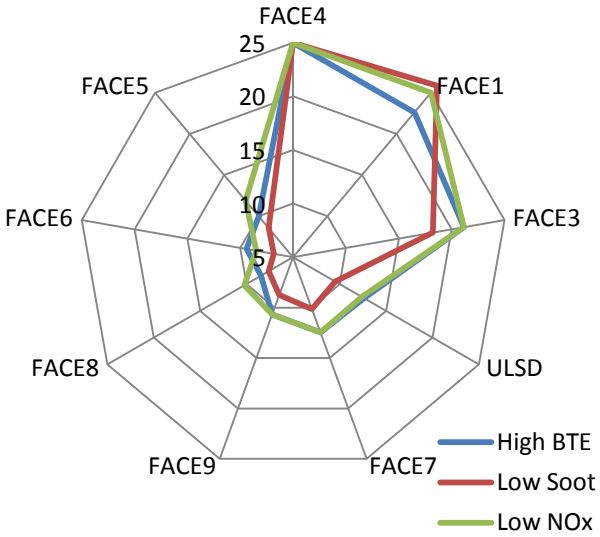

Figure 66: SOI (deg BTDC) for Optimal Single Injection Tests

Similar to the split injection strategy, HC emissions (presented in Figure 67) were greatest (~2-6 times greater) for the low CN fuels, particularly FACE 4 (~ 6 times greater). HC emissions from the medium and high CN fuels were similar regardless of optimal tests, but FACE 9 (5-22% lower) and FACE 6 (9-17% lower) emitted the lowest HC emissions for the respective CN categories.

CO emissions (Figure 68) did not trend the same as HC emissions as previously seen with the split injection strategy. Similar to conventional combustion, CO emissions for the medium and high CN fuels were generally lowest for each fuel when soot production was lowest.

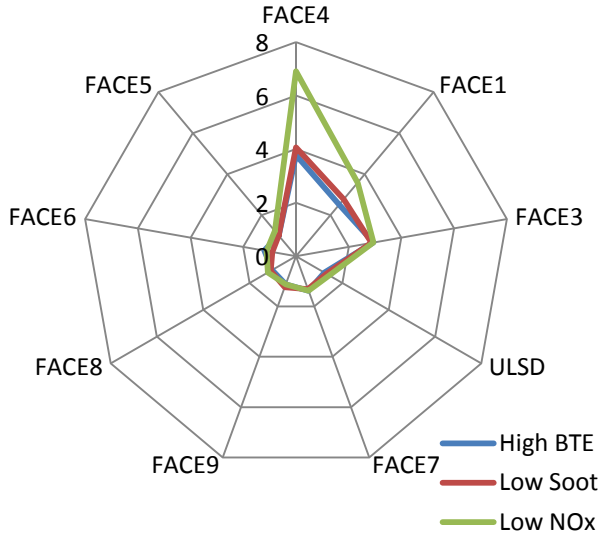

Figure 67: HC Emissions (g/kW-hr) for Optimal Single Injection Tests

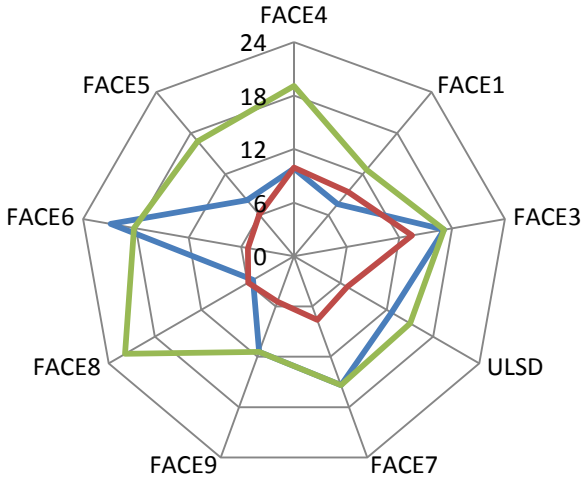

Figure 68: CO Emissions (g/kW-hr) for Optimal Single Injection Tests

NO_X emissions (Figure 69) were very low (0.08-0.38 g/kW-hr) for all fuels due to the high EGR fractions of 42-49% implemented for the single injection strategy. It was observed again that the high aromatic and T90 fuels of FACE 9 (1.1-1.5 times greater) and 8 (1.2-2.6 times greater) were the highest NO_X emissions producers within their respective CN categories, which is consistent with results presented from the split injection strategy. The lowest NO_X emissions were obtained with the low CN fuels, corresponding to non-optimal combustion phasing for FACE 4 and FACE 1 demonstrated by very low PRR in Figure 72, retarded CA50 values in Figure 73, and retarded main HRR curves in Figure 76.

Soot production (Figure 70) was greatest for the high CN fuels (0.4-684 times greater), particularly FACE 6 and FACE 8, which emitted levels double that of the split injection strategy. However, FACE 5, another high CN fuel, had (36% to 56%) lower soot than the medium CN fuels for the high BTE test. A clear CN influence on soot emissions was not as apparent as previously observed during the split injection strategy.

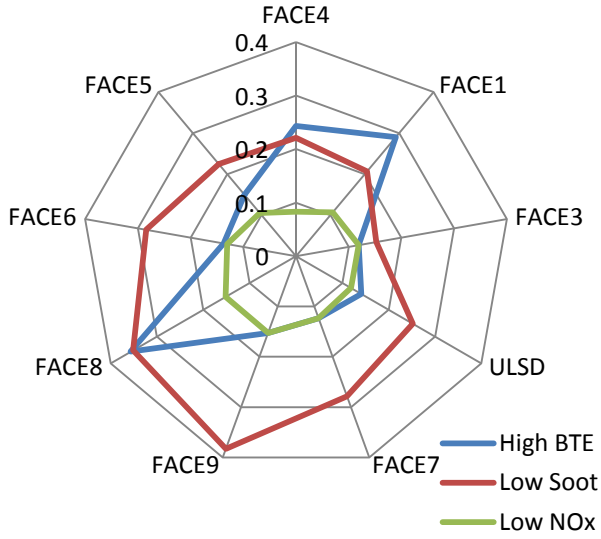

Figure 69: NO_X Emissions (g/kW-hr) for Optimal Single Injection Tests

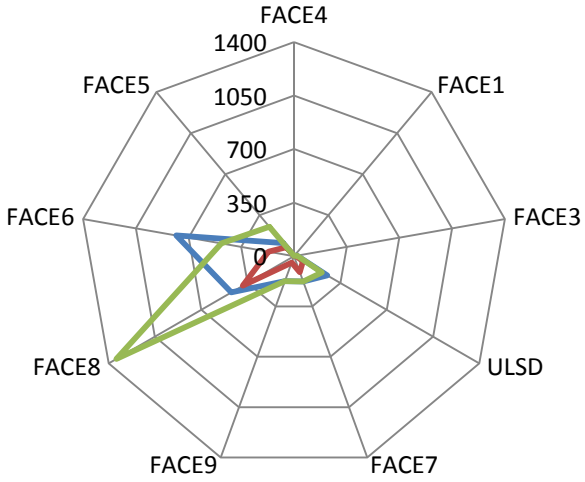

Figure 70: Soot Emissions (mg/kW-hr) for Optimal Single Injection Tests

BTE improved compared to the split injection strategy for all fuels. The low CN fuels still had the lowest BTE (Figure 71). A correlation between aromatic content and BTE was observed for the low and medium CN, and a partial correlation was seen for the high CN fuels (Figure 151, Appendix B). The maximum BTE for FACE 1, the only low CN and low aromatic content fuel, was nearly 1% higher than the other low CN fuels which had high aromatic content. Additionally, FACE 7, having the highest aromatic content of the medium CN fuels demonstrated the lowest BTE. FACE 8 (sole high aromatic content fuel of the high CN fuels), exhibited a BTE similar to the other high CN fuels during the high BTE test. For all of the other "optimal" tests, FACE 8 exhibited the lowest BTE.

Combustion phasing, represented as CA50 (Figure 73), was relatively similar for all fuels and close to the target value of 7° ATDC, with the exception of the low NO_X tests for FACE 4 and FACE 1. The retarded combustion phasing displayed in the HRR curves of Figure 76 for these low CN fuels was due to the use of high EGR rates (~47%). Additionally low PRR (~2 bar/deg and ~4 bar/deg, respectively) for the low NO_X tests of FACE 4 and FACE 1 supported this conclusion and indicated poor combustion for these tests (Figure 72).

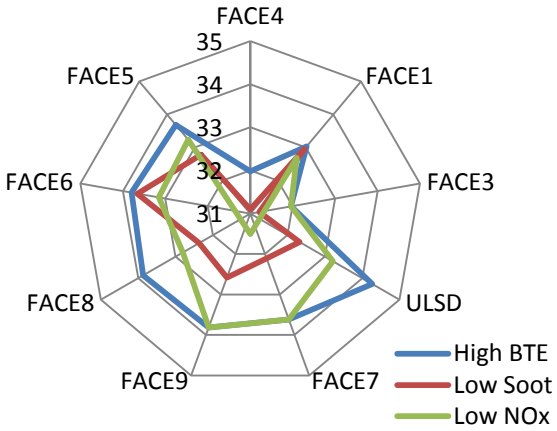

Figure 71: BTE (%) for Optimal Single Injection Tests

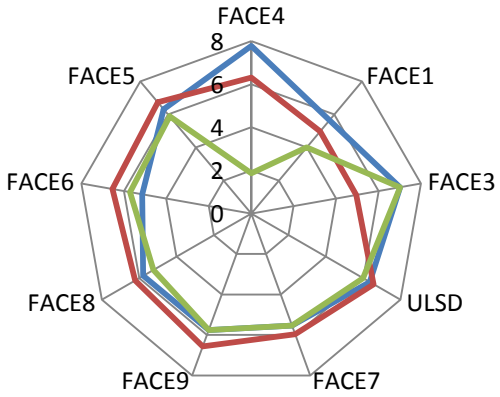

Figure 72: PRR (bar/deg) for Optimal Single Injection Tests

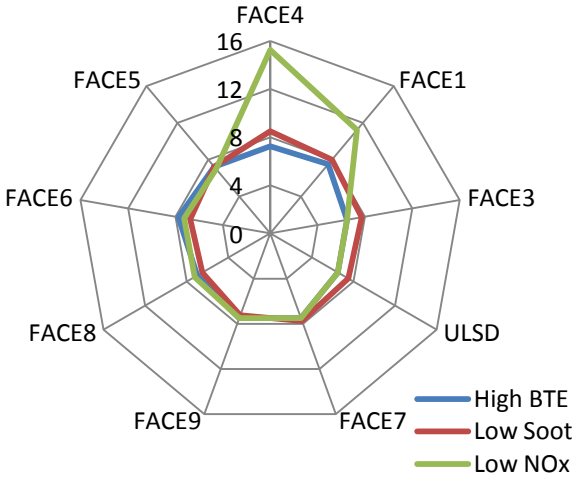

Figure 73: CA50 (deg ATDC) for Optimal Single Injection Tests

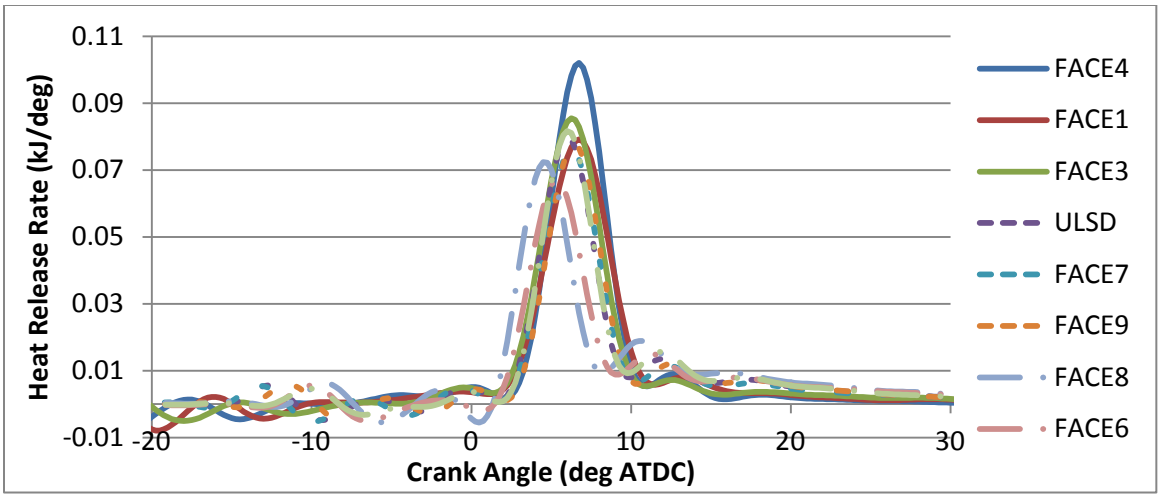

Figure 74: Calculated Heat Release Rate for Single Injection High BTE Tests

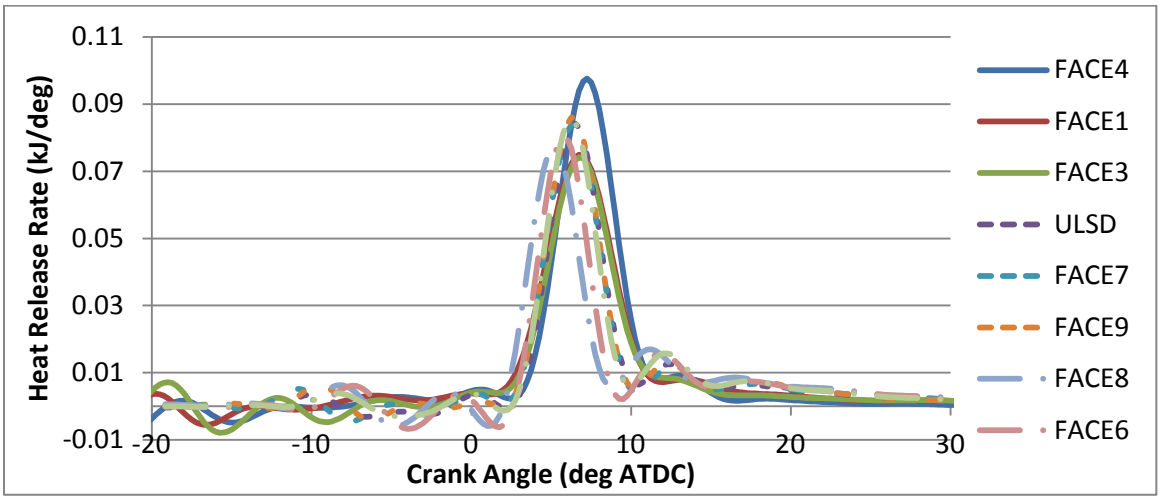

Figure 75: Calculated Heat Release Rate for Single Injection Low Soot Tests

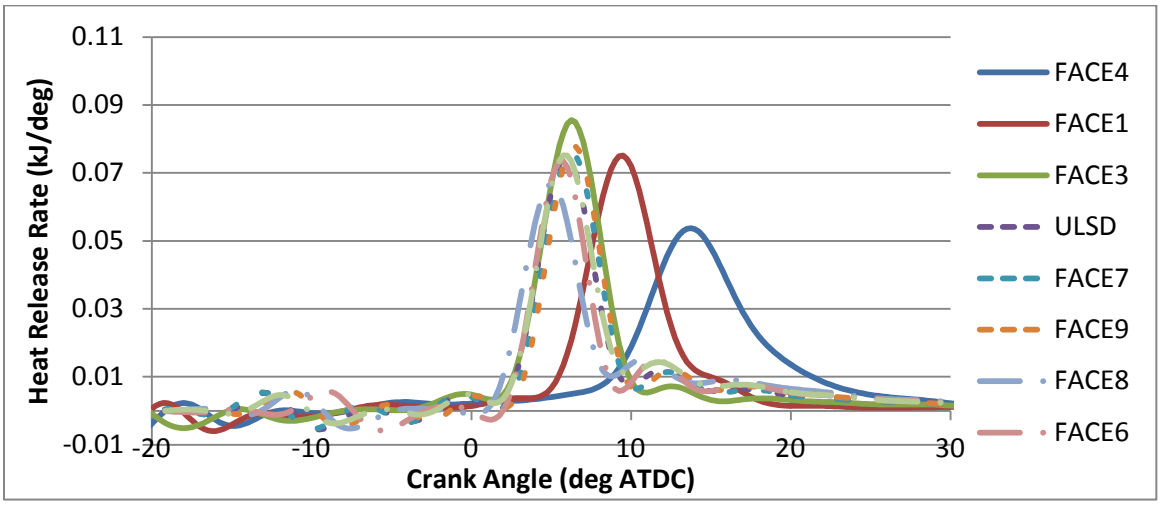

Figure 76: Calculated Heat Release Rate for Single Injection Low NO_X Tests

4.4.3 Comparable Single Injection Tests

In addition to the optimal tests selected for the single injection strategy, six tests with identical settings were selected for each fuel. Three tests performed at an intake O_2 concentration of 12.5% with varying rail pressures and three tests performed at an intake O_2 concentration of 14% with varying rail pressures were selected to demonstrate the effects of EGR and rail pressure on performance in relation to fuel properties. Figure 77 and Figure 78 present SOI timing for each intake oxygen concentration.

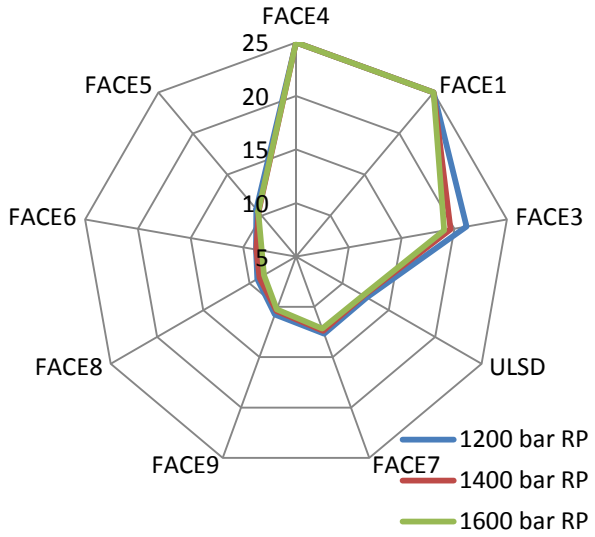

Figure 77: SOI Timing (deg BTDC) with 12.5% Intake O_2

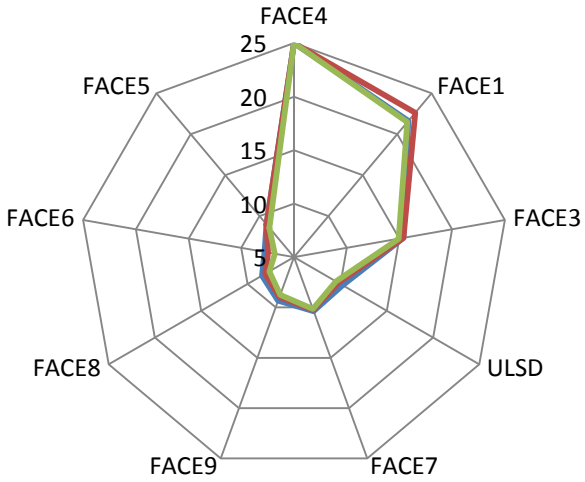

Figure 78: SOI Timing (deg BTDC) with 14% Intake O_2

HC emissions were greatest for FACE 4 and the other low CN fuels (Figure 79 and Figure 80). Increasing the intake O_2 concentrations served to reduce the HC emissions for all fuels, although a much greater reduction of 11-44% was observed for the low CN fuels. Medium and high CN fuels exhibited very similar (low) HC emissions regardless of rail pressure with FACE 6 and 9 retaining the lowest HC emissions (5-18% reduction) in their respective CN categories.

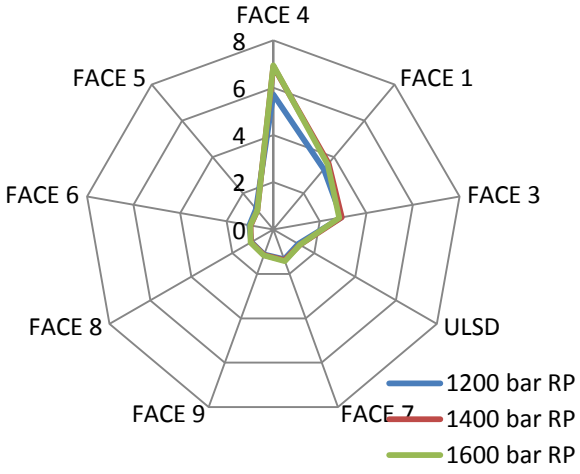

Figure 79: HC Emissions (g/kW-hr) with 12.5% Intake O_2

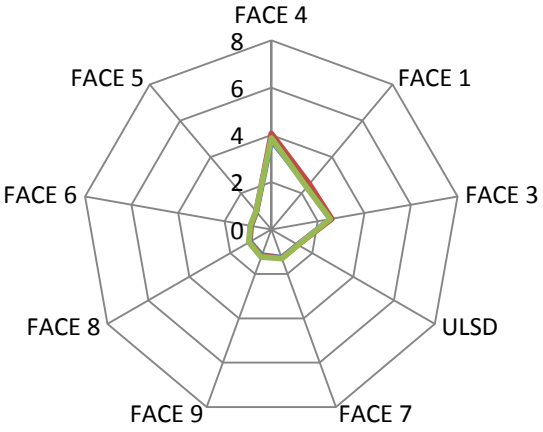

Figure 80: HC Emissions (g/kW-hr) with 14% Intake O_2

FACE 4 also produced the highest CO emissions (Figure 81 and Figure 82) at 12.5% intake O_2 concentration, although the difference between its measurements and other fuels was not as drastic as it was for HC emissions (~1.5 times greater for CO and ~3.9 times greater for HC). At 14% intake O_2, a shift was observed where FACE 3 emitted the greatest CO emissions among all fuels. Additionally, Figure 82 demonstrates that FACE 4, 3 and 7 which had among the highest aromatic content of all the fuels also produced the most CO emissions; an average ~48% increase. This aromatic and CO correlation for the FACE diesel fuels has also been reported by De Ojeda et al. [5] and Cho et al. [3].

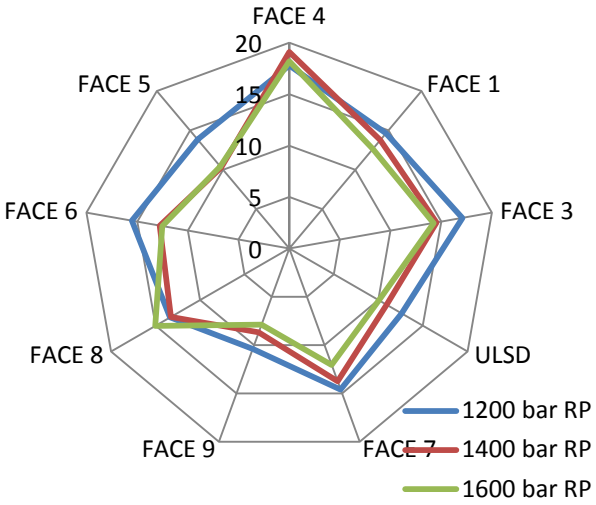

Figure 81: CO Emissions (g/kW-hr) with 12.5% Intake O_2

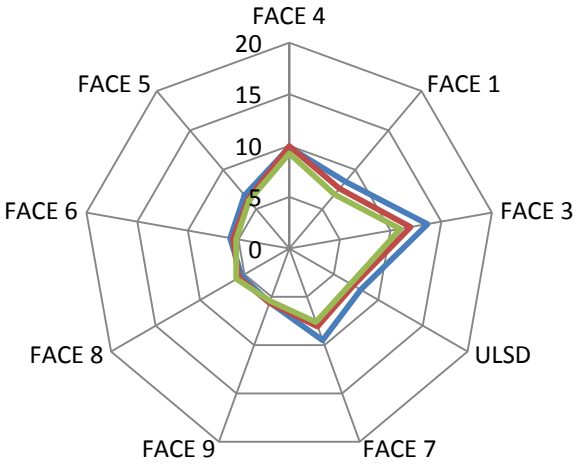

Figure 82: CO Emissions (g/kW-hr) with 14% Intake O_2

NO_X emissions presented in Figure 83 are substantially suppressed as a result of the minimal oxygen available for combustion. An increase in NO_X emissions was observed at 14% intake oxygen concentration as expected (Figure 84), yet measured levels were still lower than the majority of split injection strategy NO_X measurements. Similar to other results presented, combustion of FACE 9 and FACE 8 resulted in the highest NO_X emissions of all fuels.

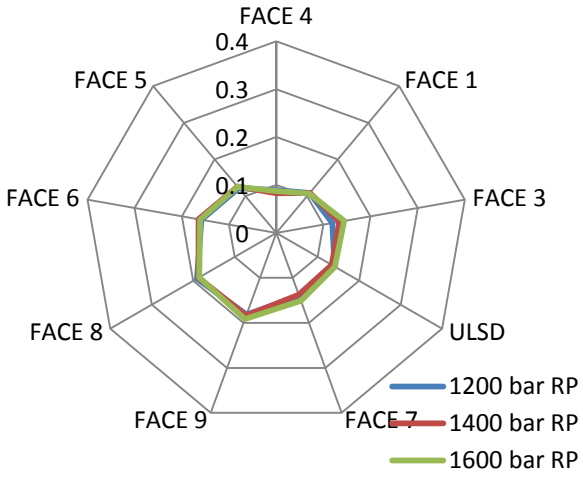

Figure 83: NO_X Emissions (g/kW-hr) with 12.5% Intake O_2

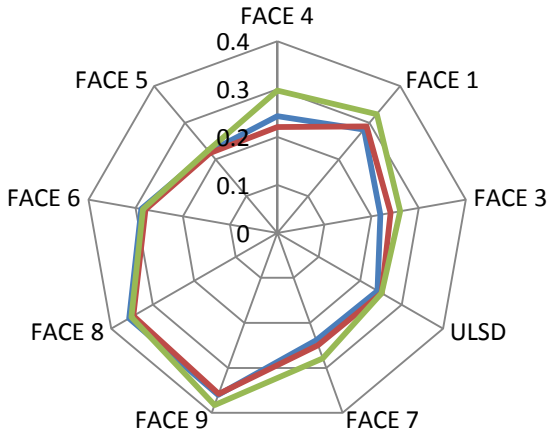

Figure 84: NO_X Emissions (g/kW-hr) with 14% Intake O_2

Comparison of soot production among all fuels (Figure 85 and Figure 86) revealed that soot emissions for FACE 8 were 1.2-498 times greater than the other fuels. FACE 6, the other high CN, high T90 fuel also produced significantly more soot than the other fuels. This suggests that high CN and high T90 together greatly enhance soot formation. FACE 5, the remaining high CN (but lower T90) fuel, produced 55-88% lower soot emissions compared to FACE 8 and FACE 6. This was also observed previously by other researchers and attributed to FACE 5's lower T90 [3, 5, 6]. However, the trend of lower soot with lower T90 does not appear to apply among the medium CN fuels. FACE 7 had the lowest T90 of the medium CN fuels, yet it produced the most soot (1.1-2.4 times higher). FACE 7 did contain the highest aromatic content of the medium CN fuels, suggesting that high aromatic content can also contribute to soot formation. Further supporting the trend, FACE 3, a low T90 fuel with high aromatic content exhibited the highest soot emissions (7-24 times higher) among low CN fuels. The scale in Figure 85 and Figure 86 prevents observation of this trend.

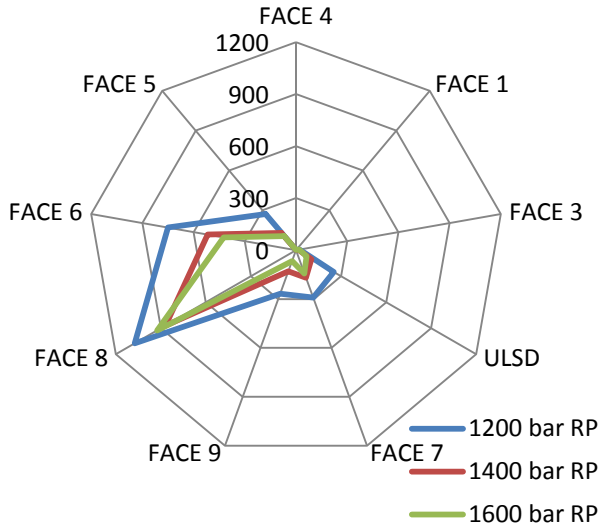

Figure 85: Soot Emissions (mg/kW-hr) with 12.5% Intake O_2

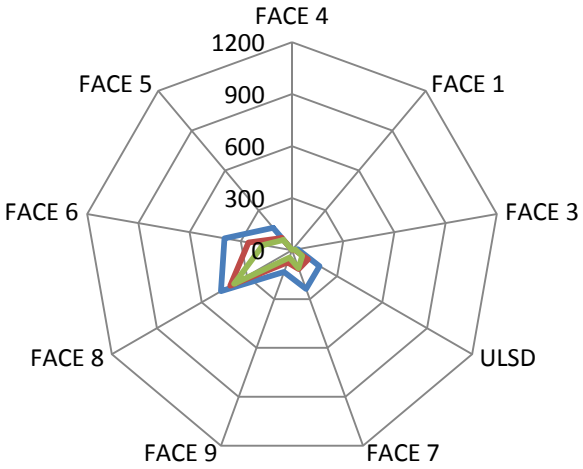

Figure 86: Soot Emissions (mg/kW-hr) with 14% Intake O_2

The BTE results are presented in Figure 87 and Figure 88. FACE 4 and FACE 3 exhibited the lowest BTE, while FACE 1 exhibited BTE on par with higher CN fuels. The single injection strategy consistently provided greater BTE (Figure 87 and Figure 88) than the split injection strategy.

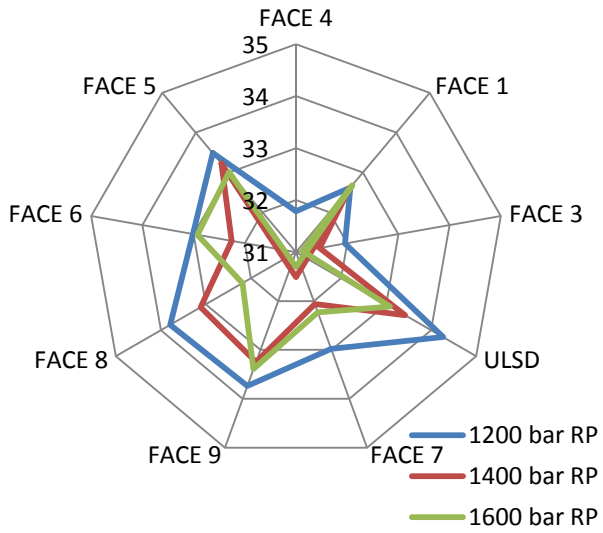

Figure 87: BTE (%) with 12.5% Intake O_2

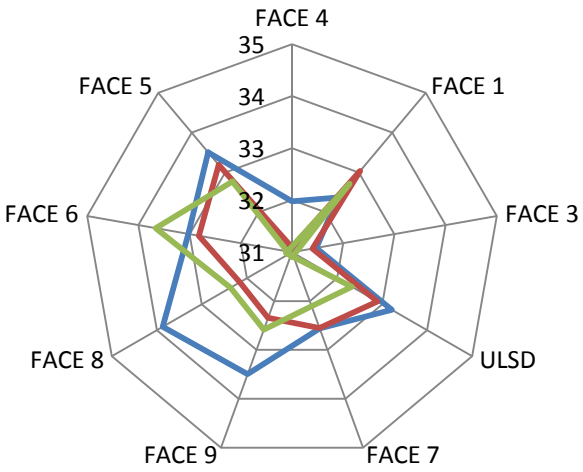

Figure 88: BTE (%) with 14% Intake O_2

Pressure Rise Rate (PRR) plots are presented in Figure 89 and Figure 90. At the 12.5% intake oxygen concentration, FACE 4 and FACE 1 had the lowest PRRs. These results correspond to the retarded combustion phasing of these fuels as seen by the CA50 plots in Figure 91 and Figure 92 and HRR plots in Figure 93 through Figure 98.

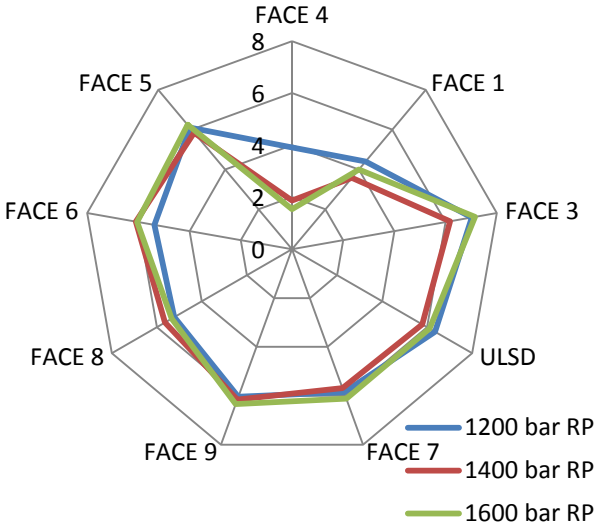

Figure 89: PRR (bar/deg) with 12.5% Intake O_2

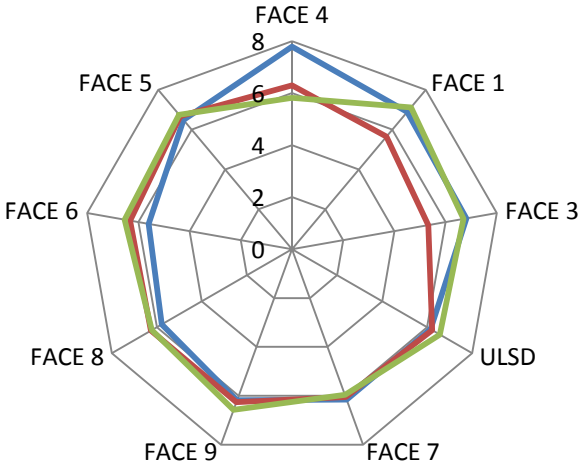

Figure 90: PRR (bar/deg) with 14% Intake O_2

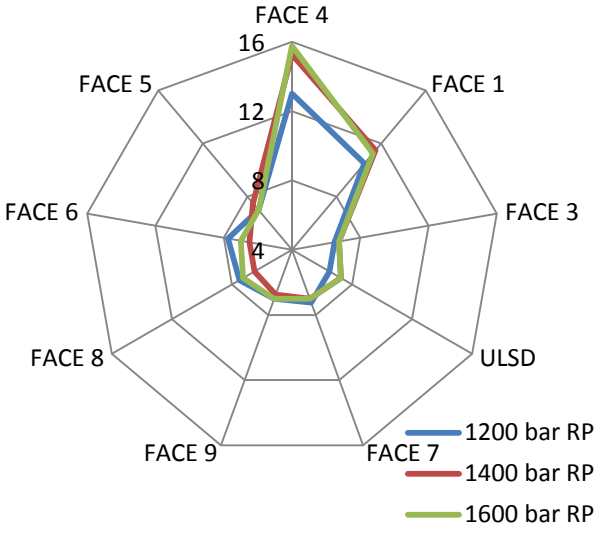

Figure 91: CA50 (deg ATDC) with 12.5% Intake O_2

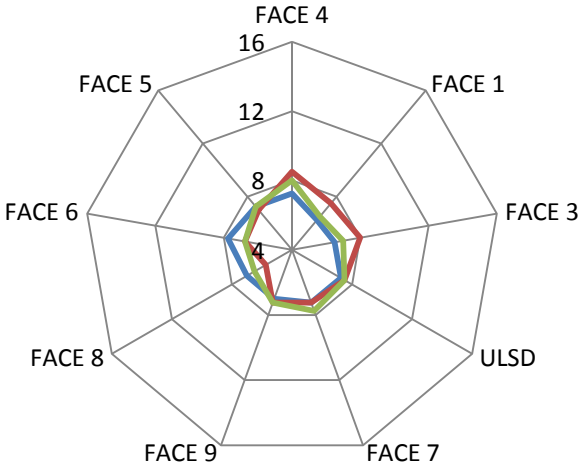

Figure 92: CA50 (deg ATDC) with 14% Intake O_2

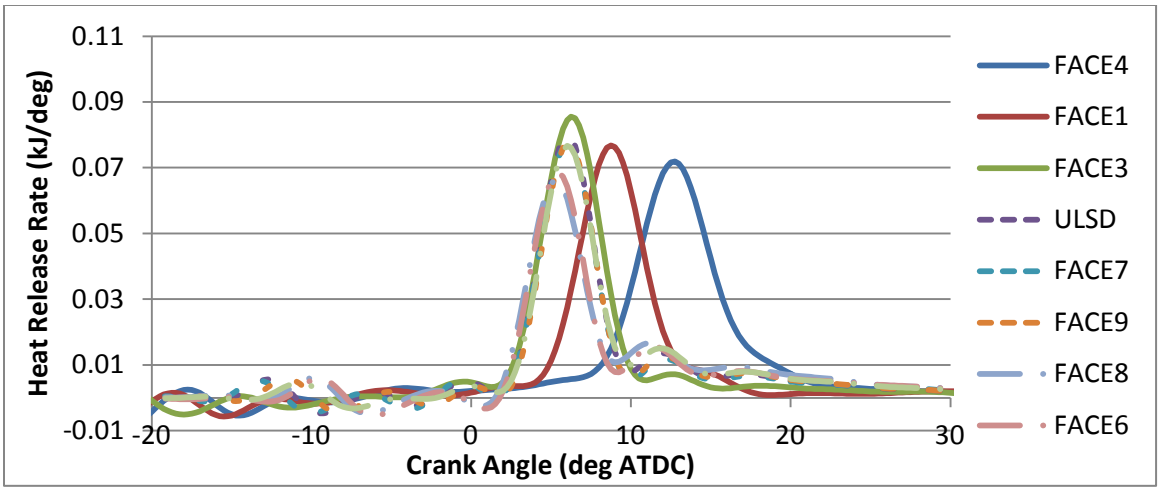

Figure 93: Calculated Heat Release Rate for 12.5% Intake O_2 1200 Bar Rail Pressure

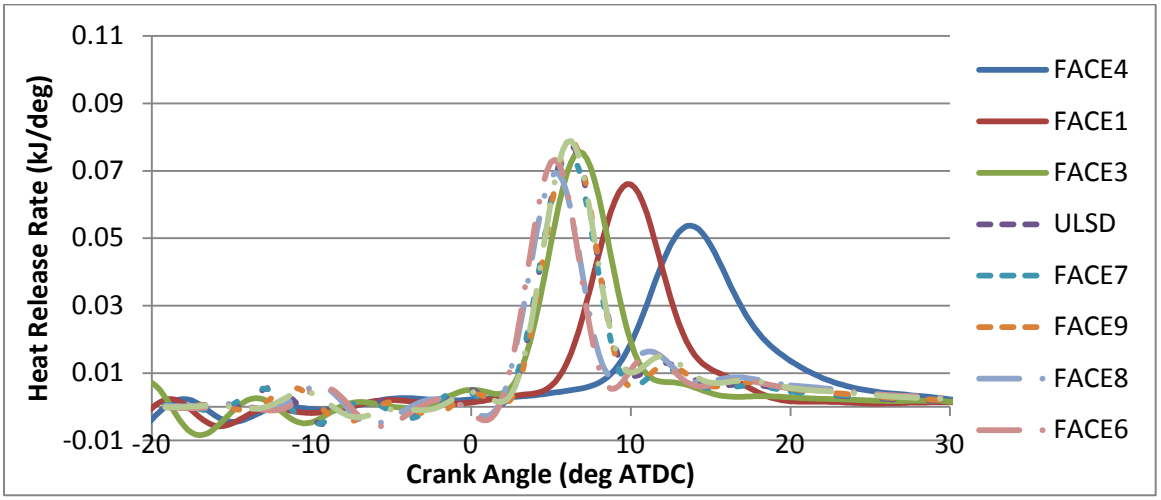

Figure 94: Calculated Heat Release Rate for 12.5% Intake O_2 1400 Bar Rail Pressure

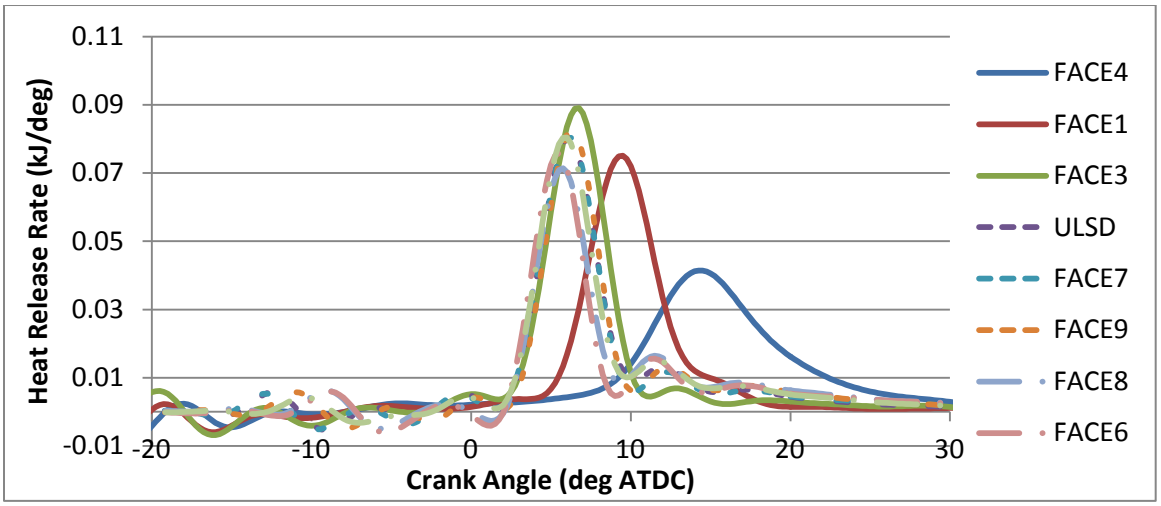

Figure 95: Calculated Heat Release Rate for 12.5% Intake O_2 1600 Bar Rail Pressure

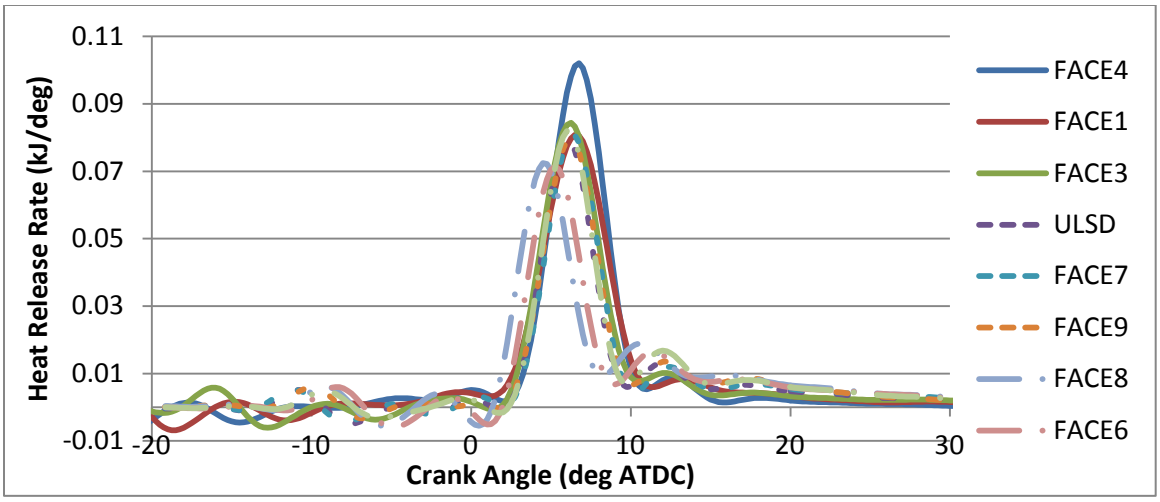

Figure 96: Calculated Heat Release Rate for 14% Intake O_2 1200 Bar Rail Pressure Test

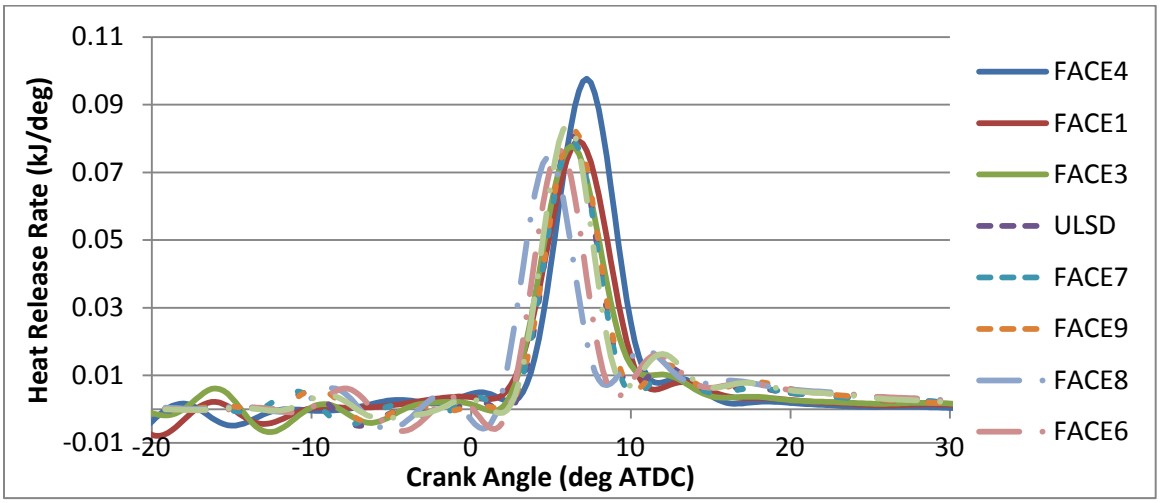

Figure 97: Calculated Heat Release Rate for 14% Intake O_2 1400 Bar Rail Pressure

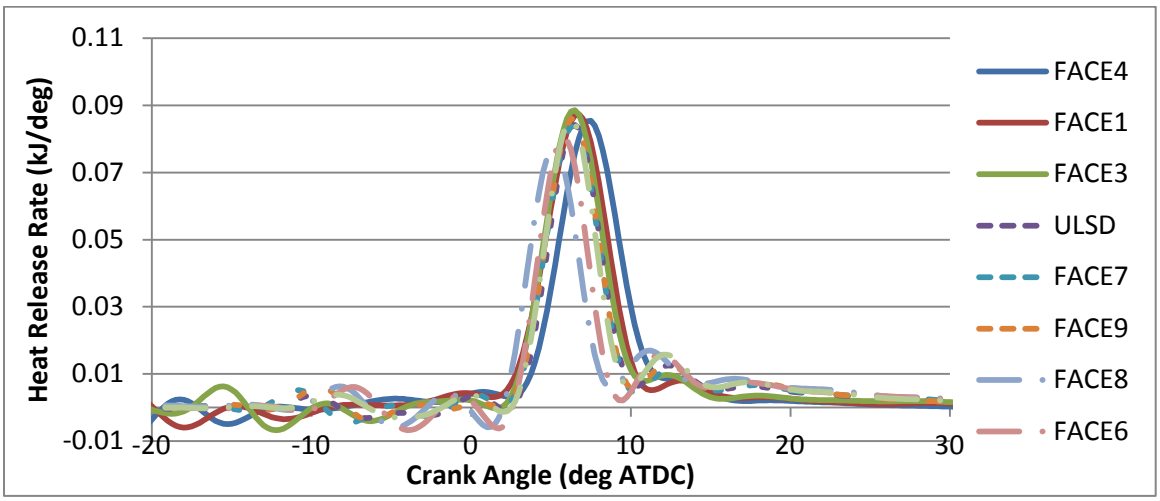

Figure 98: Calculated Heat Release Rate for 14% Intake O_2 1600 Bar Rail Pressure

4.4.4 Single Injection Emissions and Fuel Property Trends

In this section, trends of some emissions are discussed. A more complete set of comparative plots of emissions and engine performance versus fuel properties is included in Section 7.2 Appendix B. Unlike the results obtained for the split injection strategy, a linear CO emissions versus HC emissions trend was not apparent for the medium and high CN fuels operating with the single injection strategy (Figure 99). Low CN fuels may still have provided a linear trend, but the trend was much less apparent than that obtained during the split injection strategy. A clear dependence of HC emissions on CN is observed again (Figure 100), although the level of HC emissions is roughly half that observed with the split injection control strategy.

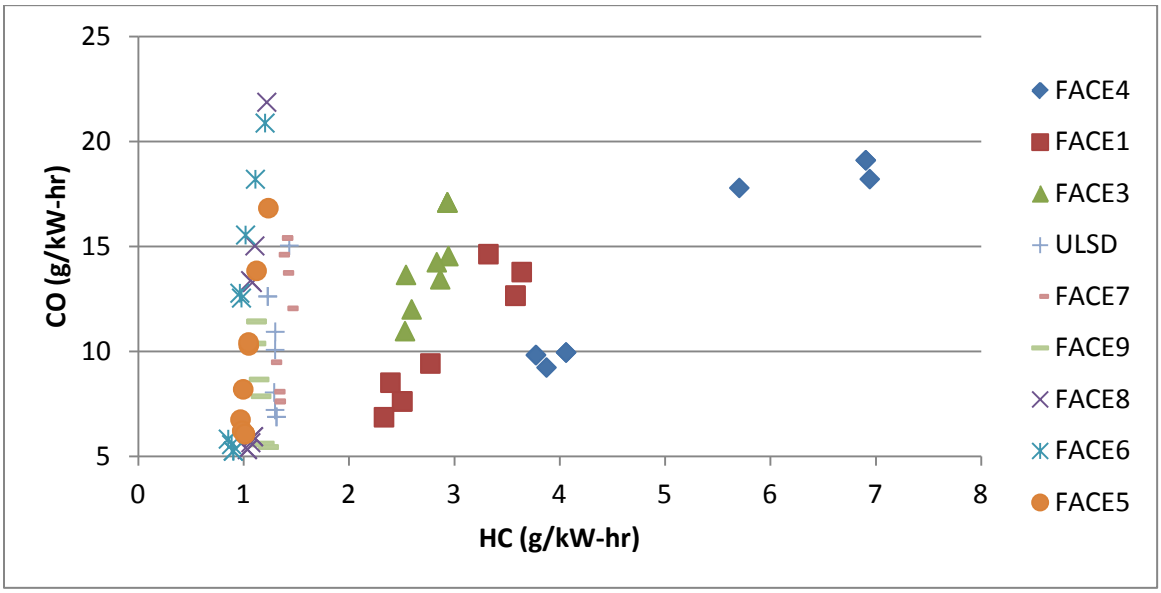

Figure 99: CO Emissions vs. HC Emissions for Single Injection Control Strategy

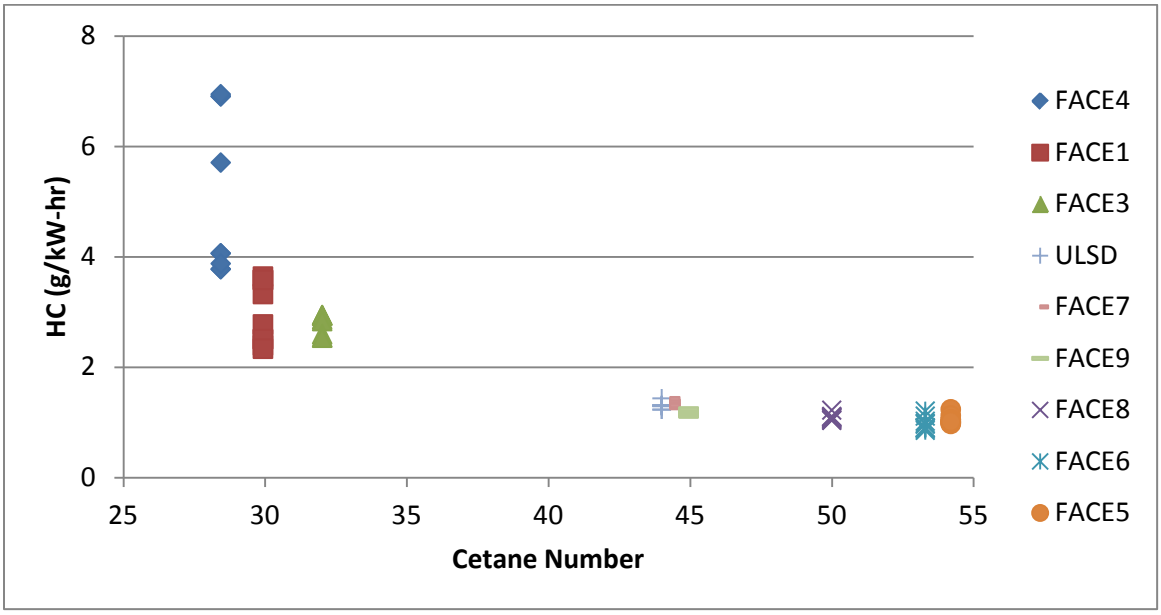

Figure 100: HC Emissions vs. CN for Single Injection Control Strategy

A comparison of soot emissions to HC emissions in Figure 101 displays a grouping of high and medium CN fuels for which soot levels varied over a wide range while HC emissions were nearly constant. The figure also shows a separate grouping of low CN fuels with almost no soot but HC emissions varying over a wide range. Plotting soot emissions versus CO emissions in Figure 102 resulted in a conventional combustion trend for the medium and high CN fuels, where higher CO emissions were observed as soot production increased. This was an effect of the shorter ignition delay experienced by the high and medium CN fuels which led subsequently to a less homogenous air and fuel mixture.

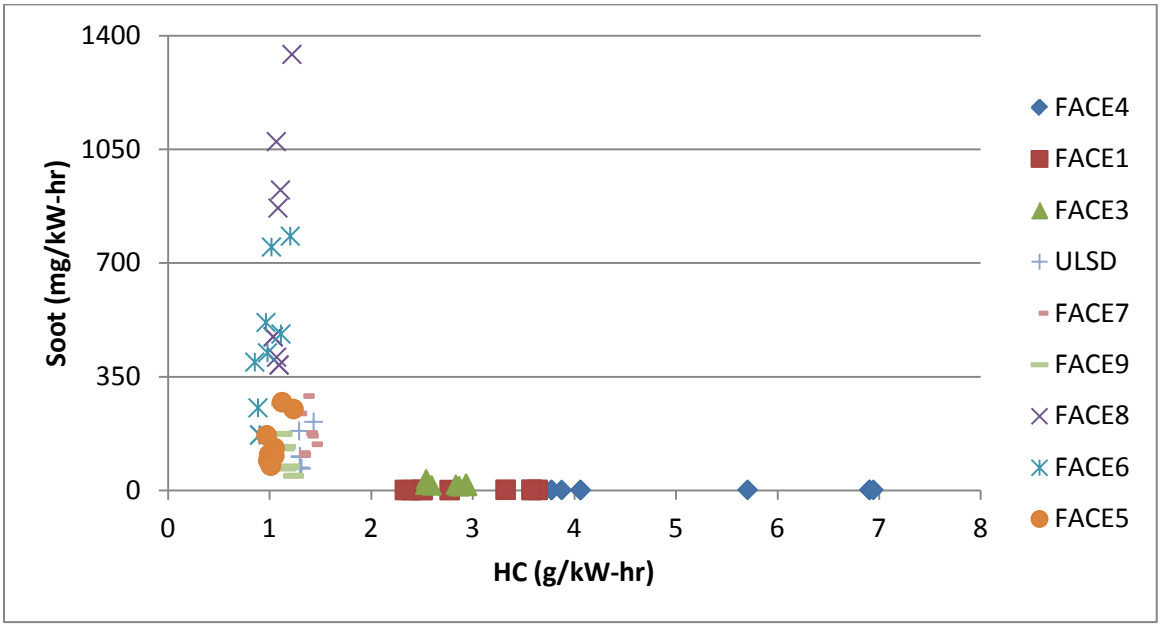

Figure 101: Soot Emissions vs. HC Emissions for Single Injection Control Strategy

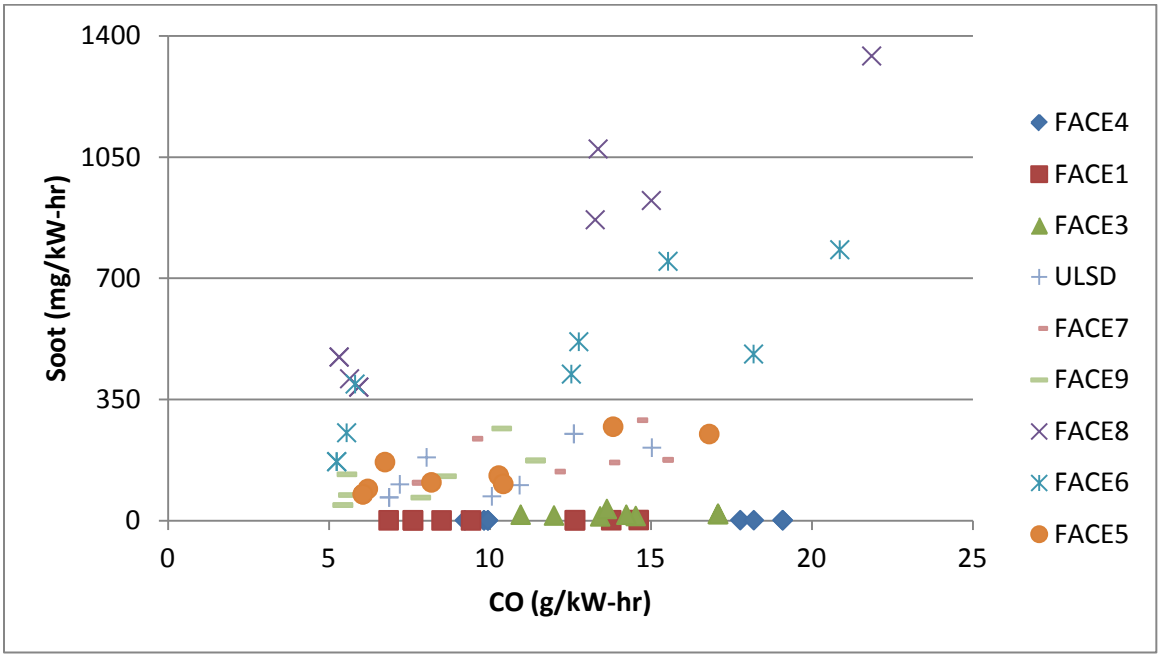

Figure 102: Soot Emissions vs. CO Emissions for Single Injection Control Strategy

Figure 103 displays a direct correlation between CO and NO_X emissions, with NO_X emissions decreasing as CO emissions increased. This resulted directly from high EGR fractions where low combustion temperatures limited CO burnout and NO_X formation. Figure 104 demonstrates again that the low CN fuels offered the best soot emissions versus NO_X emissions tradeoff as a result of the near zero soot production regardless of EGR level. This ideal tradeoff was counteracted by increased HC and CO emissions as well as reduced BTE for the low CN fuels. Similar to the split injection strategy, the medium CN fuels and FACE 5 offered a reasonable compromise between the soot emissions versus NO_X emissions tradeoff and HC emissions, CO emissions and BTE.

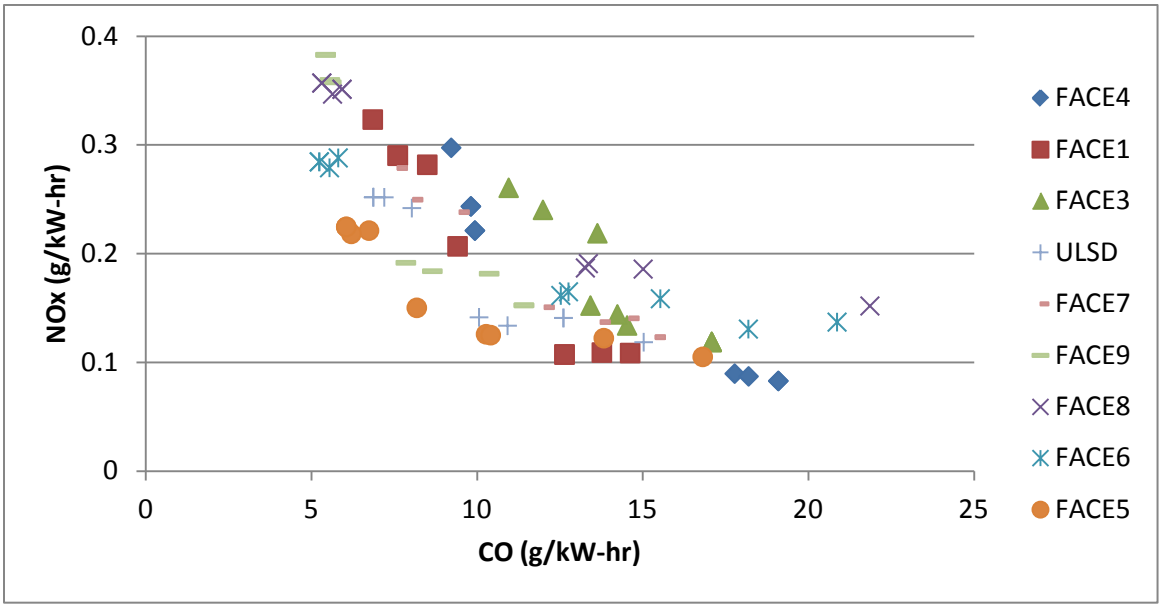

Figure 103: NO_X Emissions vs. CO Emissions for Single Injection Control Strategy

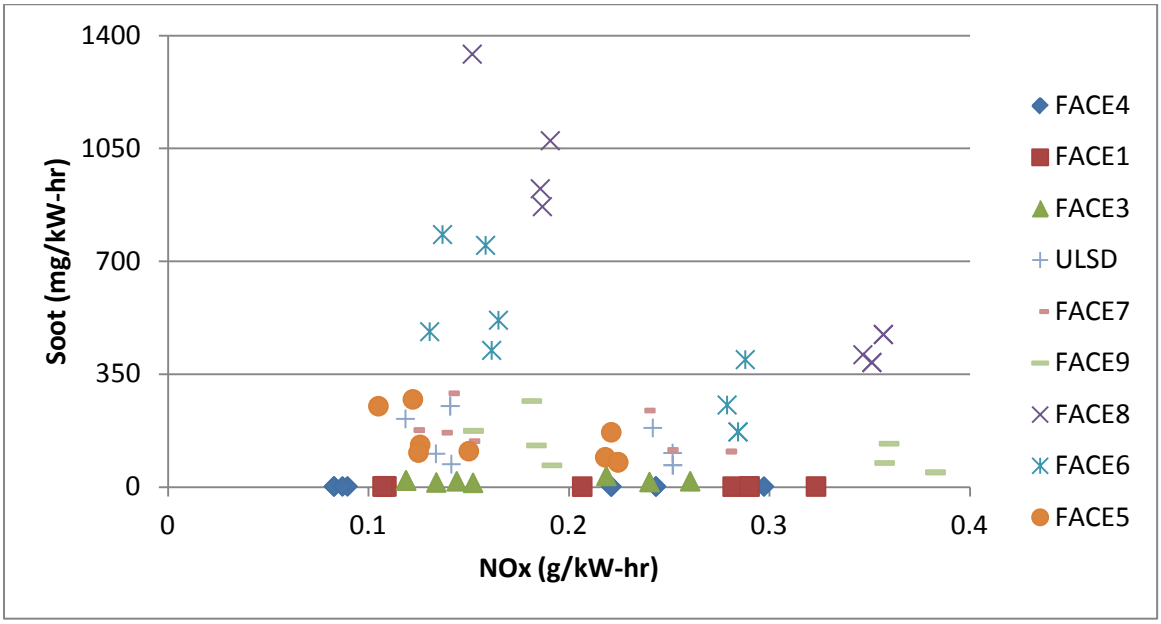

Figure 104: Soot Emissions vs. NO_X Emissions for Single Injection Control Strategy

5 Conclusions and Recommendations

Advanced combustion strategies have gained significant attention within the last decade as a potential tool to comply with tightening emissions regulations. Advanced combustion strategies seek to simultaneously produce minimal NO_X and PM emissions while retaining acceptable fuel efficiency. Achievement of such strategies depends on numerous variables, including engine hardware, engine control strategy, and fuel properties.

To investigate the effect of fuel properties on advanced combustion, a comprehensive matrix of nine fuels (FACE 1, FACE 3, FACE 4, FACE 5, FACE 6, FACE 7, FACE 8, FACE 9, and ULSD) with varying CN, aromatic content, and T90 temperature properties was utilized with a split injection control strategy and a single injection control strategy on a GM Z19DTH light-duty compression-ignition engine.

A significant effort was made to establish the engine test platform for this study. Experiments were initially performed using two separate engines (Z19DTH engine, 16-valve, and GM Z19DT engine, 8-valve) as well as three EGR coolers (EGR coolers from 1.9 L, 6.0 L, and 11.0L engines). The lower emissions, BTE, and more homogeneous combustion of the GM Z19DTH engine (16-valve) made it better suited for advanced combustion research than the GM Z19DT engine (8-valve) and it was selected to complete the study. The 1.9 L EGR cooler achieved greater BTE and more stable combustion than the 6.0 L EGR cooler. Less soot and NO_X emissions were produced when the 11.0 L EGR cooler was used with FACE 5 (high CN fuel) compared to the 6.0 L EGR cooler. To reduce the influence of engine hardware when determining fuel property effects on emissions and performance, a decision was made to use the 6.0 L EGR cooler for all fuels, noting that more desirable results could be achieved with the use of EGR coolers specifically matched to a fuel's properties.

A single engine operating condition consisting of a fixed engine speed of 2100 rpm and 3.5 bar BMEP was utilized. The split injection control strategy involved varying the start of the pilot injection, start of the main injection, and fuel split with a constant intake oxygen concentration of 16% and constant rail pressure of 1600 bar. Investigation of the single injection control strategy consisted of varying intake oxygen concentration from 12 to 14% and injection pressures from 1200 to 1600 bar while controlling the injection timing to identify the operating conditions for 50% MFB at 7° ATDC.

A repeatability study was performed to develop a standard by which emissions and performance changes among the fuels could be attributed to fuel property differences and not to the variability associated with the equipment or control strategy. Several months after the primary testing of the nine fuels, test 5 and test 40 (Table 16) were repeated 18 times each over the course of three days using the ULSD. Based on the outcome of this study, it was determined that any difference in HC emissions or NO_X emissions greater than 4% and any difference in BTE greater than 2% could be deemed significant and thus could be attributed to differences in the fuels and/or engine operating conditions rather than variability associated with the data. Similarly for CO emissions and soot emissions, a difference greater than 18% and 27%, respectively, could also be deemed significant.

Split Injection Control Strategy: Optimal Tests (High BTE, Low Soot, and Low NO_X Tests for Each Fuel)

1. The highest BTE and low soot values were achieved at the two most advanced main SOI timings tested for all fuels with the exception of the ULSD. For the low NO_X tests, the low and medium CN fuels utilized the most retarded pilot SOI timings tested, 40° BTDC and 35° BTDC respectively.
2. A correlation was observed with HC emissions increasing as CN decreased. In addition, within a given CN group, fuels with lower T90 produced less HC emissions except for the low soot test with FACE 7.
3. CO emissions correlated with HC emissions. As CN decreased CO emissions increased.
4. FACE 8 and FACE 9, which had both high T90 and high aromatic content, exhibited the highest NO_X in their respective CN categories of medium CN and high CN.
5. Low CN fuels emitted significantly less soot than the high CN fuels. In addition, FACE 6 and FACE 8 had the highest soot, which was attributed to the high CN and high T90 of those fuels.
6. FACE 4 had the lowest BTE due to incomplete combustion (evidenced by high HC and CO emissions) caused by the fuel's low CN and low volatility. For the medium and high CN fuels, the highest T90 fuels had the highest BTE.
7. Although the low CN fuels had the lowest BTE, the low CN fuels had the highest PRR due to their longer ignition delays and subsequent better mixing.

Split Injection Control Strategy: Comparable Tests (Same Pilot Timing, Main Timing, and Fuel Split for All Fuels)

1. Similar to the optimal tests, a correlation was observed between decreasing CN and increasing HC and between decreasing CN and increasing CO.
2. The trend of lower HC emissions with lower T90 observed in the optimal tests did not occur here. FACE 7 and FACE 5 (both low T90 fuels) had higher or equal HC emissions of the other fuels in their respective CN categories.
3. As expected, NO_X decreased as the main SOI was retarded. The low CN fuels exhibited lower NO_X than the other fuels due to delayed combustion phasing. As in the optimal tests, FACE 8 and FACE 9 (simultaneously high T90 and aromatic fuels) had the highest NO_X emissions of the high and medium CN fuels, respectively.
4. The low CN fuels produced the lowest soot. FACE 5, a low T90 and low aromatic fuel, produced the lowest soot for the high CN fuels. The previously mentioned T90 trend with NO_X from the optimal tests was not seen in the comparable tests by the medium or low CN fuels. Retarding the main SOI timing by 2° from 4° BTDC to 2° BTDC significantly increased soot emissions for the medium and high CN fuels.
5. The low CN fuels had the lowest BTE due to lower combustion efficiency and delayed combustion phasing.

Single Injection Control Strategy: Optimal Tests (High BTE, Low Soot, and Low NO_X Tests for Each Fuel)

1. For all fuels, the highest BTE was achieved with the two lowest rail pressures tested (1200 or 1400 bar). For the low soot tests, the medium and high CN fuels used the highest intake oxygen concentration and rail pressure tested (14% and 1600 bar respectively). For all fuels, the lowest NOx values were obtained at the two lowest intake oxygen concentrations tested (12.0% and 12.5%).
2. The low CN fuels produced the highest levels of HC emissions. FACE 4, the lowest CN fuel, emitted the highest HC emissions.
3. Although the global CO emissions versus HC emissions trend obtained for the split injection strategy was not apparent for the single injection strategy, near linear trends with differing slopes existed for the individual fuels. CO emissions had a stronger correlation with soot for the medium and high CN fuels, due to the limited ignition delay, which is similar to conventional diesel combustion.
4. NO_X emissions were at very low levels due to the high EGR rates used. Again, FACE 8 and FACE 9 (high T90 and high aromatic content fuels) had the highest NO_X emissions in their respective CN categories.
5. Similar to results from the split injection strategy, soot emissions were the highest for FACE 6 and FACE 8 likely due to the high T90 of each fuel.
6. A correlation between BTE and aromatic content was noticed (except for FACE 8's BTE test) with a lower aromatic content leading to a higher BTE.

Single Injection Control Strategy: Comparable Tests (Same Intake Oxygen and Injection Pressures for All Fuels)

1. The low CN fuels emitted the highest levels of HC emissions. FACE 4, the lowest CN fuel, emitted the highest HC emissions. The medium and high CN fuels had much lower HC emissions.
2. FACE 8 and FACE 9 (high T90 and aromatic content fuels) had the highest NO_X emissions in their respective CN categories for both split and single injection control strategies.
3. As with those tests using the split injection strategy and optimal tests using the single injection strategy, soot emissions were the highest for FACE 6 and FACE 8 due to the high CN and high T90 of each fuel.
4. FACE 3 and FACE 4 (low CN fuels) had the lowest BTE values. However, FACE 1, also a low CN fuel (but with a low T90 and low aromatic content), had a BTE similar to the medium and high CN fuels.

Overall Comparisons of Split Injection and Single Injection Control Strategies

1. The average BTE of all fuels decreased from approximately 32.6% using the single injection strategy to 30.1% using the split injection strategy, which represents an 8% reduction at this operating condition.
2. The average HC, CO and NO_X emissions decreased by 50%, 18%, and 65% respectively for the single injection strategy tests compared to the split injection tests.

3. The average soot and PRR increased by 57% and 28% for the single injection strategy tests when compared to tests with the split injection strategy.

These conclusions are valid for the tests presented in the previous sections, but cannot yet be considered valid for all fuels, test conditions and engines. Below are some recommendations for additional testing and further analysis of the existing data.

1. A regression analysis with a linear model(s) performed on the entire data set would help to determine the definitive influence of aromatic content and T90 on advanced combustion. CN was the dominant factor on engine performance and emissions, but CN often masked the effects of aromatic content and T90.
2. It would be beneficial to include engine modifications in a further study. Certain fuels lend themselves to different engine conditions. A low CN fuel prefers high intake temperatures to initiate combustion. While a high CN fuel prefers low intake temperatures for early fuel injection and therefore better mixing. Engine conditions and hardware of special interest include intake temperature, intake pressure, intake oxygen, and compression ratio.
3. Investigation of additional engine operating conditions would assist in better understanding the effects of fuel properties on engine emissions and performance while operating in advanced combustion regimes.

6 References

1. Alnajjar, M., Cannella, W., Dettman, H., Fairbridge, C., Franz, J., Gallant, T., Gieleciak, R., Hager, D., Lay, C., Lewis, S., Ratcliff, M., Sluder, S., Storey, J., Yin, H, Zigler, B., "Chemical and Physical Properties of the Fuels for Advanced Combustion Engines (FACE) Research Diesel Fuels, FACE-1, Coordinating Research Council, 2010.
2. Gallant, T., Franz, J., Alnajjar, M., Storey, J., Lewis, S., Sluder, S., Cannella, W., Fairbridge, C., Hager, D., Dettman, H., Luecke, J., Ratcliff, M., Zigler, B., "Fuels for Advanced Combustion Engines Research Diesel Fuels: Analysis of Physical and Chemical Properties," SAE Technical Paper 2009-01-2769, USA, 2009.
3. Cho, K., Han, M., Sluder, C., Wagner, R., Lilik, G., "Experimental Investigation of the Effects of Fuel Characteristics on High Efficiency Clean Combustion in a Light-Duty Diesel Engine," SAE Technical Paper 2009-01-2669, San Antonio, TX, 2009.
4. Hosseini, V., Neill, W., Guo, H., Dumitrescu, C., Chippior, W., Fairbridge, C., Mitchell, K., "Effects of Cetane Number, Aromatic Content and 90% Distillation Temperature on HCCI Combustion of Diesel Fuels," SAE Technical Paper 2010-01-2168, San Diego, CA, 2010.
5. De Ojeda, W., Bulicz, T., Han, X., Zheng, M., Cornforth, F., "Impact of Fuel Properties on Diesel Low Temperature Combustion," SAE Technical Paper 2011-01-0329, Detroit, MI, 2011.
6. Dumitrescu, C., Neill, W., Guo, H., Hosseini, V., Chippior, W., "Fuel Property Effects on PCCI Combustion in a Heavy-Duty Diesel Engine," ASME 2010 ICE Conference ICEF2010-35194, San Antonio, TX, 2010.
7. Neely, G., Sasaki, S., Huang, Y., Leet, J., Steward, D., "New Diesel Emission Control Strategy to Meet US Tier 2 Emissions Regulations," SAE Technical Paper 2005-01-1091, Detroit, MI, 2005.
8. Ballauf, Jörg, *The 9th Annual Automobile and Engine Technology Colloquium in Aachen An Overview*. Aachen, Oct. 2000. PDF.
9. Simescu, S., Ryan, T. W., Neely, G. D., Matheaus, A. C., Surampudi, B., "Partial Pre-Mixed Combustion with Cooled and Uncooled EGR in a Heavy-Duty Diesel Engine," SAE Technical Paper 2002-01-0963, Detroit, MI, 2002.
10. Nevin, R. M., Sun, Y., Gonzalez D., M. A., Reitz, R. D., "PCCI Investigation Using Variable Intake Valve Closing in a Heavy Duty Diesel Engine," SAE Technical Paper 2007-01-0903, Detroit, MI, 2007.
11. Benajes, J., Molina, S., Novella, R., Arthozoul, S., "Advanced Injection Strategies to Attain Partially Premixed Combustion Process in a Heavy Duty Diesel Engine," SAE Technical Paper 2008-01-0642, Detroit, MI, 2008.
12. Hasegawa, R., Yanagihara, H., "HCCI Combustion in a DI Diesel Engine," SAE Technical Paper 2003-01-0745, Warrendale, PA, 2003.
13. Eppring, K., Aceves, S., Bechtold, R., Dec, J., "The Potential of HCCI Combustion for High Efficiency and Low Emissions," SAE Technical Paper 2002-01-1923, San Diego, CA, 2002.
14. Kawano, D., Suzuki, H., Ishii, H., Goto, Y., Matsuo, O., "Ignition and Combustion Control of Diesel HCCI," SAE Technical Paper 2005-01-2132, Tokyo, Japan, 2005.
15. Musculus, M., "On the Correlation between NOx Emissions and the Diesel Premixed Burn," SAE Technical Paper 2004-01-1401, Detroit, MI, 2004.

16. Carlucci, P., Ficarella, A., Laforgia, D., “Effects of Pilot Injection Parameters on Combustion for Common Rail Diesel Engines,” SAE Technical Paper 2003-01-0700, Leece, Italy, 2003.
17. Musculus, M., Lachaux, T., Pickett L., Idicheria, C., “End-of-Injection Over-Mixing and Unburned Hydrocarbon Emissions in Low-Temperature-Combustion Diesel Engines,” SAE Technical Paper 2007-01-0907, Detroit, MI, 2007.
18. Weall, A., Collings, N., “Highly Homogenous Compression Ignition in a Direct Injection Diesel Engine Fuelled with Diesel and Biodiesel,” SAE Technical Paper 2007-01-2020, Japan, 2007.
19. Wagner, U., Anca, R., Velji, A., Spicher, U., “An Experimental Study of Homogeneous Charge Compression Ignition (HCCI) with Various Compression Ratios, Intake Air Temperatures and Fuels with Port and Direct Fuel Injection,” SAE Technical Paper 2003-01-2293, Costa Mesa, CA, 2003.
20. Buchwald, R., Brauer, M., Blechstein, A., Sommer, A., Kahrstedt, J., “Adaption of Injection System Parameters to Homogeneous Diesel Combustion,” SAE Technical Paper 2004-01-0936, Detroit, MI, 2004.
21. Vanegas, A., Won, H., Peters, N., “Influence of the Nozzle Spray Angle on Pollutant Formation and Combustion Efficiency for a PCCI Diesel Engine,” SAE Technical Paper 2009-01-1445, Detroit, MI, 2009.
22. Kawano, D., Naito, H., Suzuki, H., Ishii, H., Hori, S., Goto, Y., Odaka, M., Effects of Fuel Properties on Combustion and Exhaust Emissions of Homogeneous Charge Compression Ignition (HCCI) Engine,” SAE Technical Paper 2004-01-1966 Toulouse, France, 2004.
23. Pulkrabek, Willard W., *Engineering Fundamentals of the Internal Combustion Engine*. 2nd ed. Upper Saddle River, NJ: Pearson Prentice Hall, 2004. Print.
24. Bunting, B., Crawford, R., Wolf, L., Xu, Y., “The Relationships of Diesel Fuel Properties, Chemistry, and HCCI Engine Performance as Determined by Principal Components Analysis,” SAE Technical Paper 2007-01-4059, Rosemont, IL, 2007.
25. Nuszkowski, J., “The Effects of Fuel Additives on Diesel Engine Emissions during Steady State and Transient Operation”. Doctor of Philosophy Thesis, West Virginia University, 2008.
26. Szybist, J., Kirby, S., and Boehman, A., “NOx Emissions of Alternative Diesel Fuels: A Comparative Analysis of Biodiesel and FT Diesel,” Energy & Fuels, Vol. 19 No. 4, pgs. 1484-1492, 2005.
27. Woschni, G., "A Universally Applicable Equation for the Instantaneous Heat Transfer Coefficient in the Internal Combustion Engine," SAE Technical Paper 670931, Warrendale, PA, 1967.

7 Appendices

7.1 Appendix A

Appendix A includes radar plots for optimal tests of each fuel containing pertinent emissions and BTE. The values of these constituents are normalized using the factors listed in Table 22 and Table 23.

7.1.1 Split Injection Control Strategy

Table 22: Split Injection Normalizing Factors

HC Emissions	1 = 7.35 g/kW-hr
CO Emissions	1 = .943 g/kW-hr
NO_X Emissions	1 = 19.7 g/kW-hr
Soot Emissions	1 = 329 mg/kW-hr
BTE	1 = 32.8 %, 0 = 28%

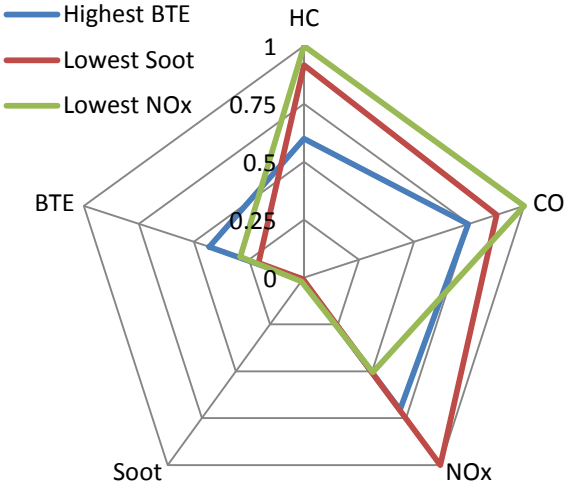

Figure 105: FACE 4

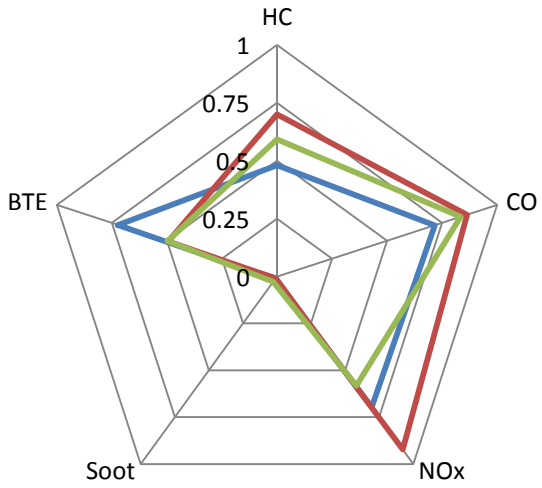

Figure 106: FACE 1

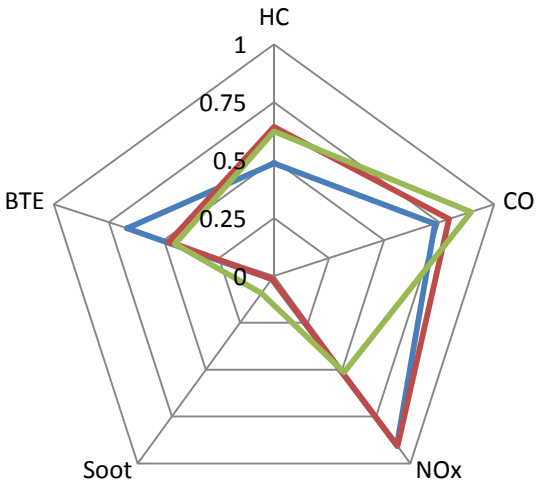

Figure 107: FACE 3

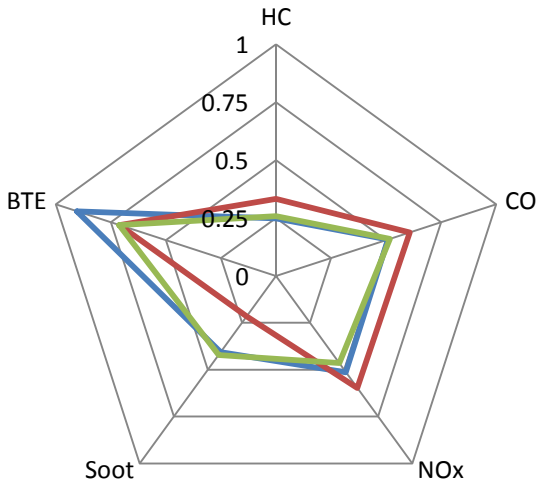

Figure 108: ULSD

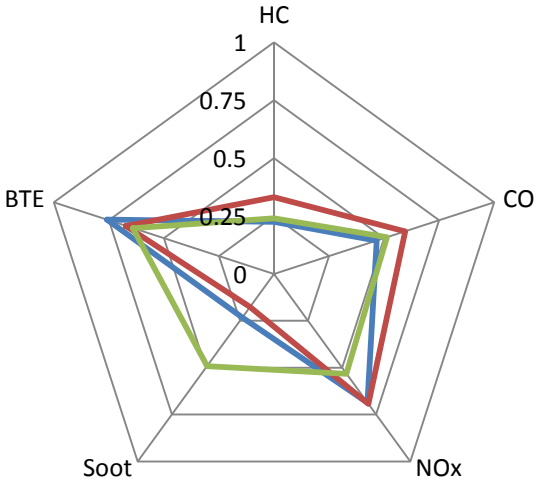

Figure 109: FACE 7

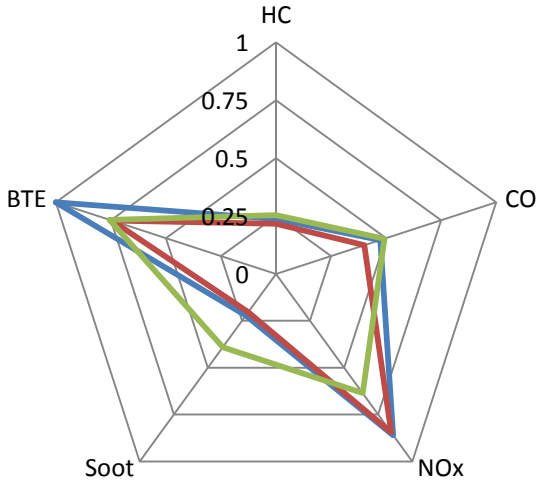

Figure 110: FACE 9

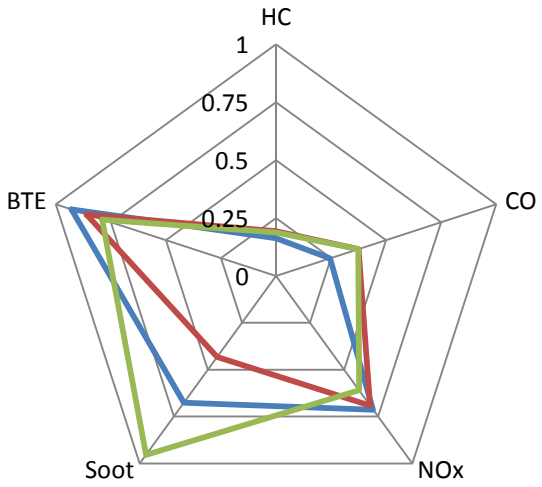

Figure 111: FACE 8

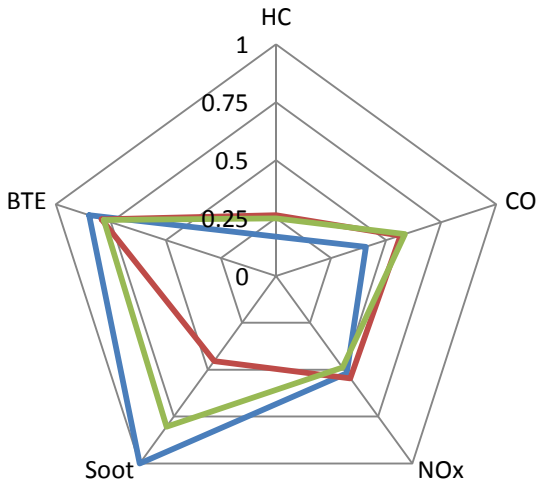

Figure 112: FACE 6

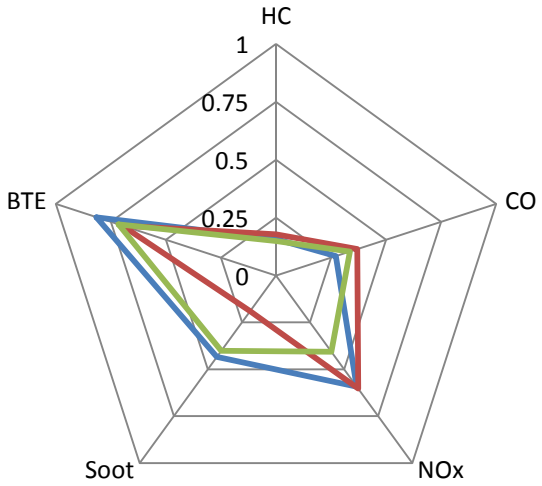

Figure 113: FACE 5

7.1.2 Single Injection Control Strategy

Table 23: Single Injection Normalizing Factors

HC Emissions	1 = 6.91 g/kW-hr
CO Emissions	1 = .383 g/kW-hr
NO_X Emissions	1 = 21.9 g/kW-hr
Soot Emissions	1 = 1324 mg/kW-hr
BTE	1 = 34.3% 0 = 30%

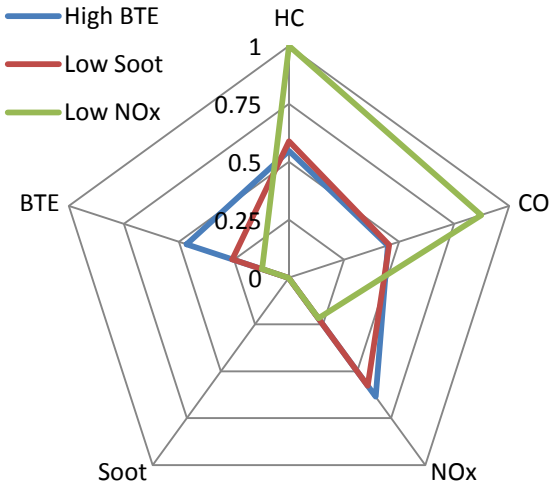

Figure 114: FACE 4

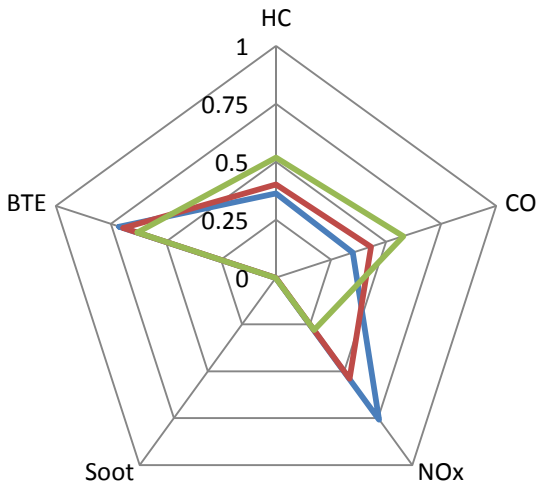

Figure 115: FACE 1

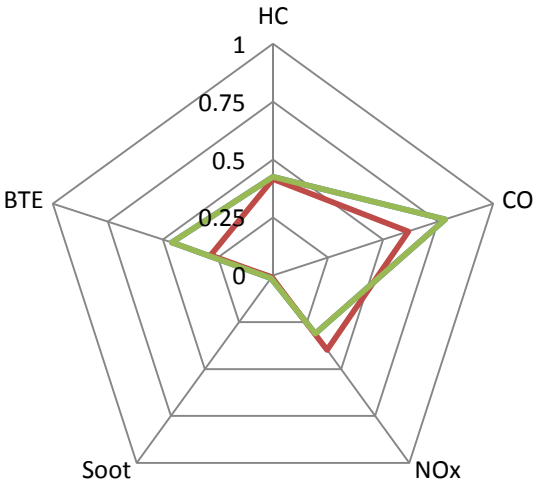

Figure 116: FACE 3

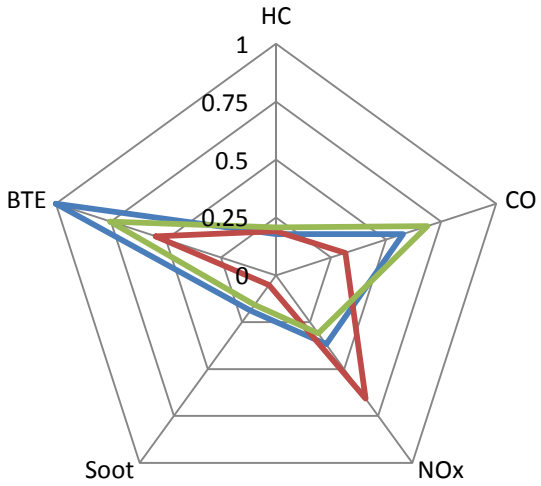

Figure 117: ULSD

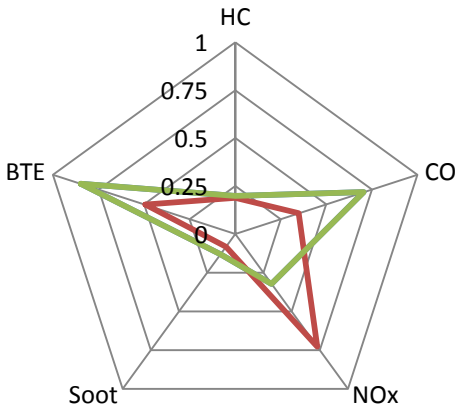

Figure 118: FACE 7

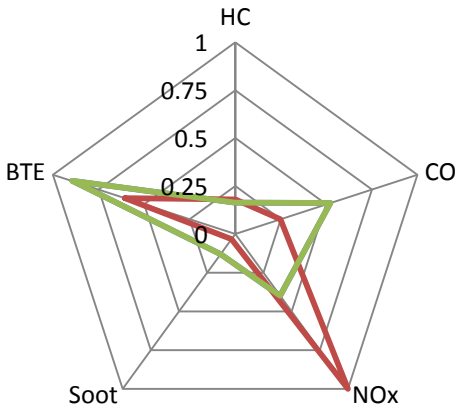

Figure 119: FACE 9

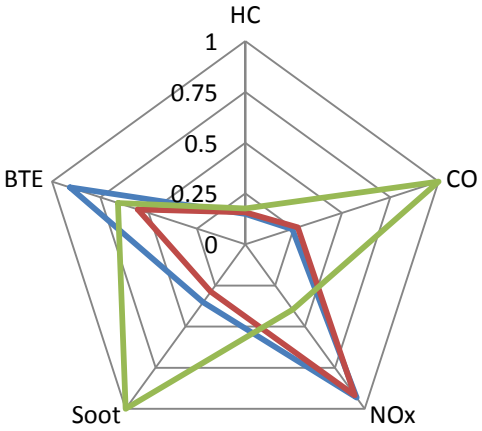

Figure 120: FACE 8

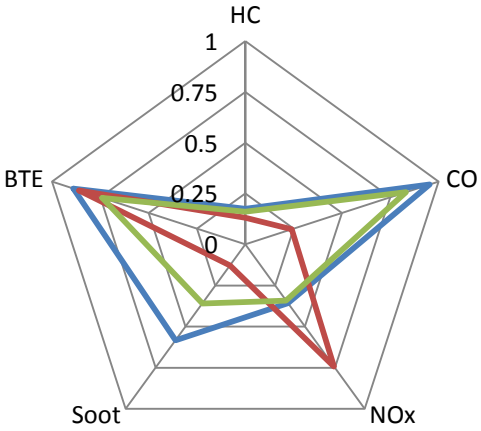

Figure 121: FACE 6

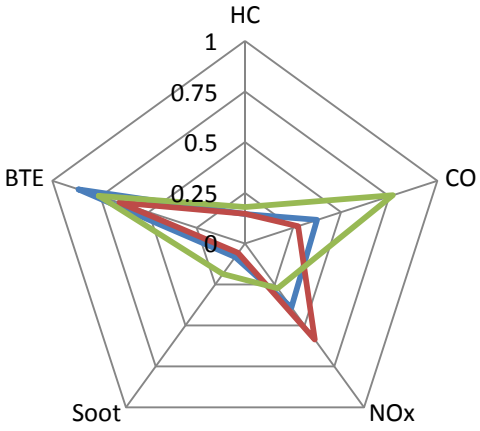

Figure 122: FACE 5

7.2 Appendix B

Appendix B includes plots of emissions, BTE, and PRR versus the primary fuel properties. These plots contain data for each fuel from the three optimal and six comparable tests discussed in Sections 4.3 Split Injection Control Strategy and 4.4 Single Injection Control Strategy of the report. Note that for some fuels nine separate data points do not appear. This is due to some optimal and comparable tests occurring at the same test conditions for a given fuel and/or some tests having similar, overlapping values for particular parameters.

7.2.1 Split Injection Control Strategy

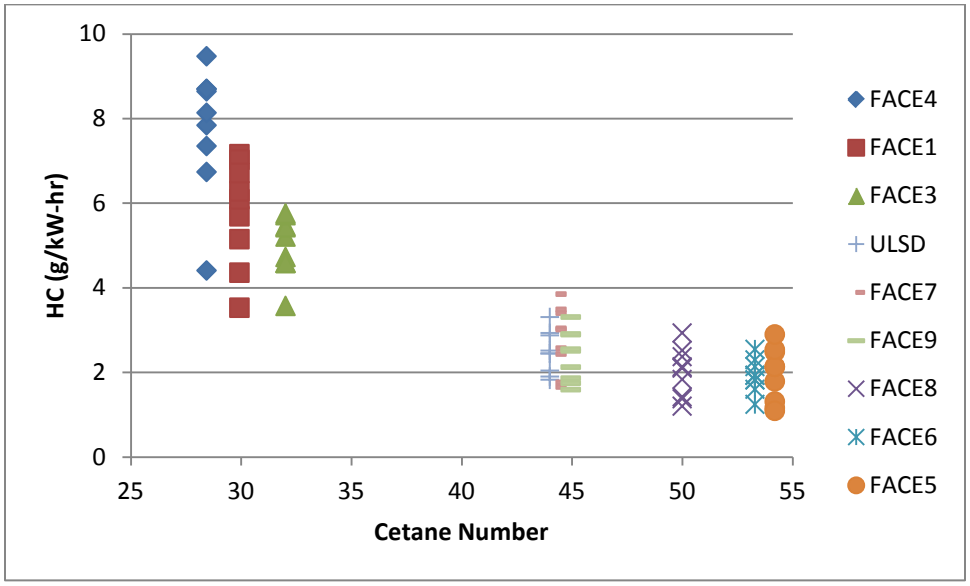

Figure 123: HC (g/kW-hr) vs. Cetane Number

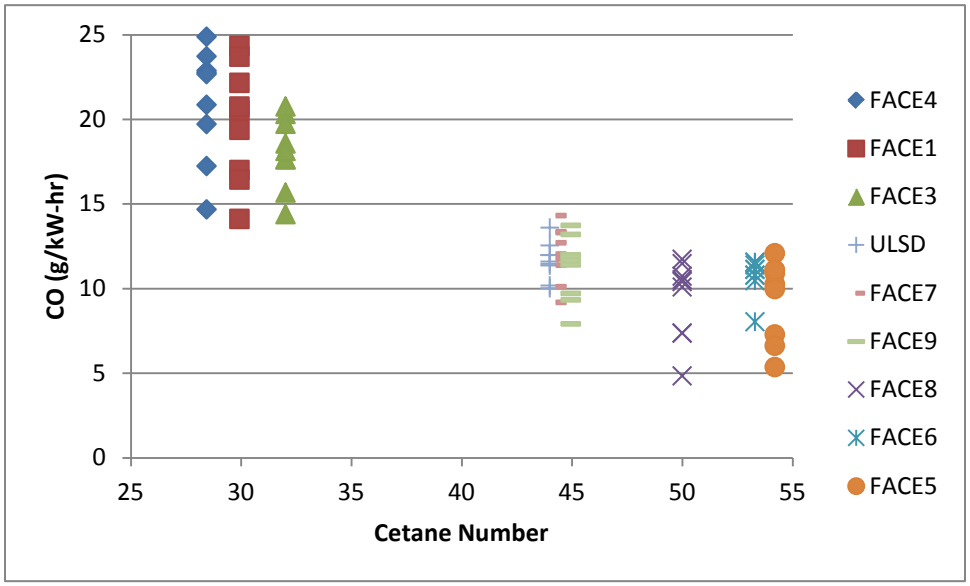

Figure 124: CO (g/kW-hr) vs. Cetane Number

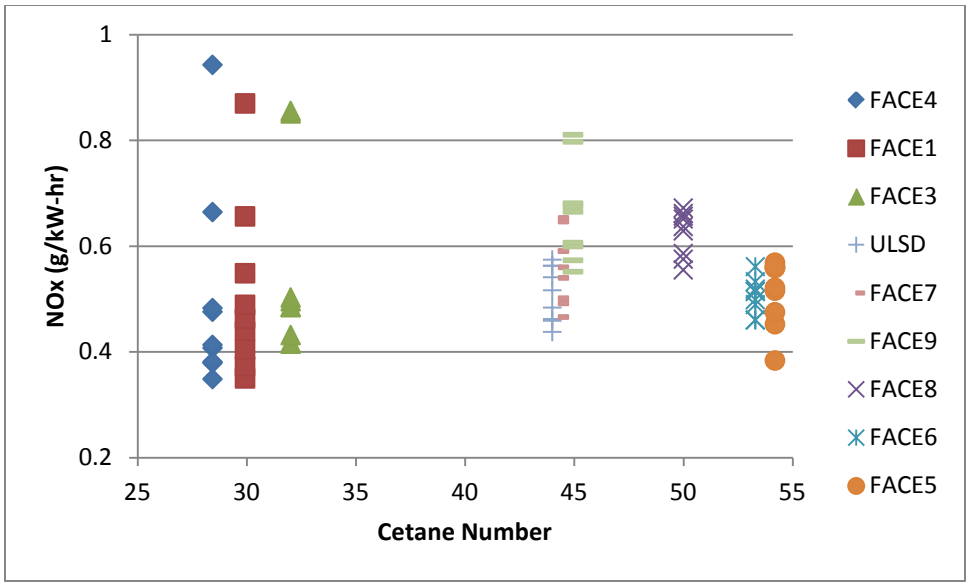

Figure 125: NO_X (g/kW-hr) vs. Cetane Number

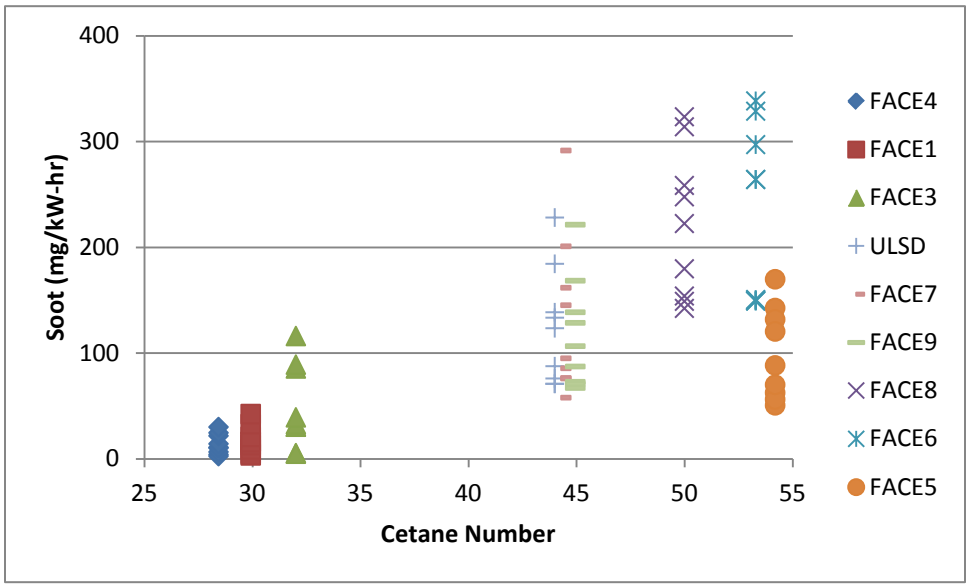

Figure 126: Soot (mg/kW-hr) vs. Cetane Number

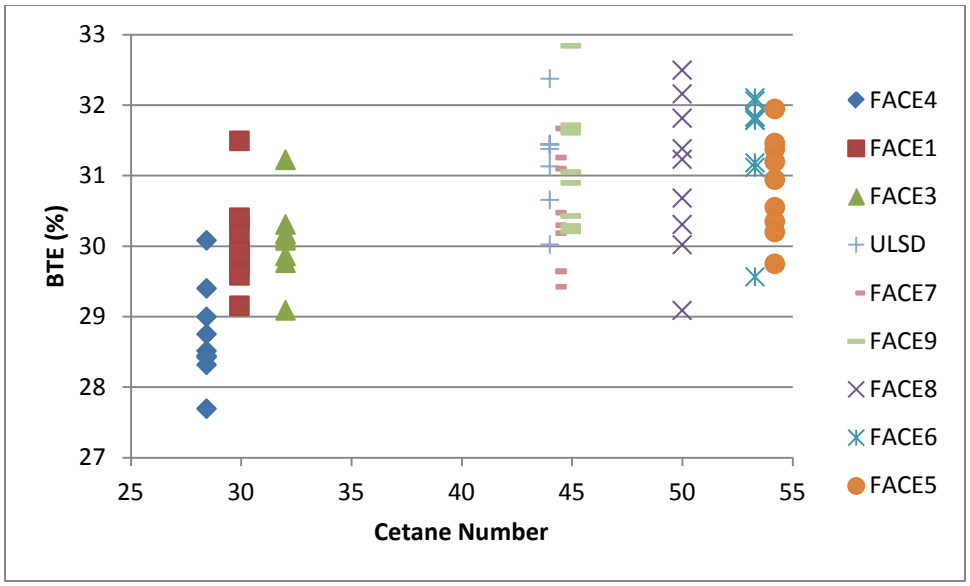

Figure 127: BTE (%) vs. Cetane Number

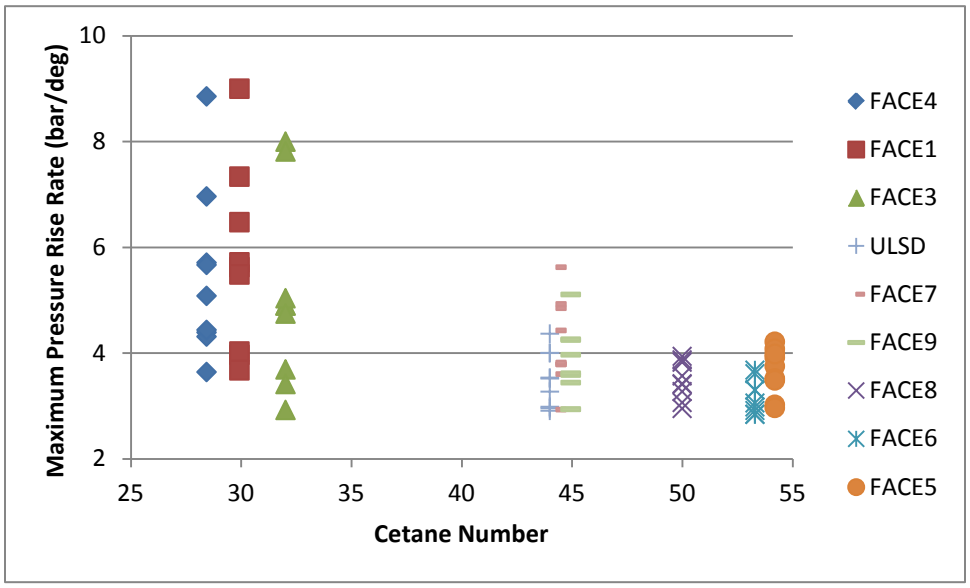

Figure 128: PRR (bar/deg) vs. Cetane Number

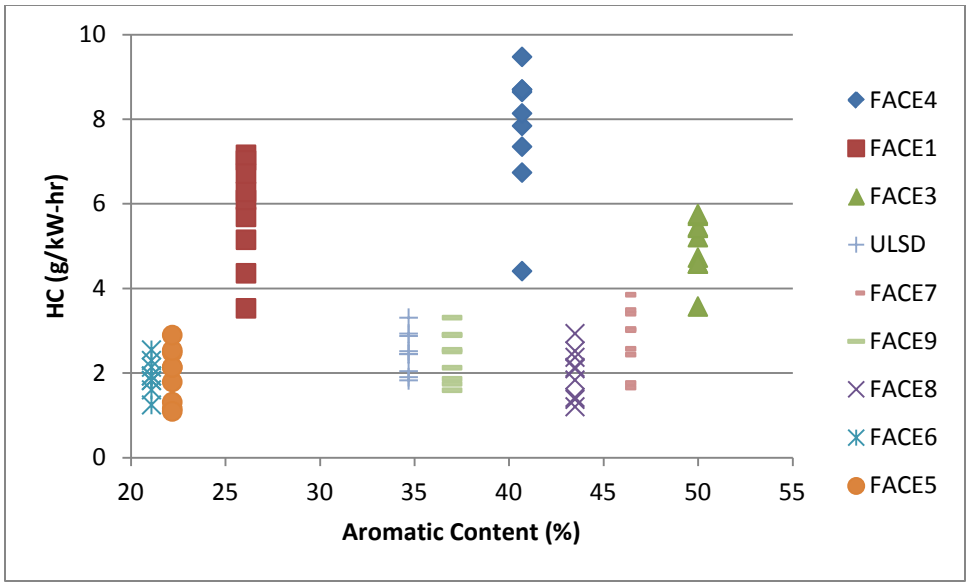

Figure 129: HC (g/kW-hr) vs. Aromatic Content (%)

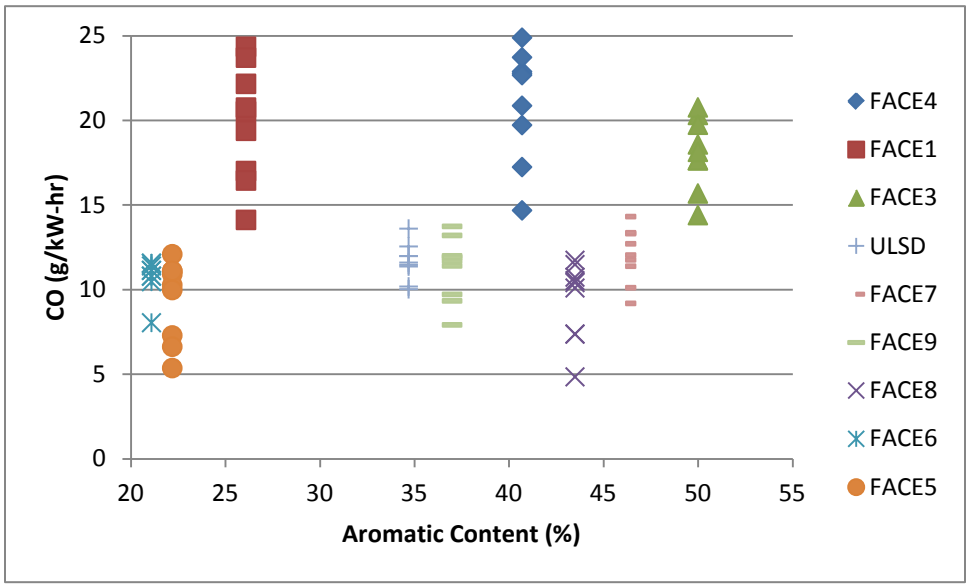

Figure 130: CO (g/kW-hr) vs. Aromatic Content (%)

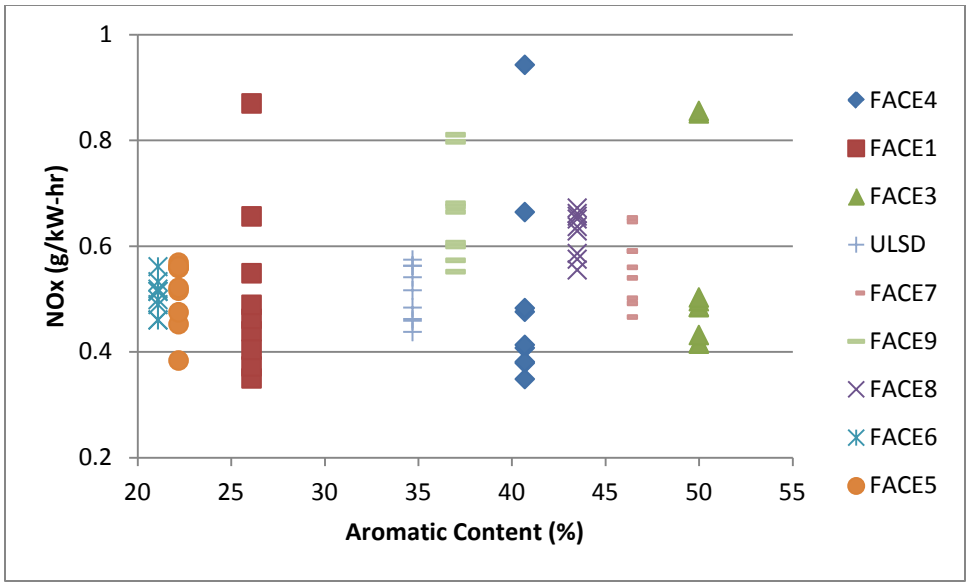

Figure 131: NO_X (g/kW-hr) vs. Aromatic Content (%)

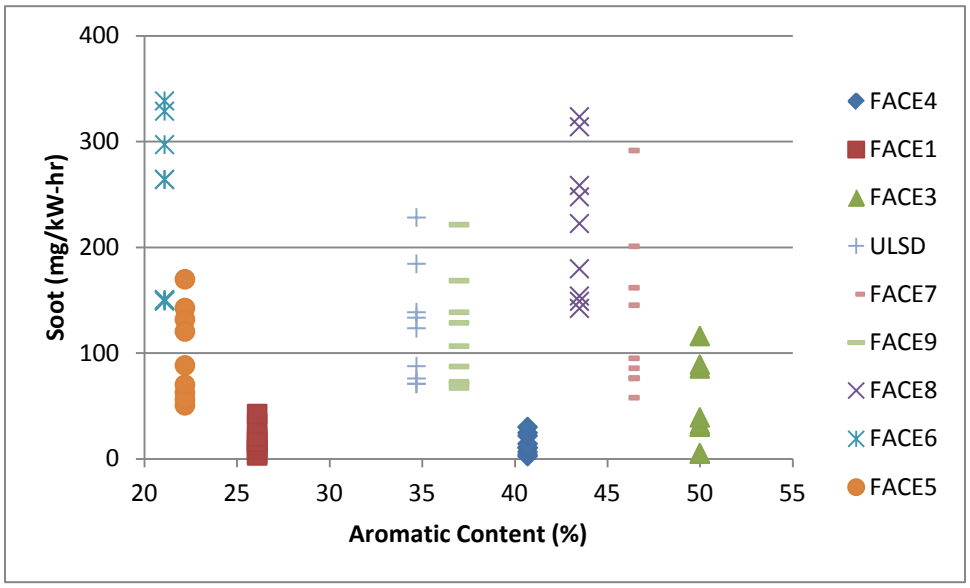

Figure 132: Soot (mg/kW-hr) vs. Aromatic Content (%)

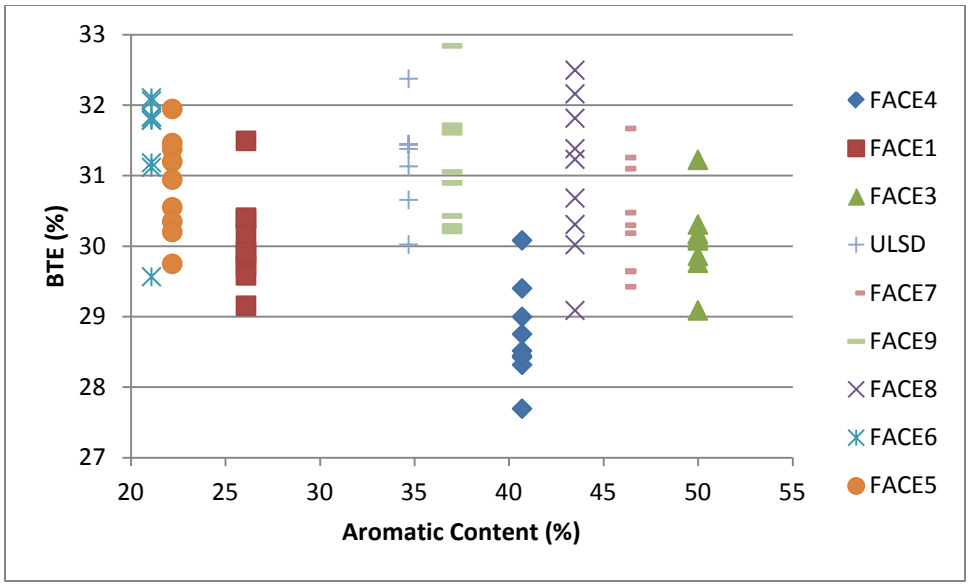

Figure 133: BTE (%) vs. Aromatic Content (%)

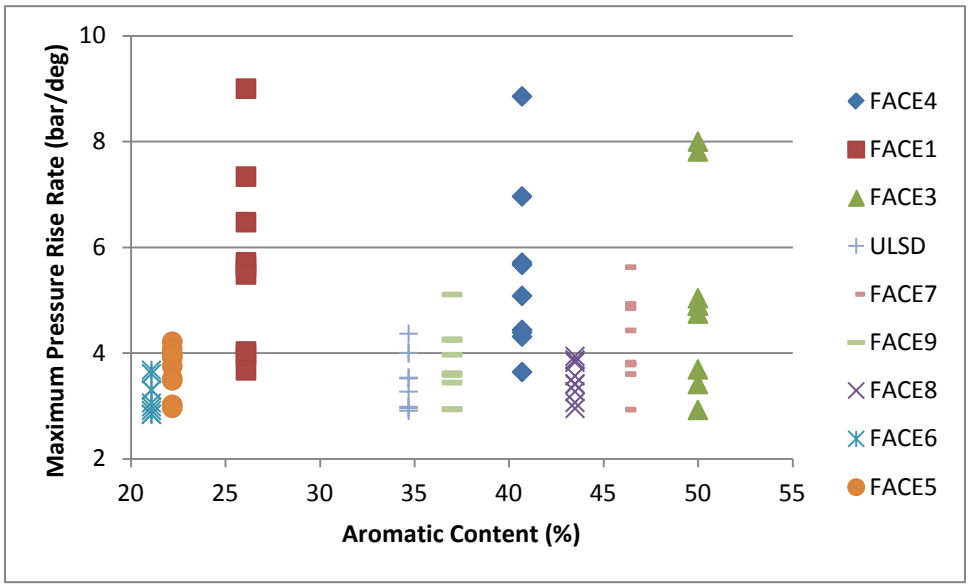

Figure 134: PRR (bar/deg) vs. Aromatic Content (%)

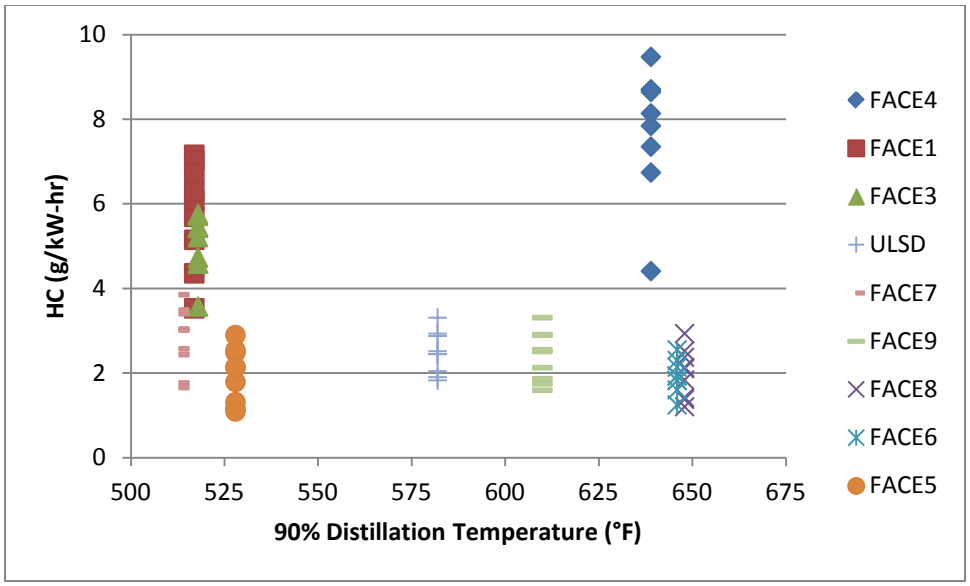

Figure 135: HC (g/kW-hr) vs. 90% Distillation Temperature (°F)

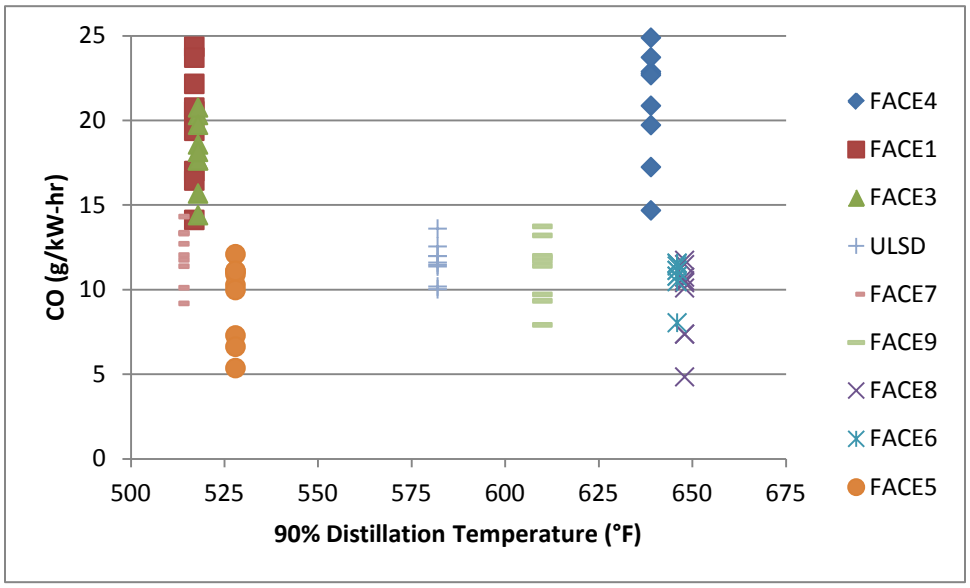

Figure 136: CO (g/kW-hr) vs. 90% Distillation Temperature (°F)

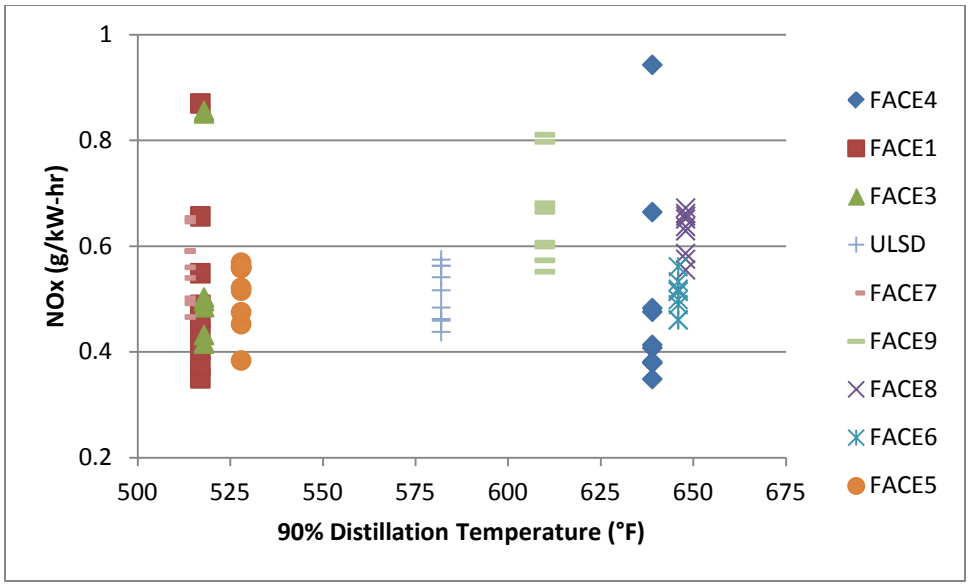

Figure 137: NO_X (g/kW-hr) vs. 90% Distillation Temperature (°F)

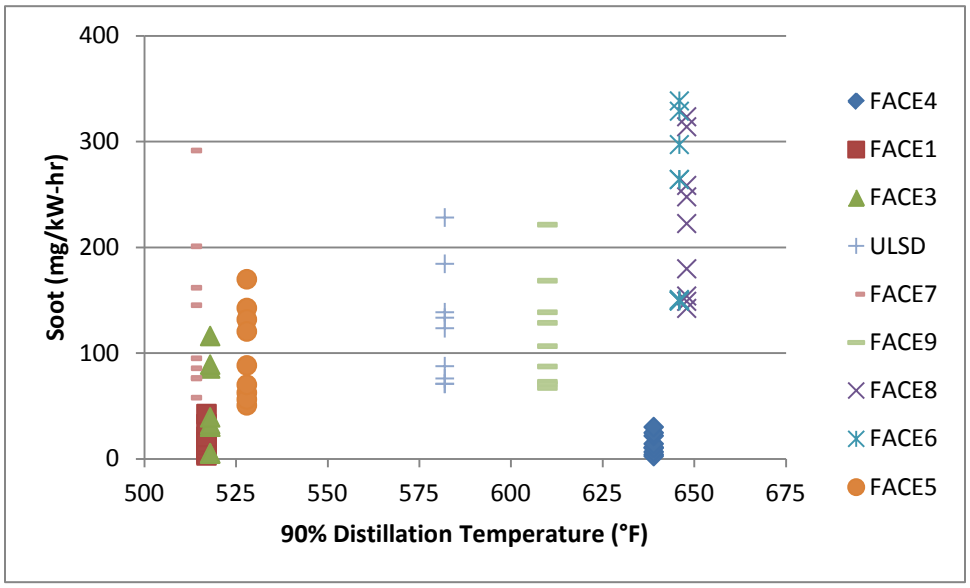

Figure 138: Soot (mg/kW-hr) vs. 90% Distillation Temperature (°F)

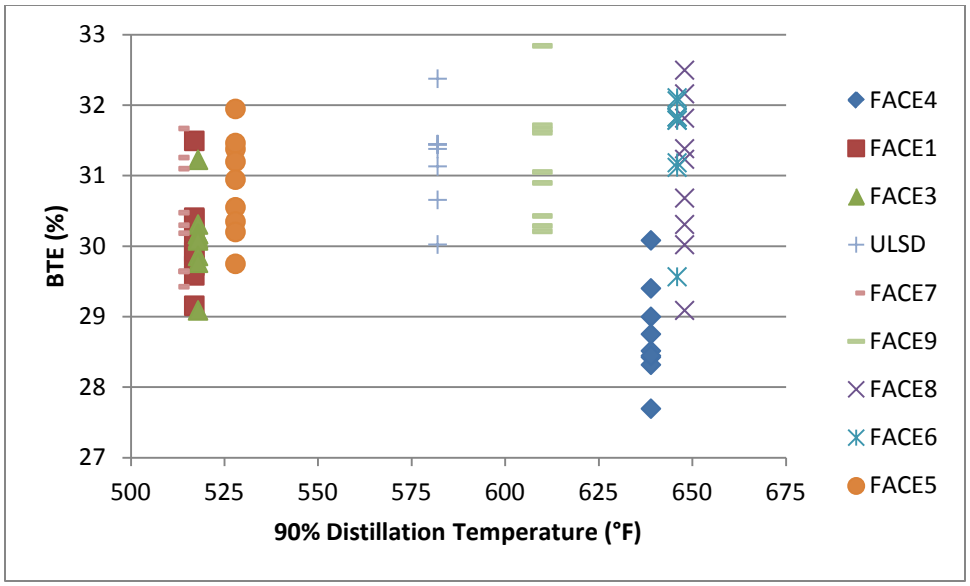

Figure 139: BTE (%) vs. 90% Distillation Temperature (°F)

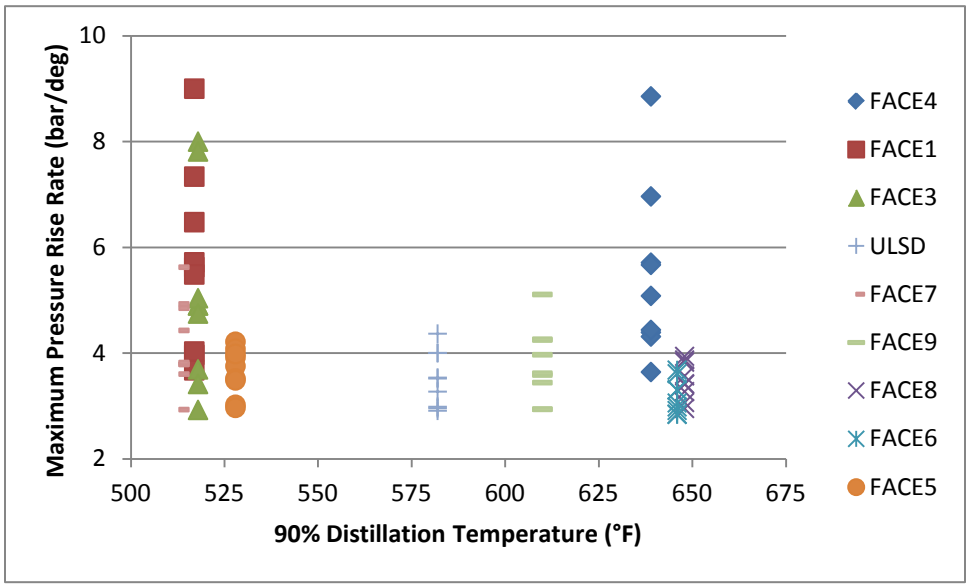

Figure 140: PRR (bar/deg) vs. 90% Distillation Temperature (°F)

7.2.2 Single Injection Control Strategy

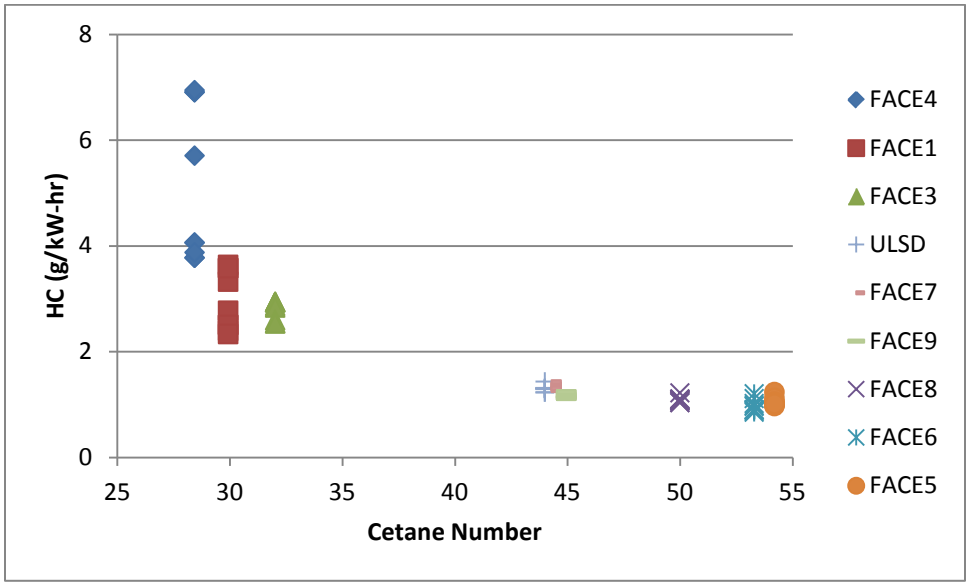

Figure 141: HC (g/kW-hr) vs. Cetane Number

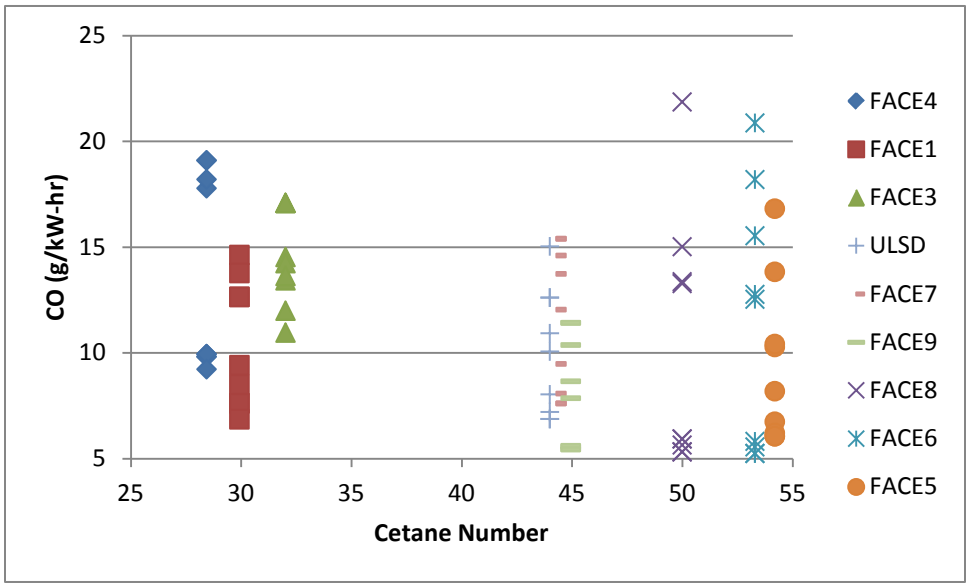

Figure 142: CO (g/kW-hr) vs. Cetane Number

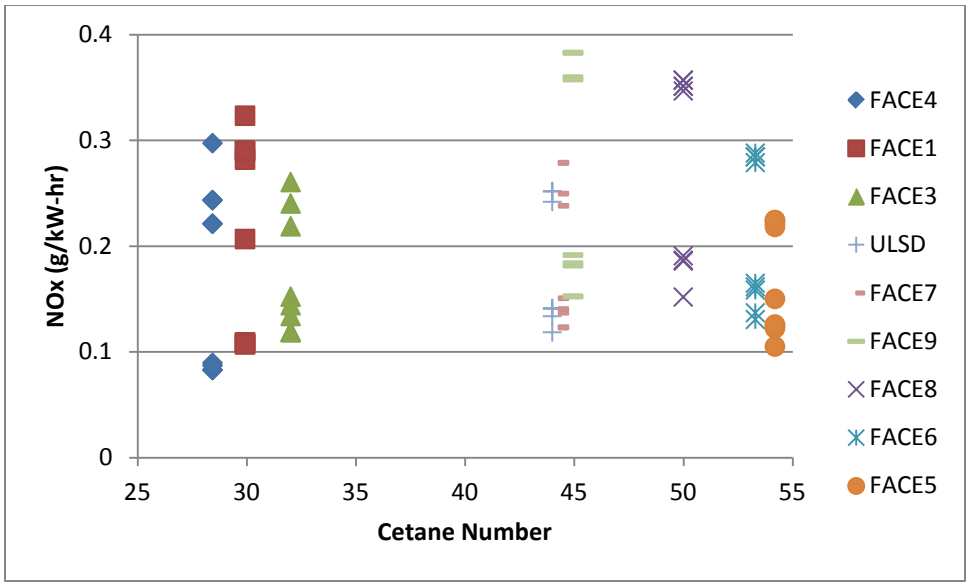

Figure 143: NO_X (g/kW-hr) vs. Cetane Number

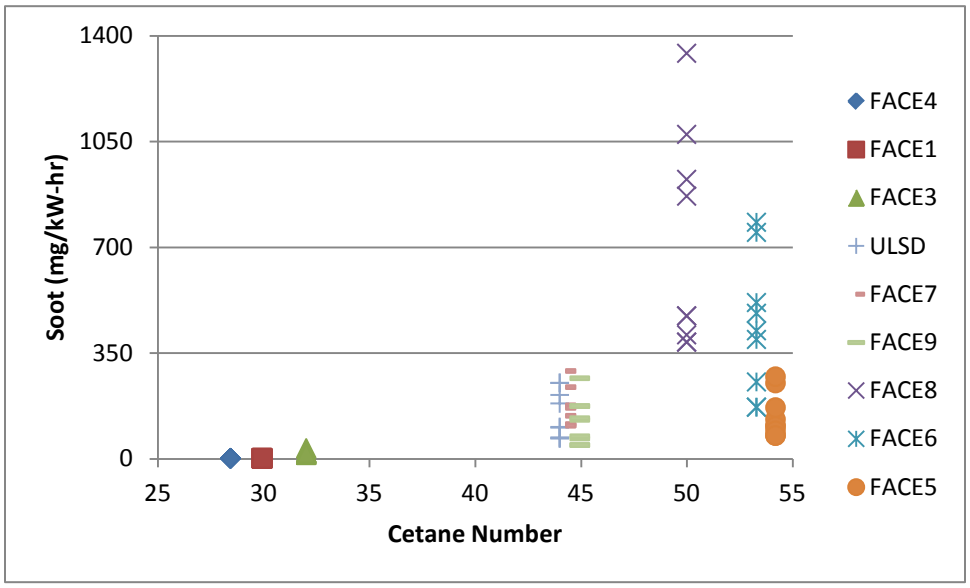

Figure 144: Soot (mg/kW-hr) vs. Cetane Number

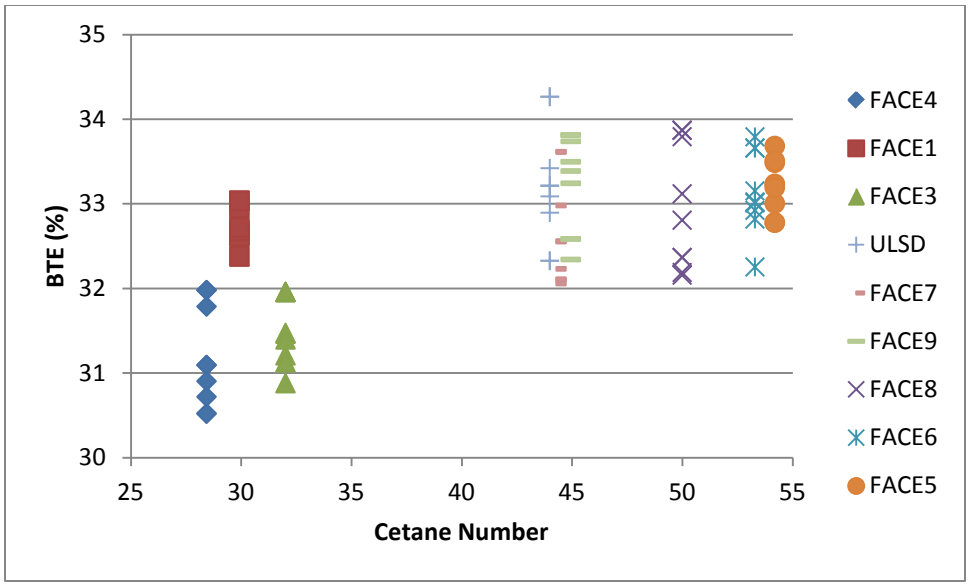

Figure 145: BTE (%) vs. Cetane Number

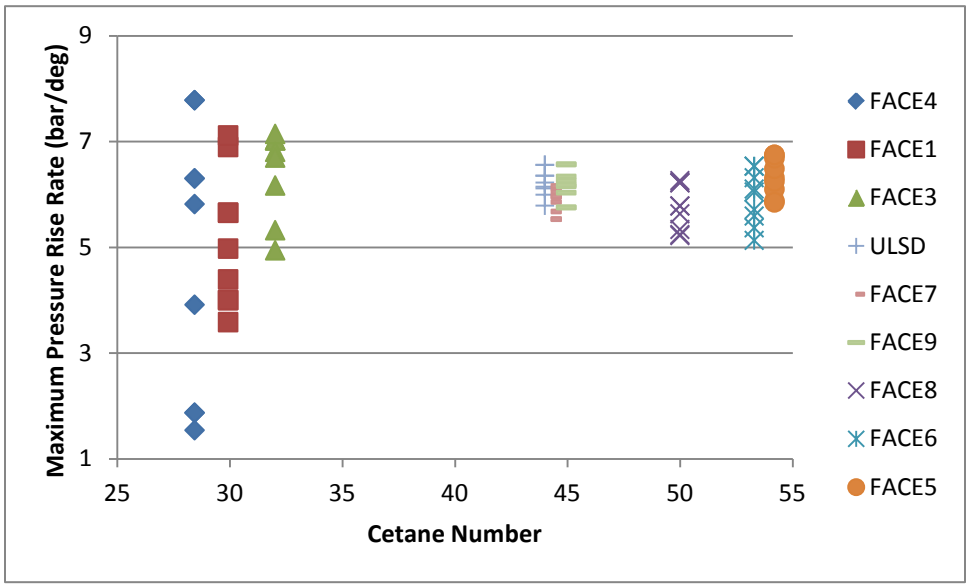

Figure 146: PRR (bar/deg) vs. Cetane Number

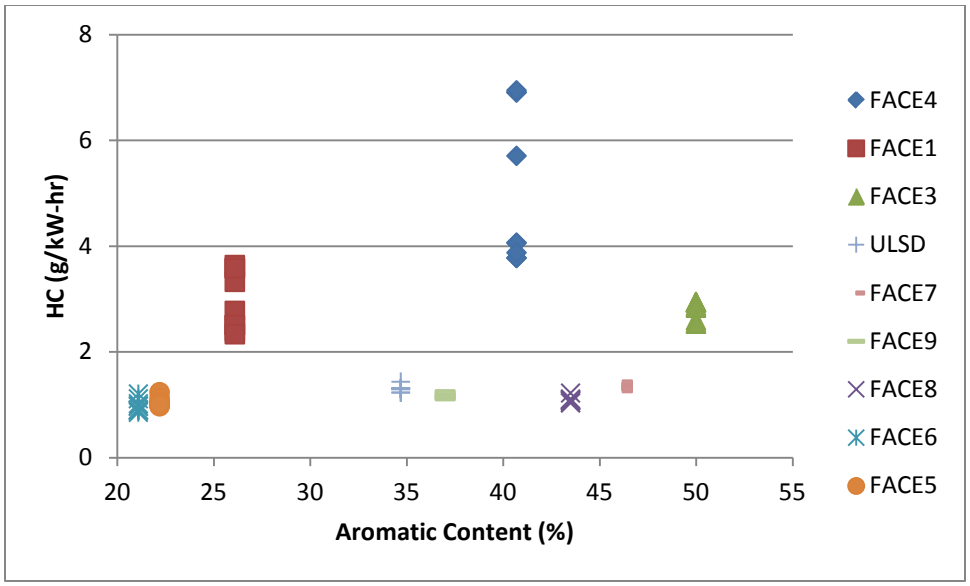

Figure 147: HC (g/kW-hr) vs. Aromatic Content (%)

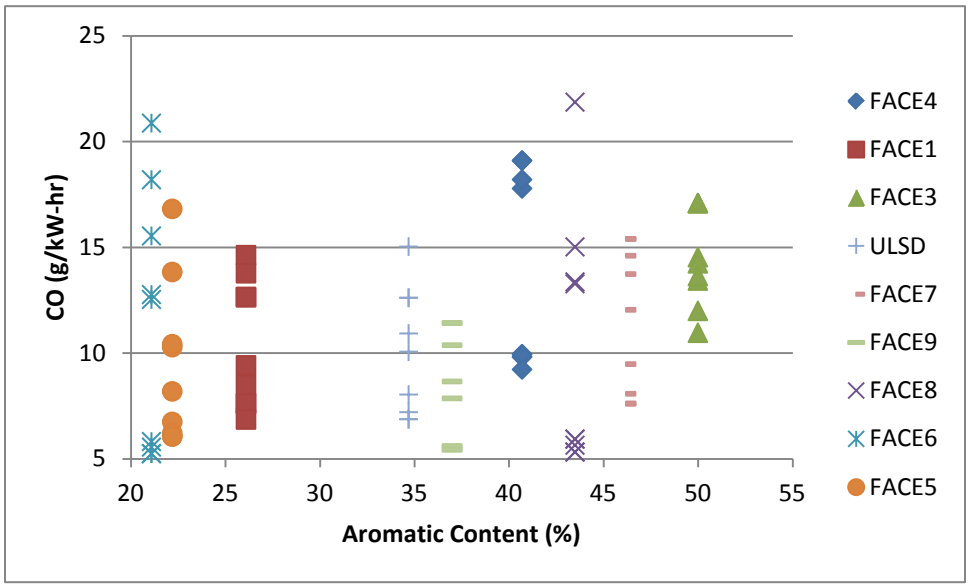

Figure 148: CO (g/kW-hr) vs. Aromatic Content (%)

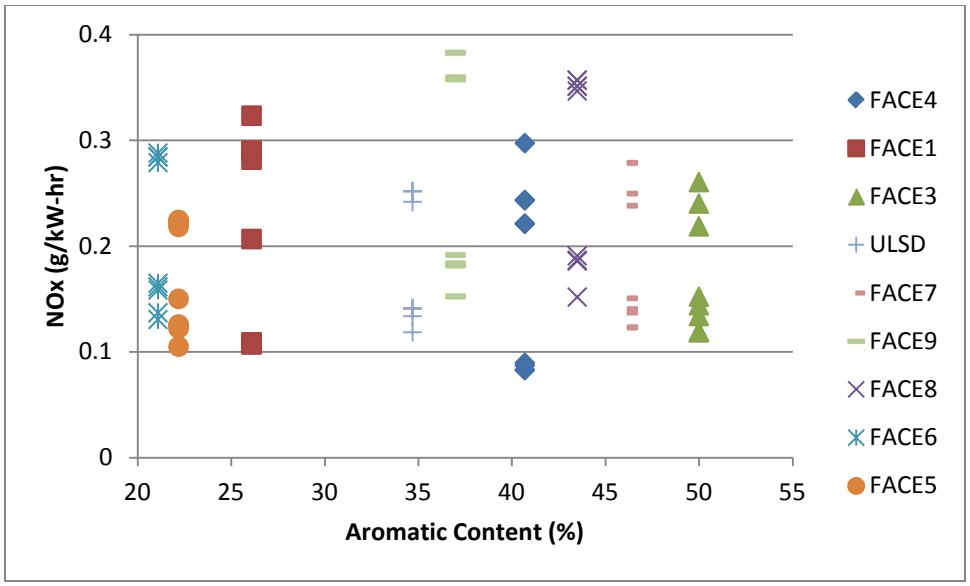

Figure 149: NO_X (g/kW-hr) vs. Aromatic Content (%)

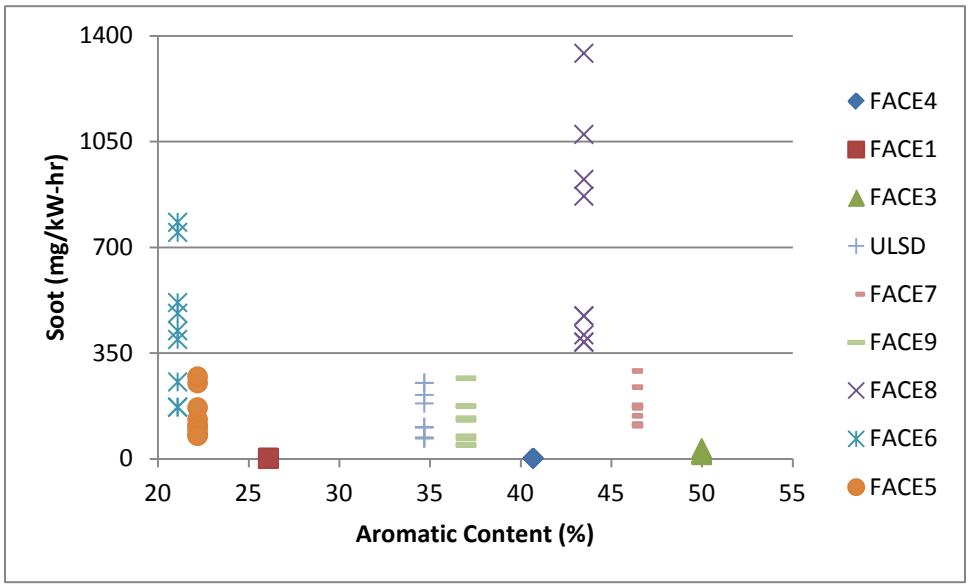

Figure 150: Soot (mg/kW-hr) vs. Aromatic Content (%)

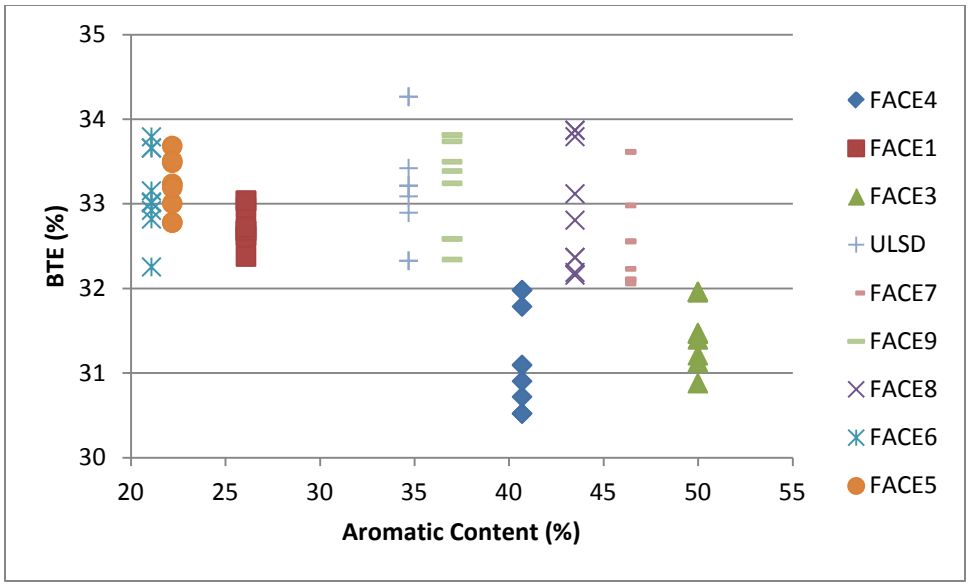

Figure 151: BTE (%) vs. Aromatic Content (%)

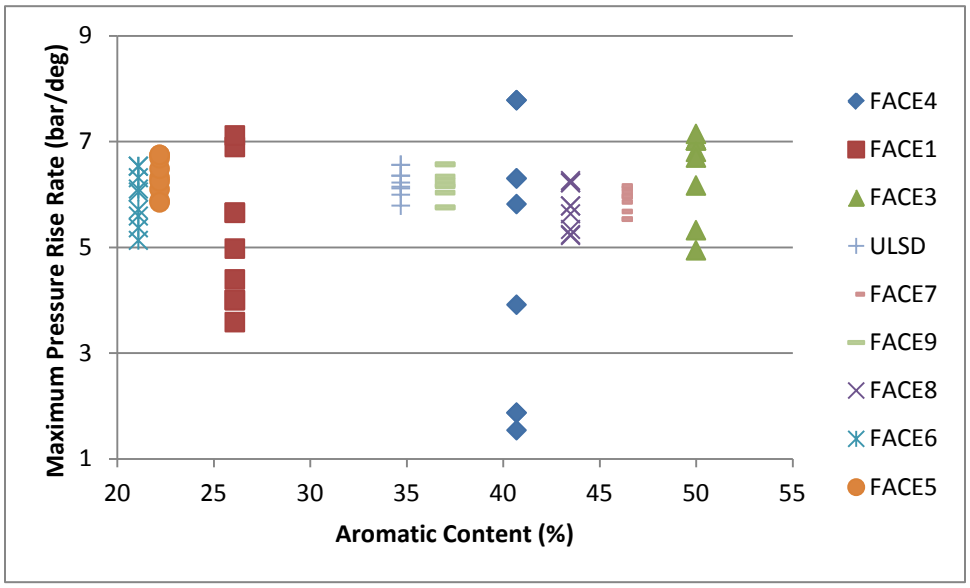

Figure 152: PRR (bar/deg) vs. Aromatic Content (%)

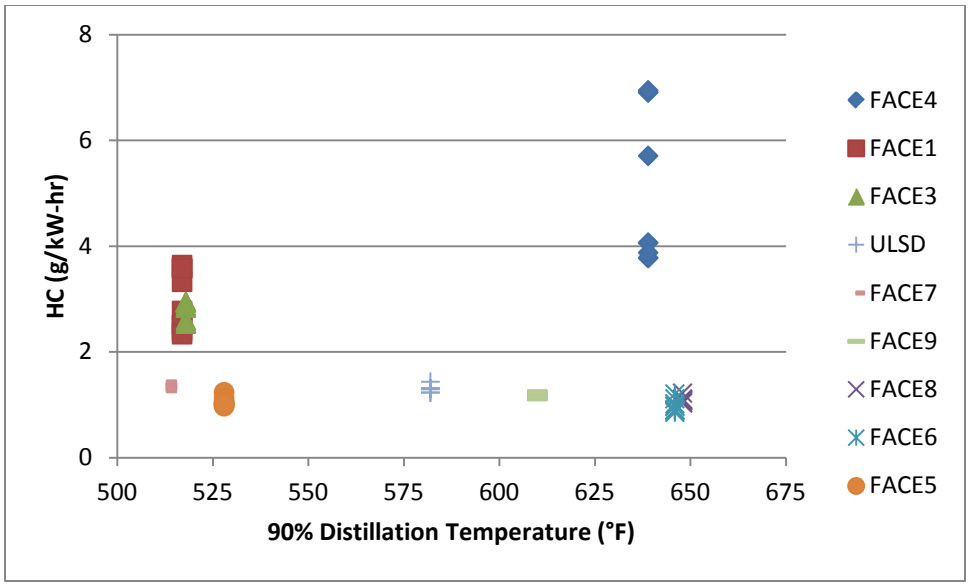

Figure 153: HC (g/kW-hr) vs. 90% Distillation Temperature (°F)

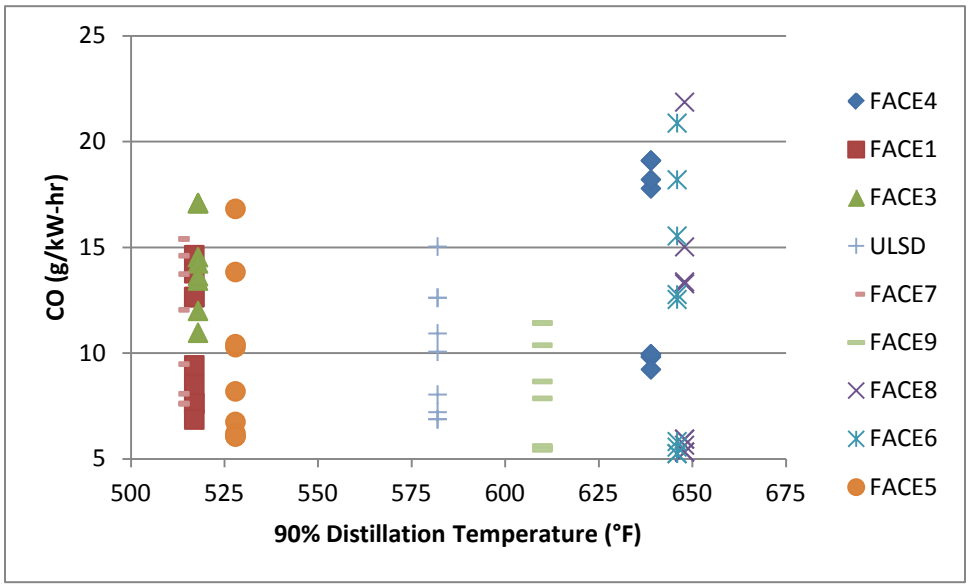

Figure 154: CO (g/kW-hr) vs. 90% Distillation Temperature (°F)

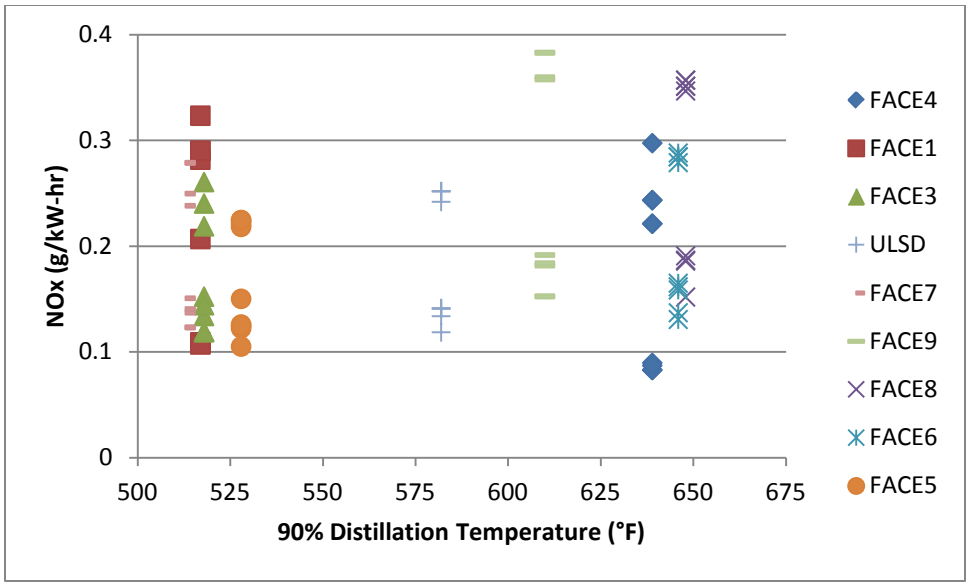

Figure 155: NO_X (g/kW-hr) vs. 90% Distillation Temperature (°F)

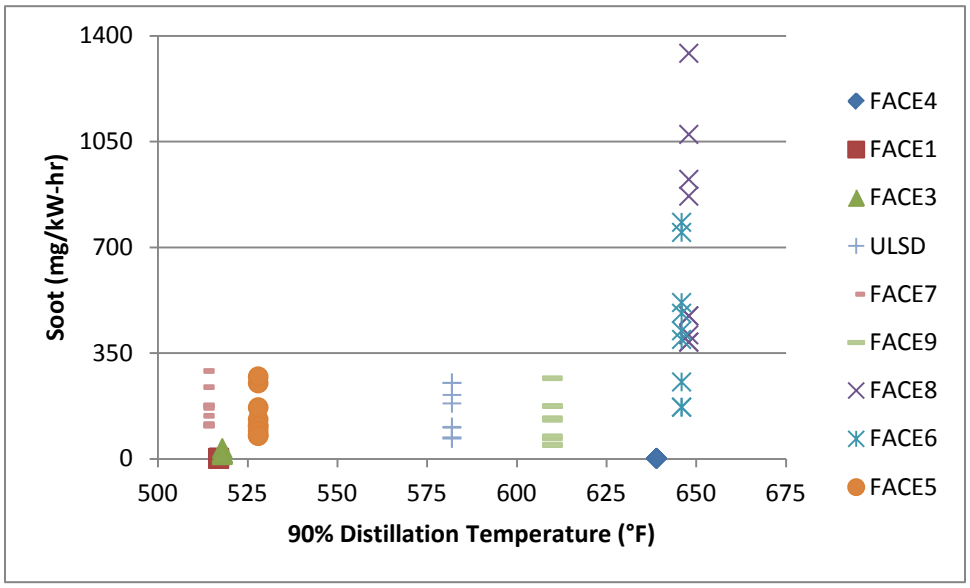

Figure 156: Soot (mg/kW-hr) vs. 90% Distillation Temperature (°F)

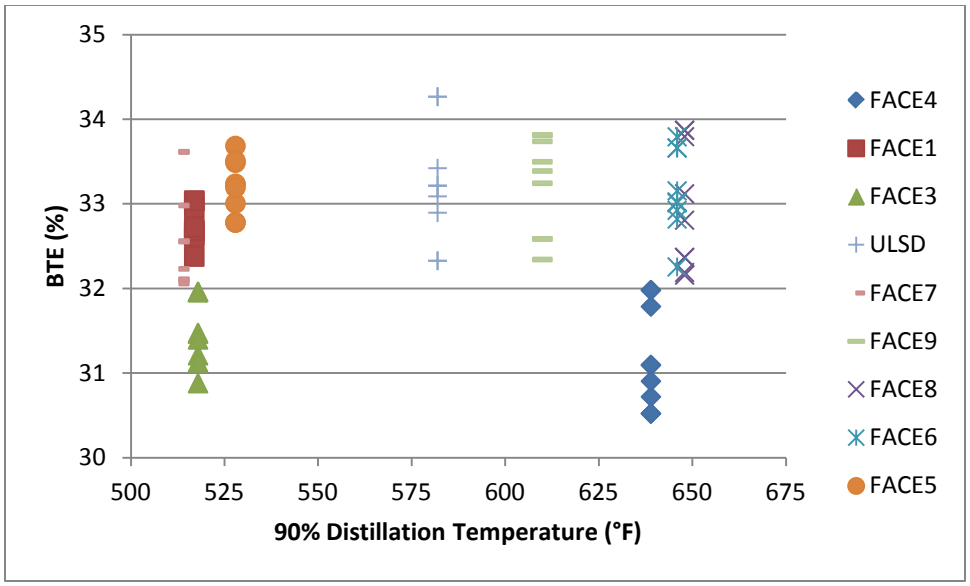

Figure 157: BTE (%) vs. 90% Distillation Temperature (°F)

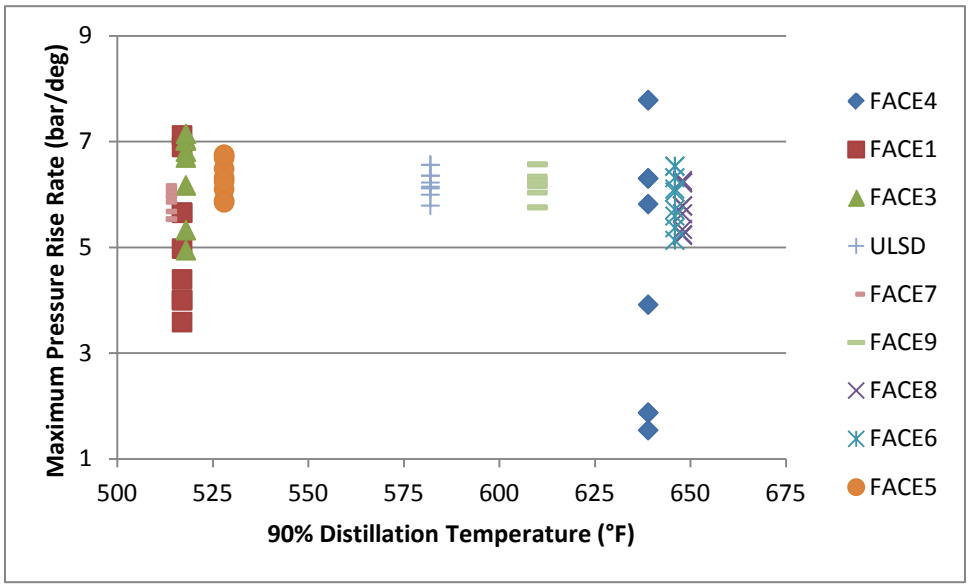

Figure 158: PRR (bar/deg) vs. 90% Distillation Temperature (°F)

7.3 Appendix C

Appendix C includes data summaries for the split injection and single injection control strategies for each fuel. This data is contained in a compressed folder included with the AVFL-16 final report submission labeled “AVFL-16 Individual Test Data.” Within this compressed folder data specific to each fuel is contained in individual Excel workbooks labeled according to the fuel name. This data is available from CRC upon request.